



Norwegian University of  
Science and Technology

# Rational calculation of sea margin

**Anna Karina Magnussen**

Marine Technology

Submission date: June 2017

Supervisor: Sverre Steen, IMT

Norwegian University of Science and Technology  
Department of Marine Technology





**NTNU – Trondheim**  
Norwegian University of  
Science and Technology

# Rational calculation of sea margin

Anna Karina Magnussen

Spring 2017

MASTER THESIS

Department of Marine Technology

Norwegian University of Science and Technology

Supervisor: Professor Sverre Steen





## **MASTER THESIS IN MARINE TECHNOLOGY**

**SPRING 2017**

**FOR**

**FOR**

**Anna Karina Magnussen**

### **Rational calculation of sea margin**

The speed-power performance of ships is usually predicted for an idealized trial condition, with a clean hull and negligible waves and wind. When the ship is in normal operation, with some hull fouling as well as waves and wind, the power required to reach a certain speed is higher than the speed originally predicted and measured on the delivery sea trial. This increase is usually expressed as a sea margin, which is normally added to the power. A typical value for the sea margin is 15%. The value of the sea margin is set according to tradition and some practical experience, but it is not normally based on proper calculations utilizing knowledge about the actual ship, her condition, and her operational profile.

It is known that added resistance due to waves and wind will be relatively larger for slow ships than for fast ships, and that they will be relatively larger for a given vessel if the speed is reduced. Also, the size of the ship and the area of operation might be important parameters. Thus, it might be argued that the sea margin should be speed dependent, and that it should be set using calculations including operational area and ship particulars. Furthermore, it is known that the frictional resistance increase due to hull condition can be more than 15% of the total.

The sea margin is important for accurate estimation of fuel consumption and therefore operating cost. It should probably depend on speed, as argued above, and it should also depend on the trade of the ship.

The objectives of the master thesis are:

- To develop, implement and test method to calculate the sea margin, using knowledge of the actual ship and operation.
- Compare the calculated sea margin with actual achieved sea margin on actual ships in operation, but utilizing the cooperation with ship owners in SFI Smart Maritime.

In the thesis the candidate shall present his personal contribution to the resolution of problem within the scope of the thesis work.

Theories and conclusions shall be based on mathematical derivations and/or logic reasoning identifying the various steps in the deduction.

The thesis work shall be based on the current state of knowledge in the field of study. The current state of knowledge shall be established through a thorough literature study, the results of this study shall be written into the thesis. The candidate should utilize the existing possibilities for obtaining relevant literature.



The thesis shall be organized in a rational manner to give a clear exposition of results, assessments, and conclusions. The text should be brief and to the point, with a clear language. Telegraphic language should be avoided.

The thesis shall contain the following elements: A text defining the scope, preface, list of contents, summary, main body of thesis, conclusions with recommendations for further work, list of symbols and acronyms, reference and (optional) appendices. All figures, tables and equations shall be numerated.

The supervisor may require that the candidate, in an early stage of the work, present a written plan for the completion of the work. The plan shall include a budget for the use of laboratory or other resources that will be charged to the department. Overruns shall be reported to the supervisor.

The original contribution of the candidate and material taken from other sources shall be clearly defined. Work from other sources shall be properly referenced using an acknowledged referencing system.

The thesis shall be submitted electronically (pdf) in DAIM:

- Signed by the candidate
- The text defining the scope (this text) (signed by the supervisor) included
- Computer code, input files, videos and other electronic appendages can be uploaded in a zip-file in DAIM. Any electronic appendages shall be listed in the main thesis.

The candidate will receive a printed copy of the thesis.

Supervisor : Professor Sverre Steen  
Start : 12.01.2017  
Deadline : 11.06.2017

Trondheim, 12.01.2017

Sverre Steen  
Supervisor

# Preface

This masters thesis on rational calculation of sea margin is the final work of a two year masters degree in Marine Technology at the Norwegian University of Science and Technology (NTNU) in Trondheim. The thesis has been carried out in the spring semester of 2017 and is a part of the hydrodynamics specialization.

The idea of the assignment came from the Marine Technology Institute. I choose this topic for my thesis as I found it interesting and it gave room for innovation and creativity.

A great thank you goes out to the supervisor of this thesis, Professor Sverre Steen. He has made time for guidance meetings throughout the semester and has helped me greatly in the development of the method proposed in the thesis.

I would also like to give thanks to PhD candidate Jarle A. Kramer whom has given much guidance on the understanding and creation of the route simulation. Acknowledgments also goes to SFI Smart Maritime who has provided data used in this thesis.

The reader of this thesis should preferably have a basic understanding of marine hydrodynamics.

Trondheim, 2017-06-10

*Anna Karina Magnussen*

Anna Karina Magnussen





# Summary

The sea margin is an important parameter when designing a ship. The sea margin describes how much added power is required in operational conditions compared to the calm water conditions in order to maintain a speed in environmental and deteriorative effects. Traditionally a 15% sea margin has been used, based on experience or data from similar ships.

In this thesis a method for calculating a rational sea margin has been developed and implemented. A literary study on sea margins has been performed in order to understand what progress has been made on the subject and what elements the new method should include. Parts of the method is based on elements introduced in the the literary study.

Calculation methods for the added resistance due to environmental and deteriorative effects have been reviewed in order to account for these effects in the proposed method.

A route simulation has been developed and implemented in the method. The simulation requires a route and a constant speed as input and delivers weather data for the last five years. The sea margin is calculated using this weather data, ship parameters and model test data.

The added resistance due to wind and waves are calculated using methods from the ISO 15016 standard. The effects of water temperature and density on the resistance has been evaluated. It was found that these changes represents a small difference in the overall results and were thus neglected. The deteriorative effects are represented by a fouling allowance which is assumed constant.

The method is explained in detail, with a presentation of the underlying methods and assumptions used. The method is programmed in MatLab and the thesis provides instructions on how to use it.

The proposed method was tested for a case ship in three routes using a specified constant speed. The routes defined in this thesis were from Amsterdam to New York, from Malaysia to

Brazil and from Georgetown to Cape Town. The sea margins for these routes using the proposed method were found to be 18.60%, 18.25% and 19.81%, respectively. These values are higher than the traditional 15% sea margin. Thus, a ship operating at the specified speed in these routes will have an underestimated power if the traditional sea margin is implemented.

Using measured operational data for the case ship the sea margin for the average speed was found to be 31.21%. Using the proposed method for the same route and speed gave a corresponding calculated sea margin of 20.70%. This indicates that the proposed method gives an underestimation of the required power in operational conditions for the case ship.

However, these results are slightly unreliable, as the case ship is operated at a constant power. Also, the effect of fouling on the actual ship is not known, which can contribute to a large increase in resistance and power. The fouling effect of the measured data is dependent on when the last hull cleaning was performed.

The sea margin is known to be speed dependent. The results from the proposed method using varying speeds have been evaluated. This showed that the added resistance margin and the sea margin both decrease with increasing speed.

# Sammendrag

Sjømarginen er en viktig parameter i forbindelse med skipsdesign. Sjømarginen beskriver hvor mye ekstra kraft som kreves i operasjonstilstander sammenlignet med tilstander for stille vann for å opprettholde en hastighet i vær og vind. Tradisjonelt har en 15% sjømargin blitt brukt, basert på erfaring eller data fra lignende skip.

I denne oppgaven har en metode for å beregne en rasjonell sjømargin blitt utviklet og implementert. Et litteraturstudie om sjømarginer har blitt utført for å forstå hva som har blitt gjort før innen temaet og hvilke elementer den nye metoden burde inneholde. Deler av metoden er basert på elementer som er introdusert i litteraturstudiet.

Beregningsmetoder for tilleggsmotstand på grunn av vær og begroing av skroget er vurdert for å redegjøre for disse effektene i den foreslåtte metoden.

En rutesimulering er utviklet og implementert i metoden. Simuleringen krever at en rute og en konstant hastighet er spesifisert og leverer værdata for de siste fem årene. Sjømarginen beregnes ved bruk av disse værdataene, skipsparametre og modelltestdata.

Tilleggsmotstanden som følge av vind og bølger beregnes ved bruk av metoder fra ISO 15016-standarden. Motstandsøken på grunn av endringer i vanntemperatur og tetthet har blitt evaluert. Det ble funnet at disse endringene representerer en liten forskjell i resultatene og dermed ble disse bidragene utelatt fra metoden. Et konstant begroingstillegg på motstanden er tatt med i metoden for å representere bidraget begroing vil ha.

Metoden er forklart i detalj, med en presentasjon av de underliggende metodene og antagelsene som brukes. Metoden er programmert i MatLab og oppgaven gir instruksjoner om hvordan den skal brukes.

Den foreslåtte metoden ble testet for et skip i tre ruter med en spesifisert konstant hastighet. Ruter definert i denne oppgaven er fra Amsterdam til New York, fra Malaysia til Brasil og fra

Georgetown til Cape Town. Sjømarginene for disse rutene ved anvendelse av den foreslåtte metoden ble funnet til å være henholdsvis 18.60%, 18.25% og 19.81%. Disse verdiene er høyere enn den tradisjonelle sjømarginen på 15%. Dermed vil et skip som opererer ved den angitte hastigheten i disse rutene ha en underestimert effekt hvis den tradisjonelle sjømarginen er implementert.

Ved bruk av målte operasjonsdata for skipet ble sjømarginen for gjennomsnittshastigheten funnet til å være 31.21%. Ved å bruke den foreslåtte metoden for samme rute og fart ble den tilsvarende sjømarginen beregnet til å være 20.70%. Dette indikerer at den foreslåtte metoden gir en underestimering av den nødvendige kraften i operasjonstilstanden for skipet. Disse resultatene er imidlertid litt upålitelige, da skipet drives med konstant effekt. Effekten av begroing på selve skipet er ikke kjent, noe som kan bidra til en stor økning i motstand og kraft. Effekten av begroing i de målte dataene er avhengig av når den siste skrogrenjeringen ble utført.

Sjømarginen er avhengig av hastighet. Resultatene fra den foreslåtte metoden ved bruk av varierende hastigheter er blitt evaluert. Dette viste at både tilleggs-motstandsmarginen og sjømarginen minker med økende hastighet.

# Contents

Preface . . . . .	i
Summary . . . . .	ii
Sammendrag . . . . .	v
Nomenclature . . . . .	xvi
<b>1 Introduction</b>	<b>1</b>
1.1 Background . . . . .	1
1.2 Problem Formulation . . . . .	2
1.3 Objectives . . . . .	2
1.4 Structure . . . . .	3
<b>2 The Sea Margin</b>	<b>5</b>
2.1 Definitions Used In Literature . . . . .	6
2.2 Definition Used In This Thesis . . . . .	8
2.3 Components Of The Sea Margin . . . . .	8
2.3.1 Environmental Effects . . . . .	8
2.3.2 Deteriorative Effects . . . . .	9
<b>3 Literary Study</b>	<b>13</b>
3.1 Existing Methods Of Calculating Sea Margin . . . . .	13
3.2 Service Margin Method . . . . .	13
3.3 Levine And Hawkins' Method . . . . .	14
3.4 Swift's Method . . . . .	17
3.5 Statiak's Method . . . . .	20

3.6	ITTC Method . . . . .	22
3.7	Cho, Kim And Kim's Prediction Of Sea Margin . . . . .	24
<b>4</b>	<b>Increase Of Resistance</b>	<b>27</b>
4.1	Environmental Effects On Added Resistance . . . . .	28
4.1.1	Added Resistance Due To Wind . . . . .	29
4.1.2	Added Resistance Due To Waves . . . . .	29
4.1.3	Added Resistance Due To Water Temperature And Water Density . . . . .	32
4.1.4	Effect Of Current . . . . .	33
4.2	Deteriorative Effects . . . . .	34
4.2.1	Increase Of Resistance Due To Roughness . . . . .	34
4.2.2	Increase Of Resistance Due To Fouling . . . . .	34
<b>5</b>	<b>New Method</b>	<b>37</b>
5.1	Defining The Route . . . . .	38
5.2	Weather Data . . . . .	39
5.2.1	Grib Files From ECMWF . . . . .	39
5.2.2	Time Intervals . . . . .	41
5.3	Route Simulation . . . . .	41
5.4	Resistance Increase Due To Environmental Factors . . . . .	43
5.4.1	Resistance Increase Due To Wind . . . . .	44
5.4.2	Resistance Increase Due To Waves . . . . .	46
5.4.3	Evaluation Of $R_{AS}$ . . . . .	48
5.5	Resistance Increase Due To Deteriorative Effects . . . . .	48
5.5.1	Resistance Increase Due To Roughness . . . . .	48
5.5.2	Resistance Increase Due To Fouling . . . . .	49
5.6	Powering Prediction . . . . .	49
5.7	Exclusion Of Extreme Weather Conditions . . . . .	51
5.8	The Sea Margin . . . . .	52
5.9	Validation Of Wave Resistance In ShipX . . . . .	53

<b>6</b>	<b>MatLab Code</b>	<b>55</b>
6.1	Input Parameters . . . . .	55
6.1.1	Route Simulation . . . . .	55
6.1.2	Sea Margin Calculation . . . . .	56
6.2	Route Simulation . . . . .	57
6.3	Sea Margin Calculation . . . . .	58
6.3.1	Added Resistance . . . . .	58
6.3.2	Resistance Due To Wind . . . . .	58
6.3.3	Resistance Due To Waves . . . . .	59
6.4	Powering Prediction . . . . .	59
<b>7</b>	<b>Case Ship</b>	<b>61</b>
7.1	Selection And Presentation Of The Case Ship . . . . .	61
7.2	Calculating The Sea Margin For The Measured Operational Data . . . . .	62
<b>8</b>	<b>Results</b>	<b>65</b>
8.1	Evaluation Of $R_{AS}$ . . . . .	65
8.2	Case Ship In Simulated Routes . . . . .	66
8.3	Sea Margin From Operational Data . . . . .	80
8.4	Application Of Method In Varying Speed . . . . .	81
<b>9</b>	<b>Discussion</b>	<b>83</b>
9.1	Evaluation Of $R_{AS}$ . . . . .	83
9.2	Sea Margin From Route Simulations . . . . .	84
9.3	Sea Margin From Measured Operational Data . . . . .	84
9.4	Speed Dependence Of Added Resistance And Sea Margin . . . . .	85
9.5	Proposed Method In Comparison With Existing Methods . . . . .	85
9.6	Limitations Of The Method . . . . .	86
<b>10</b>	<b>Conclusion And Further Work</b>	<b>87</b>
10.1	Summary And Conclusion . . . . .	87
10.2	Recommendations For Further Work . . . . .	89

<b>References</b>	<b>90</b>
<b>A Digital Appendix</b>	<b>95</b>
<b>B STAWAVE-2 Calculations</b>	<b>97</b>
<b>C ShipX Graph</b>	<b>101</b>
<b>D MatLab Code - Route Simulation</b>	<b>103</b>
<b>E Evaluation Of Temperature Change</b>	<b>141</b>



# List of Figures

2.1	Speed-power relationship for trial and average conditions (Swift, 1975), p.2 . . . .	6
2.2	Illustration of oil rig and supply ship in rough and icy weather (University of Stavanger, 2013) . . . . .	8
2.3	Fouling of ship propeller and hull (The Motor Ship, 2016) . . . . .	9
2.4	Hull roughness over time (Hellio and Yebra, 2009) . . . . .	11
3.1	Typical speed-power diagram in calm water (Levine and Hawkins, 1970), p. 8 . . .	15
3.2	Expression $k = \frac{R_{AV}}{R_T} = f(Fn)$ (Stasiak, 2004), p. 32 . . . . .	21
4.1	Determination of added resistance (Grin, 2015), p.183 . . . . .	27
4.2	Definition of $L_{BWL}$ , (ISO, 2015) p. 51 . . . . .	30
4.3	Parametric transfer function of mean resistance increase in regular waves, (ISO, 2015) p. 52 . . . . .	31
5.1	Example of path created in Google Earth from Amsterdam to New York . . . . .	38
5.2	Configuration of the V and U wind components given in the <i>grib</i> files. . . . .	39
5.3	Visual representation of the significant wave at an arbitrary time point. . . . .	40
5.4	Visual representation of the U component of wind at an arbitrary time point. . . .	40
5.5	The same route as shown in Figure 5.1 plotted in 2D in MatLab. . . . .	42
5.6	Definition of angles and velocities in wind resistance calculations. . . . .	44
5.7	Wind resistance coefficients for a 280 KDWT tanker with conventional bow, (ISO, 2015) p. 43 . . . . .	46
5.8	Definition of the angle of attack. . . . .	47
5.9	Full scale open water diagram for $KT/J^2$ . . . . .	49

5.10 Full scale open water diagram . . . . .	50
5.11 Mean added resistance in waves from ShipX, manipulated in MatLab . . . . .	53
7.1 The complete travel history of the case ship . . . . .	62
7.2 The ship route based on filtered data . . . . .	63
7.3 Speed power relation of the case ship based on calm water model test data and measured operational data . . . . .	64
8.1 Route from Amsterdam to New York . . . . .	66
8.2 Components of the added resistance for route crossing number 14 . . . . .	67
8.3 The operational resistance for route crossing number 14 . . . . .	68
8.4 The operational brake power for route crossing number 14 . . . . .	68
8.5 Total $P_B$ distribution for all route crossings combined, for the Amsterdam - New York route . . . . .	69
8.6 Sea margin histogram for all route crossings, for the Amsterdam - New York route .	70
8.7 Route specified for case ship . . . . .	71
8.8 Components of the added resistance for route crossing number 14 . . . . .	71
8.9 The operational resistance for route crossing number 14 . . . . .	72
8.10 The operational brake power for route crossing number 14 . . . . .	73
8.11 Total $P_B$ distribution for all route crossings combined, for the case ship specified route . . . . .	74
8.12 Sea margin histogram for all route crossings, for the case route . . . . .	75
8.13 Route from Georgetown to Cape Town . . . . .	76
8.14 Components of the added resistance for route crossing number 14 . . . . .	76
8.15 The operational resistance for route crossing number 14 . . . . .	77
8.16 The operational brake power for route crossing number 14 . . . . .	78
8.17 Total $P_B$ distribution for all route crossings combined, for the Georgetown - Cape Town route . . . . .	79
8.18 Sea margin histogram for all route crossings, for the Georgetown - Cape Town route	80
8.19 Resistance for the Amsterdam - New York route for varying speed . . . . .	81

8.20 Resistance margin and sea margin for the Amsterdam - New York route for varying speed . . . . .	82
9.1 Ocean temperatures in July and December 2016, (JPL OurOcean Portal via NASA, 2017) . . . . .	83
C.1 Coefficients for mean added resistance in waves from ShipX . . . . .	101



# List of Tables

- 5.1 The Beaufort scale (Pettersen, 2007) . . . . . 52
  
- 7.1 Presentation of the case ship . . . . . 62
  
- 8.1 Results for  $R_{AS}$  evaluation. . . . . 65
  
- 8.2 The difference between weather data simulation at a constant speed of 16 knots  
and for simulations at varying speed . . . . . 82



# Nomenclature

## Acronyms

**ISO** International Organization for Standardization

**ITTC** International Towing Tank Conference

**MCR** Maximum Continuous Rating

**PM** Pierson-Moscowitz

**SNAME** Society of Naval Architects and Marine Engineers

**ECMWF** European Centre for Medium-Range Weather Forecasts

**VLCC** Very Large Crude Carrier

## Greek

$\alpha$  Angle between the ship's heading and component waves [degrees]

$\beta$  Angle between ship heading and waves (Stasiak's method) [degrees]

$\eta_M$  Mechanical efficiency [-]

$\eta_R$  Relative rotative efficiency [-]

$\gamma$  Difference between ship heading and true wind direction [degrees]

$\omega$  Circular frequency of regular waves [ $s^{-1}$ ]

$\omega_1$  Circular frequency found from the first moment of the wave spectrum [ $s^{-1}$ ]

$\omega_2$  Circular frequency found from the second moment of the wave spectrum [ $s^{-1}$ ]

$\psi$  Ship heading [degrees]

$\psi_{WR}$  Relative wind direction [degrees]

$\psi_{WRref}$  Relative wind direction at the reference height [degrees]

$\psi_{WT}$  True wind direction [degrees]

$\rho$  Sea water density [ $kg/m^3$ ]

$\rho_A$  Mass density of air [ $kg/m^3$ ]

$\rho_S$  Water density for the actual water temperature and salt content (ISO resistance due to temperature and density) [ $kg/m^3$ ]

$\rho_S$  Sea water density [ $kg/m^3$ ]

$\rho_{S0}$  Water density for the reference water temperature and salt content (ISO resistance due to temperature and density) [ $kg/m^3$ ]

$\sigma^2$  Area under wave spectrum curve

$\zeta$  Wave amplitude [m]

$\zeta_A$  Wave amplitude [m]

$\nabla$  Displacement volume [ $m^3$ ]

## Lowercase

$g$  Gravitational acceleration [ $m/s^2$ ]

$k$  Coefficient, function of  $Fn$  [-]

$k_s$  Average roughness of hull surface [m]



$k_w$  Fixed percentage of sea margin (Service margin method) [-]

$n$  Propeller rate of rotation [revs/s]

$p(x)$  Probabilistic model of conditions defined for  $x$

$p(H_{1/3}^{(i)}, T_P^{(j)}, \alpha^{(k)})$  Probability of a wave heading  $\alpha$  with a given combination of  $H_{1/3}$  and  $T_P$

$r_{AW}(\omega, a)$  Dimensionless coefficient for increase of resistance [-]

$t$  Thrust deduction [-]

$w$  Taylor wake fraction [-]

$x$  A set of discrete random sailing conditions

## Uppercase

$A_{XV}$  The transverse projected area above the waterline including superstructures [ $m^2$ ]

$A_T$  Transverse area above waterline [ $m^2$ ]

$B$  Ship breadth [m]

$C_{AA}$  The wind resistance coefficient [-]

$C_{AA}(0)$  The wind resistance coefficient in head wind [-]

$C_B$  Block coefficient [-]

$\Delta C_F$  Roughness allowance [-]

$C_F$  Frictional resistance coefficient for the actual water temperature and water density [-]

$C_{F0}$  Frictional resistance coefficient for the reference water temperature and water density [-]

$C_{T0}$  Total resistance coefficient for reference water temperature and density [-]

$C_X$  Coefficient used to find wind resistance coefficient [-]

$D$  Propeller diameter [m]

$Fn$  Froude number [-]

$H_{1/3}$  Significant wave height [m]

$J_0$  Advance coefficient of the propeller [-]

$J_{0C}$  Advance coefficient of the propeller in calm water [-]

$K_Q$  Propeller torque coefficient [-]

$K_Q^*$  Torque coefficient found from  $J^*$  [-]

$K_{QC}$  Propeller torque coefficient in calm water [-]

$K_T$  Thrust coefficient [-]

$K_T^*$  Propeller thrust coefficient of the full scale propulsion point [-]

$L$  Waterline length of the ship [m]

$L_{OA}$  Length over all [m]

$L_{PP}$  Length between perpendiculars [m]

$L_{WL}$  Length of waterline [m]

$L_{BWL}$  Length from ship bow to 95% of maximum breadth [m]

$\Delta P$  Power increase [kW]

$\Delta P$  Power margin due to deteriorative effects (In Levine and Hawkins' method) [kW]

$P_{al}$  Power increment due to aging as a function of the life of the ship [kW]

$P_B$  Brake power [kW]

$P_{Bcalm}$  Calm water brake power [kW]

$P_D$  Delivered power [kW]

$P_{DS}$  Shaft power [kW]

$P_{DSC}$  Shaft power in calm water [kW]

$P_{hpr}$  Power increment due to deteriorative effects during a maintenance cycle for the hull-propeller interactions [kW]

$P_{hr}$  Power increment due to deteriorative effects during a maintenance cycle for the hull [kW]

$PM$  Power margin [%]

$P_{mr}$  Power increment due to deteriorative effects and plant operation inefficiencies during a maintenance cycle for the machinery [kW]

$P_{nr}$  Power increment due to various hull, propeller and machinery factors as a function of maintenance or repair cycle [kW]

$P_O$  Power increment due to plant operation inefficiencies [kW]

$P_{pr}$  Power increment due to deteriorative effects during a maintenance cycle for the propeller [kW]

$P_T$  Calm water horsepower (Service margin method) [%]

$P_{TS}$  Total horsepower (Service margin method) [PS]

$\Delta R$  Total increase of resistance [N]

$R_{AA}$  The increase of resistance due to wind [N]

$R_{AS}$  Increase of resistance due to deviation of water temperature and water density [N]

$R_{AV}$  Long term added resistance in waves [N]

$R_{AW}$  Added resistance on the ship in waves [N]

$R_{AW}$  Mean increase of resistance in short crested irregular waves (In Stasiak's method) [N]

$R_{AW}(x)$  Short term added resistance in waves [N]

$R_{AWL}$  Mean resistance in long crested irregular waves (STAWAVE-1) [N]

$R_{AWL}$  Mean increase of resistance in short crested irregular waves (STAWAVE-2) [N]

$R_{AWML}$  Motion induced resistance (STAWAVE-2) [N]

$R_{AWRL}$  Mean resistance increase due to wave reflection (STAWAVE-2) [N]

$Re$  Reynolds number [-]

$R_F$  Resistance due to friction for the actual water temperature and water density [N]

$R_{FO}$  Resistance increase due to fouling [N]

$RPM$  Rate of revolutions [revs/s]

$R_T$  Mean still water resistance [N]

$R_{T0}$  Ship resistance in calm water [N]

$R_{T0}$  Total resistance for the reference water temperature and water density (In ISO) [N]

$R_{Tcalm}$  Calm water resistance [N]

$R_{TS}$  Calm water resistance [N]

$R_{wave}$  Mean increase of resistance in regular waves [N]

$S$  Wetted surface area [ $m^2$ ]

$S(\omega, b, c)$  Spectral density function model of stationary irregular waves [ $m^2 s$ ]

$S_\eta$  Frequency spectrum [ $m^2 s$ ]

$SM$  Sea margin [%]

$T$  Wave period [s]

$T_{01}$  Mean wave period [s]

$T_1$  Characteristic period [s]

$T_M$  Draft at mid-ship [m]

$T_P$  Spectrum peak period [s]

$\Delta V$  Speed margin due to environmental effects [knots]

$V$  Ship speed [m/s]

$V_{DES}$  Design speed [knots]

$V_G$  Measured speed of the ship over ground [m/s]

$V_{LTA}$  Long term average speed [knots]

$V_S$  Speed of the ship through the water [m/s]

$V_{WR}$  Relative wind velocity [m/s]

$V_{WRref}$  The relative wind velocity at the reference height [m/s]

$V_{WT}$  True wind velocity [m/s]

$V_{WTref}$  The true wind velocity at the reference height [m/s]

$Z_a$  Vertical position of the anemometer [m]

$Z_{ref}$  Reference height for the wind resistance coefficient [m]

# Chapter 1

## Introduction

### 1.1 Background

The speed-power performance is important when designing a ship. It defines how much power is required to obtain a certain speed. Speed-power requirements are often specified in the contract for the ship design. This relationship is usually predicted for idealized conditions, with no wind, calm seas and a clean hull. In operating conditions the ship will experience an increase in resistance due to environmental effects, like wind and waves, and deteriorative effects like fouling and corrosion. To account for this increase the designer usually adds a percentage on the required power, expressed as a sea margin. A typical value for the sea margin is 15%.

The value of the sea margin is often determined based on tradition or practical experience, and is thus not dependent on ship parameters, condition of the ship or operational profile. This can lead to an over or under estimation of the resistance of the ship, which is not desirable in regards to fuel consumption and therefore operating cost.

The added resistance due to waves and wind will be dependent on the speed of the vessel. It is known that slow ships generally have a larger added resistance than fast ships and that for a given vessel the added resistance increases as the speed decreases. The operational area and the size of the ship might also influence the added resistance.

It is desirable to develop a new method for calculating the sea margin, which takes actual parameters into account. These parameters include the ship particulars, condition and operational profile.

A literary study was performed in the autumn of 2016 as a project thesis identifying what progress has been made on the subject. This was done in order to better understand the problems related to the calculation of sea margin.

## 1.2 Problem Formulation

In this thesis a complete method for calculating the sea margin shall be proposed, developed and tested. The method is to take operational profile into account, as well as ship particulars, environmental and deteriorative factors.

After the method is developed, it is to be tested for a case ship. The results from the method shall then be compared to the actual sea margin from a ship in operation.

## 1.3 Objectives

The main objectives of this master thesis:

1. Define the sea margin and identify its components.
2. Perform a literary study on methods of calculating the sea margin and other operational margins.
3. Investigate the increase in resistance by reviewing methods of calculating the effect of environmental and deteriorative components.
4. Develop a method for calculating the sea margin based on the following parameters:
  - Ship route.
  - Actual weather data for the route.
  - Added resistance due to wind and waves.
  - Added resistance due to fouling.
  - Ship parameters and model test data.
5. Implement the method for a case ship and review the results.

## 1.4 Structure

This paper consists of 10 chapters. A large part of Chapters 2-4 are a part of the 2016 project thesis on the subject.

In Chapter 2 the different definitions of the sea margin is reviewed, emphasizing the definition which is to be used in this paper. Components of the sea margin are reviewed.

In Chapter 3 the different methods and approaches for calculating the sea margin published over the years are reviewed.

Chapter 4 is a study of the different components which affects the increase in resistance and a review of how to calculate them.

Chapter 5 presents the new method of calculating the sea margin, with detailed instructions on how to use it.

Chapter 6 gives a presentation on how the MatLab code for the method is structured.

Chapter 7 presents the case ship the method is to be tested for and calculations of the measured operational sea margin.

Chapter 8 contains the results of the method for the case ship, as well as comparison to the measured operational data of the ship.

In Chapter 9 the results are discussed, as well as limitations of the method and comparisons between the proposed method and methods studied in the literary study.

In Chapter 10 the conclusion of the thesis and recommended further work is presented.





# Chapter 2

## The Sea Margin

When designing a ship it is important that the correct propulsion system is determined for the ship to attain the correct speed in operational conditions. To verify this, a sea trial is conducted in ideal conditions and with a clean hull to find the ship's performance in terms of power, speed and propeller shaft speed under prescribed ship conditions (ISO, 2015).

The ideal condition is defined as no wind, no waves, no current and in deep water of 15°C (ISO, 2015). However, the results attained from sea trials will not represent the normal operational conditions of a ship. In operational conditions the ship will experience an increase in resistance due to environmental effects like wind and waves, and an increase due to deteriorative effects like fouling and corrosion. To obtain the performance of the ship in operational conditions, the sea margin is introduced.

The sea margin accounts for the environmental and deteriorative effects by making a correction between the calm water trial power and the average service condition power. Figure 2.1 shows the difference in the speed-power relationship for sea trial conditions and for the ship in operational conditions. If this difference is not taken into account, the power will be underestimated which will lead to ships being designed for the wrong average service condition and thus an economic loss. If the sea margin is too low, reliability with respect to arrival time will also be low, and the safety might be at risk (Grin, 2015).

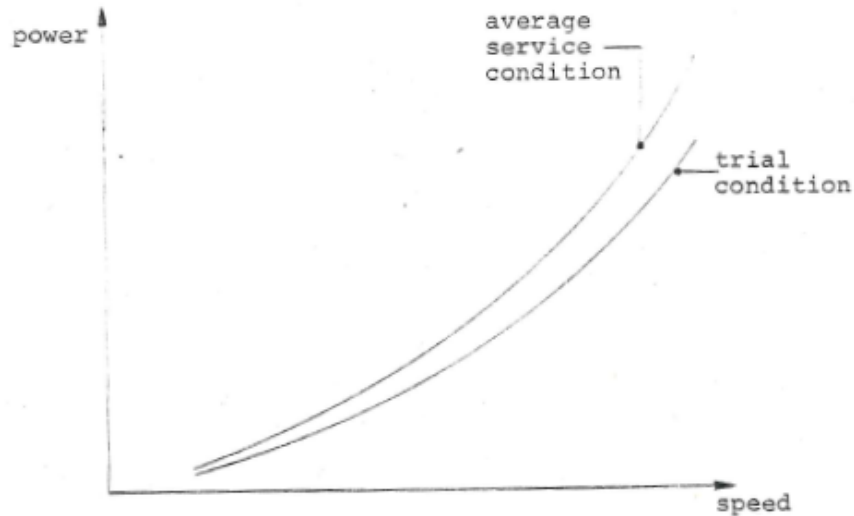


Figure 2.1: Speed-power relationship for trial and average conditions (Swift, 1975), p.2

## 2.1 Definitions Used In Literature

There has been many overlaying definitions of different operational margins over the years. The main definition of the sea margin has in large parts remained the same, but under different names. In earlier literature the margin is often referred to as a service margin, but is defined in the same way as the more modern sea margin.

Levine and Hawkins (1970) defines the service margin as a performance margin provided to enable a ship to move between two or more points within a time period. This implies that the ship is able to achieve a certain average speed over this time period. It is measured in relation to a specified trial condition in a new, clean ship in standard sea water with no wind and a calm sea.

Swift (1975) defines the service margin as an allowance for the differences in the power requirements of a ship in its trial condition and in its average service condition. The service margin is considered to be composed of two parts. The first part is an environmental margin to take factors like wind, current, sea state, water temperature, ice and fog into account. The second is a deteriorative margin to account for the effects of fouling and corrosion of hull, propeller and machinery system, as well as machinery wear and erosion of propeller and machinery system.

Arribas (2007) defines a sea margin or a weather margin as an allowance to take environmental effects on the behavior of the ship into account. The allowance is added to the calm water

resistance, which is used as a first estimation of the required power of a ship. The calm water resistance is found without considering the behavior of the sea in which the ship will operate. Arribas mentions typical sea margin values at 15-30% of the calm water power for the ship.

ITTC (2008*b*) defines the sea margin, or powering margin, as the margin which should be added to the speed-power relationship estimation for a newly built ship in ideal weather conditions to estimate ship operations in realistic conditions. Environmental effects such as wind and waves on the route, shallow water, steering effects and air- and water temperature based either on experience or on statistical values should be taken into account in the powering margin. Additionally, the effects of fouling and aging of the hull and propeller surface should also be taken into account.

The value of this margin if no model tests or reliable performance data for the ship under trial runs are available should be taken as 15 to 25% on the specified MCR power for the sea margin. This value will then consider environmental, operational and aging effects.

Molland et al. (2011) recognizes the service power margin which must be added to the basic clean hull calm water power to maintain speed in service. By adding this margin, the total installed propulsive power can be estimated. He assumes a margin for roughness and fouling, which typically would be 10% if the hull was to be cleaned with two year intervals. A weather margin for wind and wave effects is assumed, which will vary dependently of where the ship is to operate. The weather margin will typically have a value of 10-30%. A total service power margin can be approximated as a sum of the margins mentioned above. With the examples of roughness and fouling margin of 10% and a weather margin of 15% the total margin will be 25%.

Cho et al. (2016) defines the power margin as the additional power needed to maintain a certain speed in the actual sea area divided by the actual total power calculated in real sea.

#### **Comments on the definitions of sea margin**

Many of these definitions are in principle the same, although some are described with more detail. Some of the methods have specified that the sea margin can be divided into environmental and deteriorative effects, while some have not. This is an important detail, which will be included in the definition used in this paper.

## 2.2 Definition Used In This Thesis

The definition of the sea margin which will be used in this thesis is as follows:

**Sea margin:** *The margin which should be added to the calm water performance in order to account for environmental and deteriorative effects in normal operational condition.*

This definition accounts for the resistance increase due to environmental effects such as wind, sea state, fog, sea water temperature and ice. It also accounts for the resistance increase due to deteriorative effects such as hull and propeller corrosion and erosion. Normal operation is specified, as the sea margin should not account for extreme weather.

## 2.3 Components Of The Sea Margin

### 2.3.1 Environmental Effects

The sea margin will in large part be dependent of the environment which the ship operates in.

The environmental components can be defined as involuntary (Levine and Hawkins, 1970). This means that the ship operator can not do anything about the effect these components have on the ship. These components are in some cases defined as a speed margin, as they are changeable in nature and by increasing the speed in good weather the time lost under adverse conditions can be made up for.

The environmental factors include wind, fog, sea water temperature, ice and currents and waves.



Figure 2.2: Illustration of oil rig and supply ship in rough and icy weather (University of Stavanger, 2013)

## Wind, Waves, Current And Sea Water Temperature

The effects of wind, waves, current, sea water temperature and density will have an impact on the increase of resistance in operational condition and will be examined more closely in Chapter 4.

## Fog And Ice

The effects of fog and ice will not be considered in this paper. Fog will not directly influence the increased resistance of the ship but can cause a voluntary speed reduction by the ship operator.

Ice will directly influence the increased resistance of the ship, but the effects of this will not be considered in this paper. It is assumed that the ships considered will not be operating in areas where it is typical to encounter ice.

### 2.3.2 Deteriorative Effects

The deteriorative effects are voluntary (Levine and Hawkins, 1970). This means that the ship operator can to some degree influence how much these effects will influence the operation by changing the ship maintenance schedule. These effects are in some cases defined as an added power requirement, as they act more or less consistently once they have developed and must be overcome by a power increase to operate at a specified ship speed.

The deteriorative effects include hull fouling and corrosion, propeller corrosion, erosion and fouling, as well as machinery corrosion, erosion and fouling (Levine and Hawkins, 1970). Fouling is marine growth, like barnacles and sea weed, attaching to the hull (Steen and Minsaas, 2013). Figure 2.3 shows a ship with fouling of the hull and propeller.



Figure 2.3: Fouling of ship propeller and hull (The Motor Ship, 2016)

## Fouling And Corrosion

The texture of a ship hull is a continuously changing parameter, which has a large effect on the performance of a ship (Carlton, 2012). A large part of the ship's power is needed to overcome the viscous friction between the water and the hull (Swain et al., 2007). The hull roughness effect can be considered as an addition to the viscous friction of the hull (Carlton, 2012). The hull surface roughness can be considered to contain permanent roughness due to unevenness in the steel plates and temporary roughness due to marine growth (Carlton, 2012).

A typical ship hull has an anti-fouling coating which gives off a poison from the surface (Steen and Minsaas, 2013). The poison protects against marine growth, but will gradually wash away until no effect will be present (Steen and Minsaas, 2013). If anti-fouling provision has not been provided, the effect of fouling can under the right circumstances relatively quickly cause an increase of 30-40% in fuel consumption (Carlton, 2012).

Roughening of the propeller is caused by fouling, corrosion and erosion, which leads to an decrease in propeller efficiency (Swift, 1975). Deterioration of the machinery system leads to reduction of the power output (Swift, 1975).

The Figure 2.4 shows how the hull roughness increases over the age of the ship. The effect of hull roughness is initially rapid, but tails off parabolically. From the figure it is seen that after four years the hull roughness for the average hull will cause an increase in power to maintain speed of approximately 30 % and have a hull roughness of approximately 400  $\mu m$ .

The rate of fouling is generally a function of the anti-fouling paint quality, time spent in port and which ports are visited (Swift, 1975). The speed is also an important factor. The best conditions for fouling is when the ship is either in port or moving at slow speeds, typically less than 2 knots (Swift, 1975). For higher speeds it will be harder for the marine growth to connect to the hull surface. Other influences to fouling include seawater temperature, time at sea, season, fouling pressure, ballast and freeboard (Swain et al., 2007).

The rate of corrosion of the plating is a function of the cathodic protection and the anti-corrosion coating (Swift, 1975). The effects of fouling is apparently completely recoverable, while the effects of corrosion is almost completely recoverable, upon dry docking and sand-blasting (Swift, 1975).

The propeller will be prone to less fouling, as the movement of the propeller makes it harder

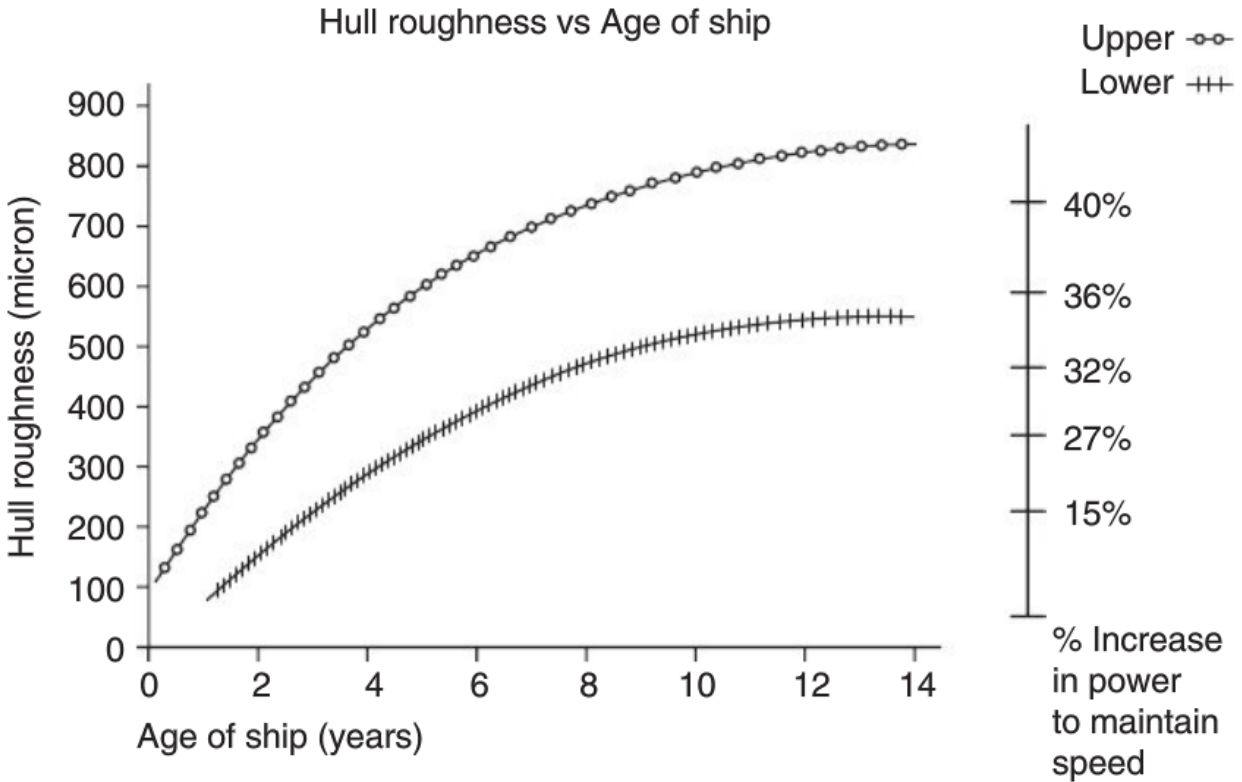


Figure 2.4: Hull roughness over time (Hellio and Yebra, 2009)

for marine growth to attach. However, there will be corrosion and erosion effects, the latter having the possibility of causing severe effects if cavitation is present as well (Swift, 1975).

Through a dialog with a representative for a shipping company, the usage of the sea margin in operational conditions was discussed. With a daily monitoring of ship data in operational conditions the power of the ship is found. This is then corrected for wind and waves. The resulting sea margin is used in order to evaluate the fouling of the ship. If the fouling is at a degree which is unacceptable, the ship must have a hull cleaning performed. This shows that in operational conditions the effects of fouling is very important and is monitored closely.





# Chapter 3

## Literary Study

A literary study on sea margin was performed in the autumn of 2016 by the author, as a part of a project thesis on the same subject.

### 3.1 Existing Methods Of Calculating Sea Margin

As previously mentioned, a fixed sea margin of 15-25 % is often used when designing ships. However, the possibility of a more rational calculation method of sea margin has been explored over the last decades.

In all of the sections below the only reference used for each section is the author(s) which published the method. The author(s) are specified in the first line of each section. Comments on the methods are not from the references unless specifically specified.

### 3.2 Service Margin Method

Up to the 1960s the service margin method was applied in most cases (Stasiak, 2004). This was a justified practical design approach to a problem which had not been thoroughly investigated or modeled yet. The problem is complex and important, and at the time this approach was the only practical solution available.

The method is quite simple to perform, using the resistance or horsepower related to the calm water conditions.

$$R_{TS}(V_E) = (1 + k_W) \cdot R_T(V_E) \quad (3.1)$$

or

$$P_{TS}(V_E) = (1 + k_W) \cdot P_T(V_E) \quad (3.2)$$

Here  $k_W \in (0.15; 0.35)$ , is the fixed percentage of service margin which the designer chooses based on experience.  $k_W$  is a resistance or horsepower coefficient which is dimensionless.  $V_E$  is the speed for which the calm water resistance  $R_T(V_E)$  or horsepower  $P_T(V_E)$  is based on.

### Comments On The Method

Of all the available methods for calculating the sea margin, this method is the simplest one. This is logical, as it is the oldest of the methods. It is also interesting to note that it is very similar to the method referred to in the assignment as the one still used today, but with a wider range for  $k_W$ .

This method does not take any specific components into account when deciding the value of the sea margin, but assumes that the value accounts for all effects influencing the ship. The value is to be within the interval 15% to 35% and chosen by the ship designer based on tradition or data from similar ships operating on the same route (Arribas, 2007). It stands to reason that this percentage will in most cases be inaccurate leading to vessels having either an over- or underestimated operational power. Overestimated vessels would then have an economically beneficial design, as it can handle more than it was calculated for. However, the underestimated vessel can experience conditions it was not designed for and thus not be able to perform as contracted.

### 3.3 Levine And Hawkins' Method

A technical report was published in the Society of Naval Architects and Marine Engineers (SNAME) titled "Comments on the service margins for ships" by Levine and Hawkins (1970). This paper recognizes that the methods used up to that point had been simplified to the point where the validity of the methods should be questioned. The authors define that the service margin should

be based on both environmental and deteriorative factors.

The paper states that to determine the service margin, decisions has to be made regarding the fundamental aspects of the proposed operation. These are decisions regarding the ship route, the long term average speed, the time period over which speed is averaged, the age of the test ship at which average speed is required and the ship displacement for normal operation during this time.

The operational profile should include details on the route which the ship is to follow with specifications of speed restrictions on parts of the route, if they are present. The environmental effects has to be taken into account, and should be presented as the occurrence of wind, sea state, ice and fog, combined with the time interval of each occurrence during the operational route.

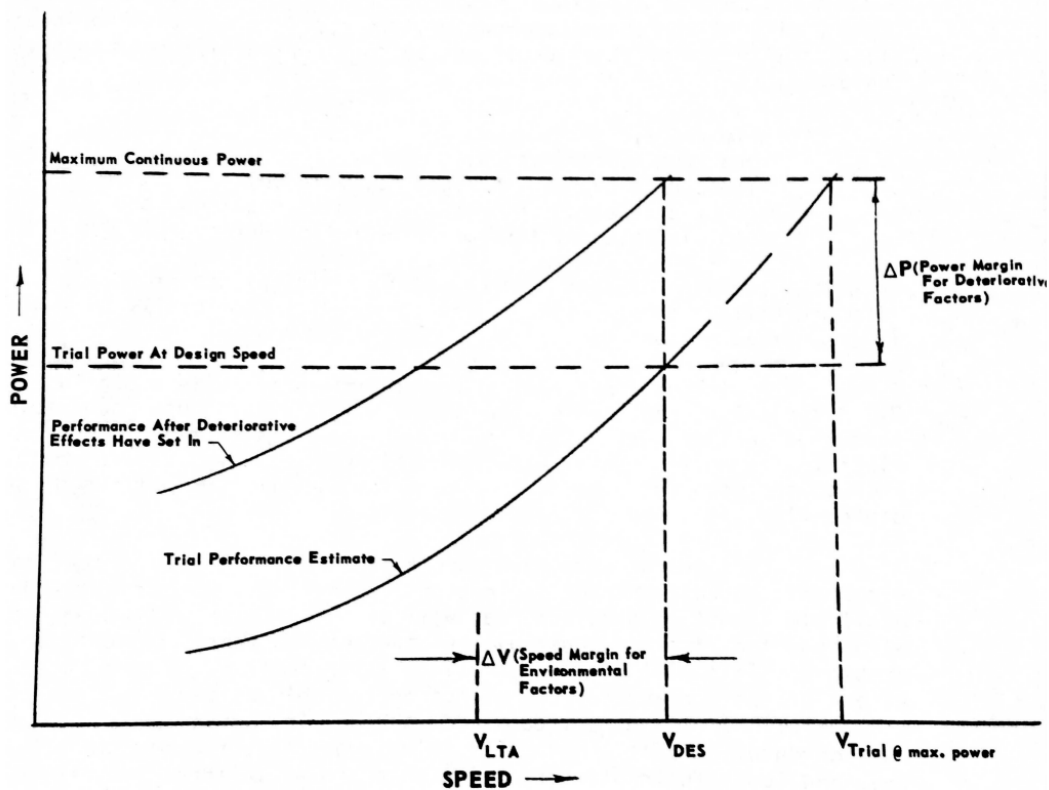


Figure 3.1: Typical speed-power diagram in calm water (Levine and Hawkins, 1970), p. 8

Figure 3.1 shows two curves; the trial performance estimate and the performance after deteriorative effects have set in and are at their maximum with regards to degradation of performance. The long term average speed is denoted as  $V_{LTA}$ , which is the required speed for oper-

ation. This is not the speed at which the ship will operate continuously, but the average speed resulting from various operational conditions and speeds over various time.

The design speed for the vessel is denoted  $V_{DES}$ , which is the calm water speed for which the hull should be optimized for. A ship must be able to achieve  $V_{DES}$  in calm weather with deteriorative effects specified in the maintenance scheduling.

As seen in Figure 3.1 the difference between  $V_{LTA}$  and  $V_{DES}$  is defined as the speed margin for environmental effects  $\Delta V$ . The margin makes sure the ship can maintain performance in the expected environmental conditions.

Likewise, the difference between trial power at design speed and the maximum continuous power is defined as the power margin for deteriorative effects  $\Delta P$ . The margin makes sure the ship can maintain performance as the deteriorative effects sets in and the ship ages.

The paper gives a detailed proposed method of calculating  $V_{LTA}$  and  $V_{DES}$  which in turn can be used to find the speed margin.

The paper states an ideal expression of the power margin needed to overcome the deteriorative effects as

$$\Delta P = (P_{al} + P_O) + \sum P_{nr} \quad (3.3)$$

where  $\Delta P$  is the power increment due to deterioration,  $P_{al}$  is the power increment due to aging as a function of the life of the ship and  $P_O$  is the power increment due to plant operation inefficiencies.  $P_{nr}$  is the the power increment due to the various hull, propeller and machinery factors as a function of maintenance or repair cycle. Each value of  $n$  signifies a different factor, i.e.  $P_{1r}$  is hull fouling,  $P_{2r}$  is hull corrosion, etc. This power increment  $\Delta P$  is a function of hull and propeller fouling, corrosion and erosion, as well as machinery plant fouling, corrosion, erosion, wear and operation. Equation 3.3 considers all of its components as a part of the deterioration over a given time period.

As measurements of the deterioration at a given time was difficult to obtain in 1970, the expression was deemed too complex, and therefore simplified as seen in Equation 3.4 to avoid large uncertainties.

$$\Delta P = P_{al} + P_{hr} + P_{pr} + P_{hpr} + P_{mr} \quad (3.4)$$

Here  $\Delta P$  and  $P_{al}$  are defined as for Equation 3.3.  $P_{hr}$ ,  $P_{pr}$  and  $P_{hpr}$  are defined as the power increment due to deteriorative effects during a maintenance cycle for the hull, propeller and hull-propeller interactions effects, respectively.  $P_{mr}$  is the power increment due to all machinery deteriorative effects as well as plant operation inefficiencies during a maintenance cycle.

The paper argues that even though some of the parameters involved are hard to find with the then current technologies, this approach will still be more accurate than the service margin method which has an arbitrary factor which is not design or operational dependent.

### Comments On The Method

This approach is in many ways more rational than the service margin method, as it takes actual design and operational parameters into account. The authors acknowledges that there is certainly uncertainty paired with the method, but with the available technology of that time, this is to be expected. This method includes many of the parameters which needs to be evaluated in a rational approach to calculate the sea margin, but at the time it was presented it could not be implemented due to limited technology.

## 3.4 Swift's Method

Swift (1975) published a paper called "An approach to the rational selection of the power service margin". This paper suggests an effective power service margin to be used more realistically by a designer employing the conventional approach to ship design. He defines this margin as the margin of the power installed to attain the expected speed in service over that required to power the ship at the same speed in the trial condition.

The conventional service margin method does not consider the stochastic nature of ship speed in operation. Swift's approach takes the random nature of the ship's speed in service particularly into consideration.

To do this, Swift suggests a decision model for which the speed is developed, which serves as the basis for the expected speed. The decision model presented is a simplification of the problem. In 1975 there were not sufficient data or modeling procedures to account for a idealistic decision model. An idealistic model would include all the environmental and deteriorative ef-

fects the ship would encounter over its lifetime, and calculate a speed based on this, which in turn would be used to in calculations of the measure of merit. The measure of merit, or the merit factor is an economical measurement.

In this model it is assumed that the ship is on a pre-specified course, where the percentage of time spent in each area of the route with a specific heading is known. Additionally the sea state frequency of occurrence which the ship will encounter is calculated from seaway data statistics.

From these sea states the added drag, and hence the speed, of the ship is calculated from seakeeping tables. These seakeeping tables are also used to find the ship motions for each sea state and quantitative values of the voluntary speed reduction are determined. The speed found in each sea state is then combined with the probability of the relative frequency of that sea state to find the expected speed for the ship in operation.

The approach of finding the sea margin proposed by Swift is a modification of the conventional approach to preliminary ship design using a power service margin. This approach consists of six steps as described below. This description does not include all the information given in the paper, for all details see Swift (1975).

- **Step 1:** Reading of user input.

Here one considers the particulars given in the design. The ship particulars include length, beam, draft, depth, etc. The route particulars include the round trip distance and the percentage of total time spent in each area of the route with a specific heading.

- **Step 2:** Calculation of ship weights and costs.

By using design relationships involving the principal characteristics of the ship, the machinery type and the installed horsepower, the ship costs and weights are calculated.

- **Step 3:** Calculation of the frequency of occurrence of each sea state.

By using sea state statistics and the route input data, the frequency of occurrence of each sea state is calculated for the particular route.

- **Step 4:** Calculation of the expected speed in service.

Using all of the installed horsepower, the calm water speed is determined using the powering standard series for each year in service with arguments for hull deteriorative effects.

At this calm water speed the added resistance is found by interpolation of seakeeping tables for each sea state, which leads to calculation of the speed of this sea way. Motion constraints are to be evaluated at each seastate. If the constraints are violated, the speed is to be reduced until the constraints are satisfied. By combining the frequency of occurrence of each sea state and the speed of the ship in that sea state, the expected speed of the ship over its lifetime is found.

- **Step 5:** Calculation of the annual operation costs and the transportation capacity.

The annual operating cost is found using the port time, service days and route data, as well as the ship characteristics, the installed horsepower and the expected speed in service. By using the payload found in step 2 and the number of round trips per year, the annual transport capacity is found.

- **Step 6:** Evaluation of the measure of merit.

The measure of merit is evaluated using the economic input data, the operating costs, the calculated initial investment and the transport capacity.

Both the long- and short-term deteriorative effects experienced by the ship in service are taken into account in the power service margin.

Swifts effective powering margin is defined in Equation 3.5.

$$\left[ \frac{\text{Installed horsepower}}{\text{Calm water horsepower for mean service speed}} - 1 \right] \cdot 100 \quad (3.5)$$

By using his method on two sample studies; a tanker and a container ship, Swift found the effective power service margin to be 11% and 18%, respectively.

### Comments On The Method

This approach to a rational power service margin is more of a specification on how to estimate the calm water horsepower for mean service speed. The formulation provided for the effective power service margin is not a new formulation, but based on more exact parameters than earlier.

This paper considers economical factors in a larger degree than the ones studies earlier in this chapter. The economical aspect of the problem is not considered in this thesis.



### 3.5 Stasiak's Method

Stasiak (2004) published a paper on sea margin where he acknowledges that there are many difficulties involved in creating more accurate values of the sea margin. These difficulties can be found both in the lack of interest for the problem to be solved as well as in the solution itself. Stasiak specifies that he believes the service margin method will be in use for some time in the future, but that it should be continuously updated according as new technology is developed. This way the  $k_W$  coefficients will have a higher degree of accuracy and be based on ship parameters.

Stasiak presents a wave service margin coefficient model in order to contribute to a rationalization of the determination of real ship resistance and horsepower. This wave service margin coefficient is a part of the service margin coefficient used in the service margin method.

In Stasiak's paper he outlines a method for calculating the long-term prognosis of the increased resistance of a ship moving in head waves, i.e. at  $\beta = 180^\circ$ . By doing this one can make use of the seakeeping ability methods, consisting of a generalization of the long-term prognosis of the additional ship resistance in waves,  $R_{AV}$ .

The increase of resistance is determined as a probabilistic estimation of a mean value of a set of random short-term additional resistance  $R_{AW}(x)$  prognosis for a ship moving with constant speed  $V$ .

$$R_{AV} = \sum R_{AW}(x) \cdot p(x) \quad (3.6)$$

In Equation 3.6  $x$  is a set of discrete random sailing conditions, each with resistance increase values determined as a short-term prognosis.  $x = \{a, b, c\}$  where the elements defined in the set are ship loading conditions, sailing regions and sea states with wave condition characteristics, respectively.

$p(x) = p(a) \cdot p(b) \cdot p(c|b_1)$ , which is a probabilistic model of the conditions defined for  $x$  or a combined probability function of  $a$ ,  $b$  and  $c$  which are discrete random variables.

The short-term prognosis of resistance increase  $R_{AW}(x)$  is determined in accordance with the superposition principle.

$$R_{AW}(x) = 2 \int_{\omega} r_{AW}(\omega, a) \cdot S(\omega, b, c) \cdot d\omega \quad (3.7)$$

In Equation 3.7,  $r_{AW}(\omega, a)$  is the dimensionless coefficient for increase of resistance determined from ship model tests in head sea for waves of different frequencies.  $S(\omega, b, c)$  is a spectral density function model of stationary irregular waves. The form of this model is specific to the sea region  $b$  in which the vessel is to operate, as well as sea state characteristics  $c = c(H_{1/3}, T_1)$ . Here  $H_{1/3}$  is the significant wave height and  $T_1$  is the characteristic period.

The paper calculates the increased resistance  $R_{AV}$  for three vessels; a tanker, a container carrier and a ro-ro ship. The Froude numbers for each ship are calculated normally. From this a coefficient function  $k$  is defined as a function of the Froude number, as shown in Figure 3.2.

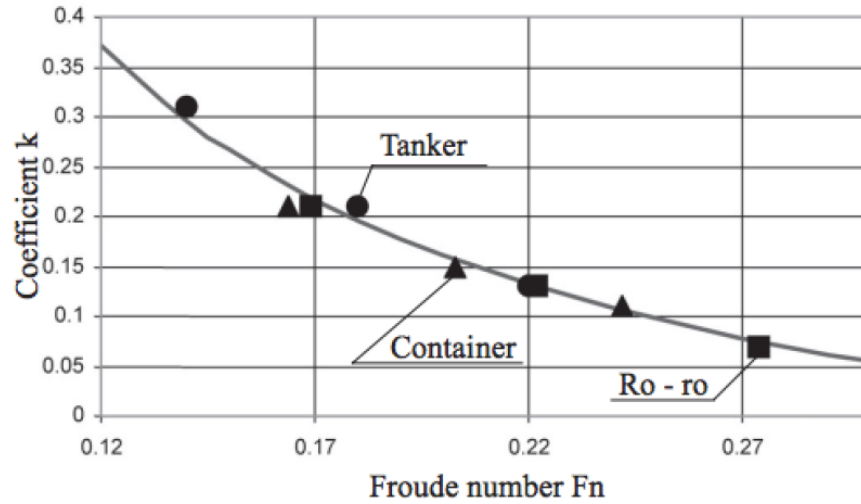


Figure 3.2: Expression  $k = \frac{R_{AV}}{R_T} = f(Fn)$  (Stasiak, 2004), p. 32

The points in Figure 3.2 are calculated from the equation in the figure text, and the full line of the graph in the figure is found from Equation 3.8.

$$k = \frac{R_{AV}}{R_T} = \frac{0.0635}{Fn} - 0.157 \quad (3.8)$$

In Equation 3.8  $F_n$  is in the interval between 0.12 and 0.30 and  $R_T$  is the mean still water resistance.

The coefficient  $k$  is a part of  $k_W$ , which is defined in the same way as under Chapter 3.2.  $k$  is the wave service margin representing the increase of resistance or power due to waves.

## Comments On The Method

This method was only predicted for the head sea condition, i.e. for a  $\beta$  of  $180^\circ$ . This is the most extreme condition with respect to resistance increase, so the results should be taken as an upper estimation.

This method takes only the wave part of the problem into account. The method does not take the change of course into account, which is needed in a complete model. The model does not take deteriorative effects or the effects of the other environmental components than waves into account.

As this method is meant to improve the service margin method by defining a wave service margin, these limitations are to be expected. Thus, Stasiak presents a solution to a part of the problem but not a complete solution.

## 3.6 ITTC Method

ITTC (2008*b*) have published recommended procedures and guidelines for predicting powering margins.

The thrust and torque coefficients,  $K_T$  and  $K_Q$ , are corrected for changes in the submergence of the propeller caused by ship motions and waves.

The added power in a regular waves has to be calculated. To do this the full scale propulsion point is found from Equation 3.9.

$$K_T^* = \frac{R_{T0} + R_{AW}}{\rho n^2 D^4 (1 - t)} \equiv const \cdot J_0^2 \quad (3.9)$$

where  $K_T^*$  is the propeller thrust coefficient of the full scale propulsion point, where the effects of thrust loss and added resistance are included.  $\rho$  is the water density,  $n$  is the propeller rate of rotation,  $D$  is the propeller diameter and  $t$  is the thrust deduction.  $R_{T0}$  is the ship resistance in calm water and  $R_{AW}$  is the added resistance on the ship in waves. In  $R_{AW}$  the effects of wind and wave resistance and increase of resistance caused by fouling and roughness increase should be included. Thus the total resistance is considered.

The relative propulsion power increase of the ship is found from Equation 3.10.

$$\frac{P_{DS}}{P_{DSC}} = \frac{K_Q}{K_{QC}} \left( \frac{J_{0C}}{J_0} \right)^3 = \frac{K_Q}{K_{QC}} (1 - w)^3 \quad (3.10)$$

where  $P_{DS}$  is the shaft power,  $K_Q$  is the propeller torque coefficient,  $J_0$  is the advance coefficient of the propeller and  $w$  is the Taylor wake fraction. Subscript  $C$  means "for calm water" for all the parameters.

When calculating the sea margin according to this method, several assumptions has been made. The waves are long crested and consistent with a narrow banded process. Due to these assumptions the wave record can be cut into successive regular wave parts, each with a circular frequency  $\omega$  and an amplitude  $\zeta$ . Then the probability density function can be calculated for these parameters. The probability density function will depend on the area under the wave spectrum curve,  $\sigma^2$  which is related to the significant wave height through the formula  $\sigma^2 = H_{1/3}^2/16$ . Other parameters the function will depend on are the circular frequencies,  $\omega_1$  and  $\omega_2$ , defined by the first moment and second moment of the wave spectrum. Assuming a Pierson-Moscowitz (PM) spectrum these moments are calculated using equations dependent on the spectrum peak period  $T_P$ .

For a given sea state the power increase and heading is found from Equation 3.11.

$$\frac{P_{DS}}{P_{DSC}} = \int_0^\infty d\zeta \int_{-\infty}^\infty d\omega \cdot f(\zeta, \omega) \frac{K_Q}{K_{QC}} (1 - w)^3 \quad (3.11)$$

This method utilizes a scatter diagram to find the probability  $p$  of each combination of  $H_{W1/3}$ ,  $T_P$  and heading. All of these parameters are needed to calculate the power increase in a particular route or set of routes. In addition to the scatter diagram, a calculation of the relative time period spent in the domain of each scatter diagram is needed.

When all of the above steps are followed, the powering margin (PM) can be calculated from Equation 3.12.

$$PM = \left( \sum_i \sum_j \sum_k p(H_{1/3}^{(i)}, T_P^{(j)}, \alpha^{(k)}) \cdot \int_0^\infty \int_{-\infty}^\infty f(\zeta, \omega) \cdot \frac{K_Q}{K_{QC}} \cdot (1 - w)^3 d\omega d\zeta - 1 \right) \cdot 100\% \quad (3.12)$$

In Equation 3.12,  $p(H_{1/3}^{(i)}, T_P^{(j)}, \alpha^{(k)})$  is defined as the probability of a wave heading  $\alpha$  with a given combination of  $H_{1/3}$  and  $T_P$ . The summation of these over  $i$ ,  $j$  and  $k$  will be 1 as shown in Equation 3.13.

$$\sum_i \sum_j \sum_k p(H_{1/3}^{(i)}, T_P^{(j)}, \alpha^{(k)}) = 1 \quad (3.13)$$

To find the definition of the operation, the area of operation and the time spent in a given area, one should consult the ship operator and the client the ship is to be designed for.

In the occurrence of having no model test or reliable data available, the sea margin is defined to be in the interval of 15-25% on the specified MCR power. This value of the sea margin will include the effects of operation, environment and aging.

### Comments On The Method

This method is the most specific in terms of formulations in comparison with the previously studied methods. This is probably because it was published much more recently, when more sophisticated methods of calculation and modeling were available. The value of the sea margin percentage if no data is available is very similar to the service margin method.

## 3.7 Cho, Kim And Kim's Prediction Of Sea Margin

In a paper by Cho, Kim and Kim a prediction method for calculating the sea margin is suggested for a specific route (Cho et al., 2016). The paper suggests using a 3D Rankine panel method for the regular wave resistance and the Probabilistic Operating Condition on a specific route to calculate the sea margin.

The paper defines the sea margin to be calculated as shown in Equation 3.14.

$$\frac{P_{total}(V_S)}{P_{calm}(V_S)} - 1 = SM \quad (3.14)$$

where  $P_{total}(V_S)$  and  $P_{calm}(V_S)$  is the power required to maintain service speed in waves and in calm water condition, respectively.  $SM$  is the sea margin in percent.

The prediction method considers a specific operational plan which can be used in the design stage of the ship. The prediction method is divided in parts:

- Operational plan of the vessel:

The operational sea area and course of the ship is defined.

- Calculation of resistance in calm sea:

The calm water resistance is found from model test or numerical analysis (CFD).

- Resistance increase due to wind:

Resistance due to wind is found from the ITTC chart (STA-JIP).

- Resistance increase due to waves:

Resistance due to waves is found using STAWAVE-1, STAWAVE-2 and 3D Rankine Panel Method.

- Prediction of power increase in waves:

Found using the resistance and thrust identify method (RTIM).

Following these steps, the paper finds a sea margin which reflects the environmental effects. The resulting sea margin for the VLCC in contract condition is found to be about 14.8 - 18.0% for a route when operating in the most frequent sea states.

### **Comments On The Method**

Of the studied methods for calculating the sea margin in this thesis, this is the most applicable one. The prediction method uses well established concepts of calculation and takes the environmental effects into account. This prediction has large similarities to the method proposed in this thesis.



# Chapter 4

## Increase Of Resistance

It is clear that the added resistance will be an important component of the sea margin. Thus, methods for calculating this must be clearly defined.

There are several different methods of finding the added resistance of a ship advancing in waves, with different approaches to the problem. For the calculation of added resistance due to waves, Faltinsen et al. (1980) has developed the direct pressure integration method. Another approach to the added resistance due to waves comes from Gerritsma and Beukelman (1972) who uses a strip theory approximation in the radiated energy method.

A calculation of added resistance due to wind is described by Molland et al. (2011), in a formulation which takes the relative wind speed into account.

These are just some of the methods which can be used to find the increase of resistance due to environmental components. A review of all of the methods for calculating resistance increase would be a study in itself, and is thus not performed.

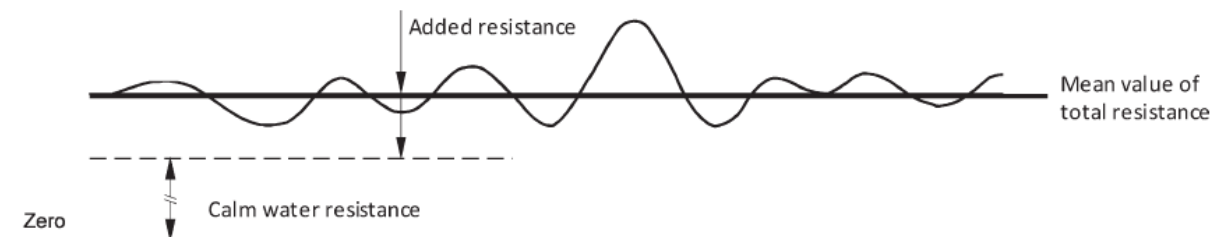


Figure 4.1: Determination of added resistance (Grin, 2015), p.183

The method for calculating the increase of resistance due to environmental effects which



will be used comes from the ISO (2015) standard. This method is easy to follow as it makes clear assumptions and is straightforward to compute. As it is an international standard it is widely recognized. To define a new method for calculating the sea margin based on increased resistance calculations from this ISO standard will thus be a good choice.

The ISO (2015) method assumes that the applicability of the method is limited to displacement type ships and small trim angles. The method is meant to be carried out for sea trials under ideal conditions. This implies low sea states and the standard defines limits for allowable wave heights during the speed-power trials.

The method does not take hull roughness or fouling into account. These are assumptions and limitations which must be considered when using the method for other conditions.

The resistance increase due to deteriorative effects are divided into roughness and fouling. The increase of resistance due to roughness is found from Townsin (1985) and ITTC (2008*a*). The increase of resistance due to fouling is not specified, as methods for obtaining this were not found.

Instead of calculating the change in power at a given speed, it is also possible to calculate the change in speed for a given power setting, and thus determining the speed loss due to added resistance. This is not studied in this paper, as this paper primarily considers the change in power at a given speed.

## 4.1 Environmental Effects On Added Resistance

ISO (2015) has published guidelines for the assessment of speed and power performance by analysis of speed trial data.

Here the environmental effects on the resistance are corrected for by estimating the increase of resistance  $\Delta R$ .

$$\Delta R = R_{AA} + R_{AW} + R_{AS} \quad (4.1)$$

where  $\Delta R$  is the total increase of resistance and  $R_{AA}$  and  $R_{AW}$  is the increase of resistance due to wind and waves respectively, in Newtons.  $R_{AS}$  is the increase of resistance due to water temperature and density deviations. The resistance value  $\Delta R$  associated with the measured power is to

be calculated for each run in the sea trials.

The ISO (2015) method uses  $\Delta R$  to correct for the environmental effects and to find calm water resistance. In this thesis it will not be corrected for, but used to find the added resistance. Thus,  $\Delta R$  can be added to the calm water resistance in order to find the actual resistance in operational conditions.

#### 4.1.1 Added Resistance Due To Wind

From ISO (2015) the increase of resistance due to wind is calculated by Equation 4.2

$$R_{AA} = 0.5\rho_A \cdot C_{AA}(\psi_{WRef}) \cdot A_{XV} \cdot V_{WRef}^2 - 0.5\rho_A \cdot C_{AA}(0) \cdot A_{XV} \cdot V_G^2 \quad (4.2)$$

where  $R_{AA}$  is the increase of resistance due to wind in newtons.  $A_{XV}$  is the transverse projected area above the waterline including superstructures in square meters and  $C_{AA}$  is the wind resistance coefficient. The coefficient is based on data from wind tunnel model tests or from data from similar ship types.  $V_G$  is the measured ship's speed over ground in meters per second.

$V_{WRef}$  and  $\psi_{WRef}$  are the relative wind velocity and direction at the reference height in meters per second and degrees, respectively.  $\rho_A$  is the mass density of air in kilograms per cubic meter.

The wind velocity and direction are to be taken as mean values over a selected period. This is because they will vary in time.

#### 4.1.2 Added Resistance Due To Waves

By superimposing the components of regular waves linearly, the irregular waves can be represented. ISO (2015) presents the STAWAVE-1 and STAWAVE-2 methods of calculating added resistance due to waves.

##### STAWAVE-1

STAWAVE-1 is a correction method which can be used when a ship has limited pitch and heave. This leads to a limitation in allowed wave heights, as the method is for low to mild sea states. The restriction for the significant wave height is  $H_{1/3} \leq 2.25\sqrt{L_{PP}/100}$ . The STAWAVE-1 method is

based on the fact that in head waves the encounter frequency is high, and thus one can neglect the effects of wave induced motions. This leads to the added resistance being dominated by the wave reflection of the hull on the waterline (ISO, 2015).

When approximating the water line geometry based on the bow section on the water line and the beam of the ship, the added resistance can be calculated as shown in Equation 4.3

$$R_{AWL} = \frac{1}{16} \rho_s g H_{1/3}^2 \sqrt{\frac{B}{L_{BWL}}} \quad (4.3)$$

Here  $R_{AWL}$  is the mean resistance in long crested irregular waves in Newtons, and acts as a substitute for  $R_{AW}$ .  $\rho_s$  is the water density in kilograms per cubic meter,  $g$  is the gravitational acceleration in meters per square second,  $B$  is the ship breadth in meters and  $H_{1/3}$  is the significant wave height in meters.  $L_{BWL}$  is the distance from the bow to 95% of maximum breadth on the waterline in meters, as shown in Figure 4.2

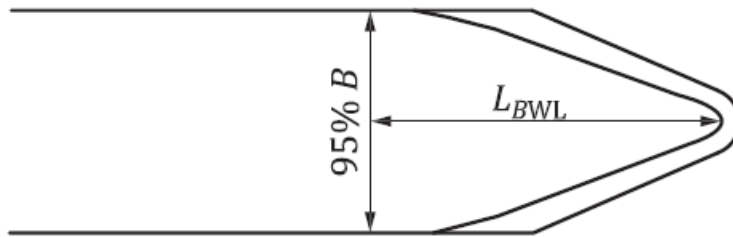


Figure 4.2: Definition of  $L_{BWL}$ , (ISO, 2015) p. 51

As mentioned, STAWAVE-1 is limited to bow waves, or waves with direction from ahead, i.e. within  $0$  to  $\pm 45^\circ$  off the bow. Waves outside this limit are omitted from the wave correction.

## STAWAVE-2

STAWAVE-2 is an empirical correction method with frequency response. The method uses main parameters such as speed and ship dimensions to approximate the transfer function of the mean resistance increase in head waves (ISO, 2015). The parametric transfer function of mean resistance increase in regular waves used in the method is shown in Figure 4.3.

This method has limitations as well. It is applicable to the mean increase of resistance in long crested irregular head waves. This means that also for this method the limit for the wave

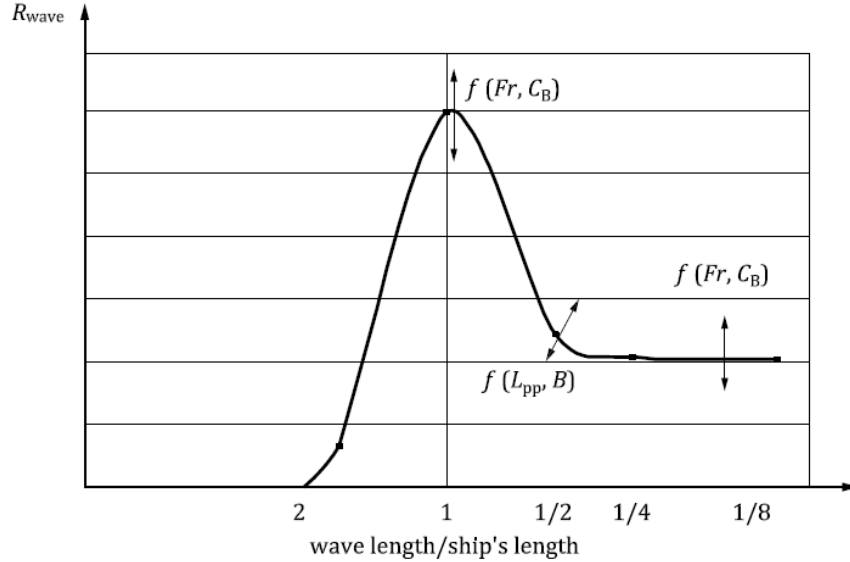


Figure 4.3: Parametric transfer function of mean resistance increase in regular waves, (ISO, 2015) p. 52

directions is within  $\pm 45^\circ$  off the bow. Waves outside of this limit are omitted. Formula 4.4 shows the main equation for this method.

$$R_{AWL} = 2 \int_0^\infty \frac{R_{wave}(\omega, V_S)}{\zeta_A^2} S_\eta(\omega) d\omega \quad (4.4)$$

Here  $R_{AW}$  is the mean increase of resistance in short crested irregular waves in Newtons. This acts as a substitute for  $R_{AW}$ .

$R_{wave}$  is the mean increase of resistance in regular waves in Newtons.  $\zeta_A$  is the wave amplitude in meters,  $\omega$  is the circular frequency of regular waves in rad/s and  $V_S$  is the speed of the ship through the water in meters per second.  $S_\eta$  is the frequency spectrum in square meter seconds. The procedure for finding  $R_{wave}$  and  $S_\eta$  is shown below.

The parameter  $R_{wave}$  is an empirical transfer function which includes the mean resistance increase due to wave reflection  $R_{AWRL}$  and motion induced resistance,  $R_{AWML}$  (ISO, 2015), as shown in Equation 4.5.

$$R_{wave} = R_{AWML} + R_{AWRL} \quad (4.5)$$

The complete formulations for establishing  $R_{AWML}$  and  $R_{AWRL}$  are found in Appendix B as

well as in the MatLab code in Appendix D.

STAWAVE-2 also complies with the following limitations:

- $75 \text{ m} < L_{PP}$
- $4.0 < \frac{L_{PP}}{B} < 9.0$
- $2.2 < \frac{B}{T_M} < 9.0$
- $0.10 < Fr < 0.30$
- $0.50 < C_B < 0.90$

To find the frequency spectrum  $S_\eta$ , the Pierson-Moscowitz type is assumed and found as shown in Equation 4.6.

$$S_\eta = \frac{A_{fw}}{\omega^5} \exp\left(-\frac{B_{fw}}{\omega^4}\right) \quad (4.6)$$

where

$$A_{fw} = 173 \frac{H_{1/3}^2}{T_{01}^4}$$

and

$$B_{fw} = \frac{691}{T_{01}^4}$$

Here  $\omega$  is the circular frequency of regular waves in rad/s,  $H_{1/3}$  is the significant wave height in meters and  $T_{01}$  is the mean wave period in seconds.

### 4.1.3 Added Resistance Due To Water Temperature And Water Density

A change in temperature or density of water will affect the ship resistance through the change in viscosity (ISO, 2015). The standard assumes a constant sea water temperature of  $15^\circ\text{C}$  and a density of  $1026 \text{ kg/m}^3$ .

From ISO (2015) the increase of resistance due to waves is calculated by

$$R_{AS} = R_{T0} \left( \frac{\rho_S}{\rho_{S0}} - 1 \right) - R_F \left( \frac{C_{F0}}{C_F} - 1 \right) \quad (4.7)$$

where

$R_{AS}$  is the increase of resistance due to deviation of water temperature and water density.  $R_{T0}$  is the total resistance for the reference water temperature and water density and is found as shown in Equation 4.8.  $R_F$  is the resistance due to friction for the actual water temperature and water density and is found as shown in Equation 4.9. All of these resistance parameters have Newton as unit.

$\rho_S$  is the water density for the actual water temperature and salt content and  $\rho_{S0}$  is the water density for the reference water temperature and salt content, both in kilograms per cubic meter.

$C_{F0}$  is the frictional resistance coefficient for the reference water temperature and water density and  $C_F$  is the frictional resistance coefficient for the actual water temperature and water density.

$$R_{T0} = \frac{1}{2} \rho_{S0} S V_S^2 C_{T0} \quad (4.8)$$

where  $S$  is the wetted surface area in square meters,  $V_S$  is the ship speed in meters per second and  $C_{T0}$  is the total resistance coefficient for the reference water temperature and density.

$$R_F = \frac{1}{2} \rho_S S V_S^2 C_F \quad (4.9)$$

where  $C_F$  is the frictional resistance coefficient for the actual water temperature and density.

#### 4.1.4 Effect Of Current

In the full speed trial data analysis presented in ISO (2015), it is also specified that correction of the effect of current on the speed must taken into account. However, in the new method this thesis is proposing, the effect of current will not be taken into account. In the data available from the route simulation there is not enough information on the current in order to include this in a reliable way. The speed will be assumed to be constant throughout the route. This will be explained further in Chapter 5.

## 4.2 Deteriorative Effects

The ISO method for calculating the increase of resistance is considered a good approach which will be used in the new method proposed in Chapter 5. However, this does not take deteriorative effects into account. Thus, other means of calculating these effects must be established.

### 4.2.1 Increase Of Resistance Due To Roughness

In the 1978 ITTC (2008a) performance prediction method, the full scale predictions include the roughness allowance as follows:

$$\Delta C_F = \left\{ 44 \left[ \left( \frac{k_s}{L} \right)^{1/3} - 10Re^{-1/3} \right] + 0.125 \right\} \cdot 10^{-3} \quad (4.10)$$

where  $\Delta C_F$  is the roughness allowance and  $k_s$  indicates the average roughness of hull surface. When no roughness is measured a standard value of  $k_s = 150 \cdot 10^{-6} m$  is used, as this is a typical value for a new ship (Molland et al., 2011).  $L$  is the waterline length of the ship in meters. This is an equation by Townsin (1985) which states the roughness allowance as Reynolds number dependent. This roughness allowance does not take the effect of fouling into account, but can it is assumed that the effect of corrosion can be included.

The added frictional resistance can then be found from the formula (Townsin, 2003):

$$\Delta C_F = \frac{\Delta R}{0.5\rho SV^2} \quad (4.11)$$

where  $\Delta R$  is the added frictional resistance in Newtons,  $\rho$  is the fluid density in kilograms per cubic meter,  $S$  is the wetted surface of the ship in square meters and  $V$  is the ship speed in meter per seconds.

### 4.2.2 Increase Of Resistance Due To Fouling

Fouling can develop quicker than roughness and can cause a much higher resistance increase (Steen and Minsaas, 2013). The main effect of fouling is that the resistance of the ship is increased due to more water being dragged forward along with the ship (Hellio and Yebra, 2009).

The calculation of increased resistance due to fouling will involve many parameters, like antifouling coatings and operational area, which makes reliable estimations difficult to attain (Steen and Minsaas, 2013).

In this thesis no specific methods for calculating the increase of resistance due to fouling has been found. There is no accurate and overall method to predict ship fouling (ITTC, 2008*b*). The only way of obtaining statistically reliable information is to study a large number of ships over extended time periods (ITTC, 2008*b*).

In light of this a fouling allowance is proposed. This is done by adding a set percentage on the calm water resistance and assuming this constant between hull cleaning intervals. According to Molland et al. (2011) an acceptable assumption of the annual increase of resistance due to fouling is at about 5%. This is approximately equal to an annual increase of the frictional resistance of 10%.

According to Hellio and Yebra (2009) the normal percentage added to the power due to propeller and hull surface roughness caused by marine growth and corrosion is 10%.

Thus, a fouling allowance of 10% of the calm water resistance is used, assuming a two year interval between hull cleanings.





# Chapter 5

## New Method

A new method for calculating a rational sea margin is proposed in this thesis. The method requires a given route and a specified constant speed for the ship. It collects weather data assuming the ship operates continuously back and forth on this route for a given time period. The route is divided into intervals where data, like the speed and weather, is assumed constant. Using weather data, the added resistance due to wind, waves and fouling is calculated for each interval in the route crossings. The added resistance is added to the calm water resistance of the ship and a powering prediction calculates the required power for each interval in the route crossings. The number of routes crossings simulated will depend on the length of the route, the ship speed and the time period to be analyzed.

The method assumes a constant speed for the whole route and moderate sea conditions. As the resulting sea margin should not represent extreme weather conditions, weather data above Beaufort 5 is omitted.

Using the calculated power in operational conditions, the sea margin is found for each interval in the route crossings and averaged in order to find a representative sea margin value for the whole route simulation.

The method proposed in this thesis consists of several key aspects. Both the environmental and deteriorative effects are taken into account, through resistance increase due to wind, waves and fouling.

A complete MatLab code for calculating the sea margin has been created in this thesis. This code is found in Appendix D. Several input files and parameters are needed in order to run the

code:

- A *kml* file containing the route coordinates, as described in section 5.1.
- Several *grib* files containing weather data for the time period the route should be simulated for, as described in section 5.2.
- Parameters from a ship model test, including open water diagram and ship particulars.

The code is created to be able to calculate the sea margin for an arbitrary ship route.

## 5.1 Defining The Route

To be able to run the code the user must have knowledge of where the ship is to operate. Google Earth is used in this method in order to define the ship route. Alternately the coordinates can be defined directly in the script. In Google Earth one can create a path consisting of a chosen number of points, which describes the route from the origin point to the destination. An example of such a path defined with five points from Amsterdam to New York is shown in Figure 5.1. It is recommended to limit the number of defining points in order to avoid possible errors in the MatLab code later. After defining the route, the path can be saved as a *kml* file in the same folder as the MatLab code is located. The *kml* file contains the longitude and latitude points of the defined route.

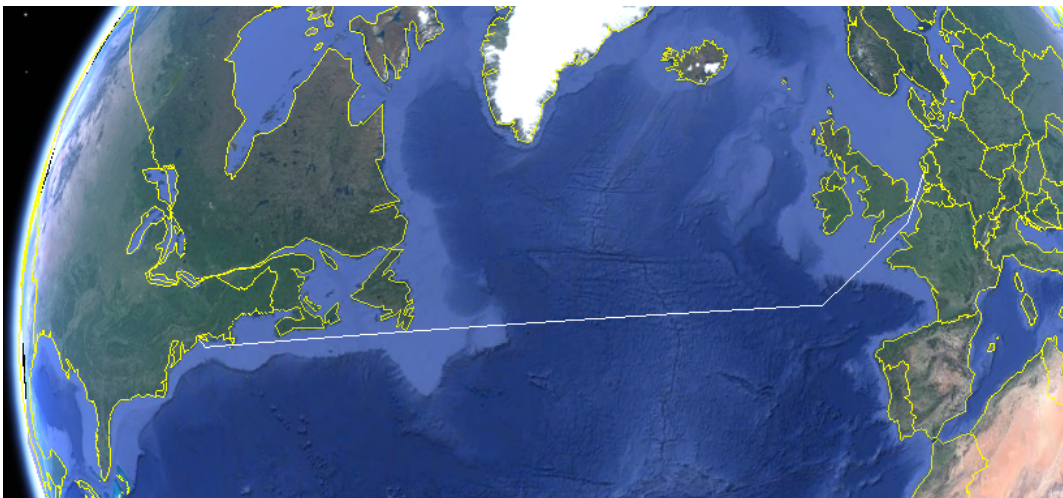


Figure 5.1: Example of path created in Google Earth from Amsterdam to New York

## 5.2 Weather Data

### 5.2.1 Grib Files From ECMWF

Data from The European Centre for Medium-Range Weather Forecasts (ECMWF) was acquired in order to find reliable weather data. This data is stored in *grib* files, and is a part of the Digital Appendix. The data base of ECMWF contains weather data from across the globe from 1979 until today.

The parameters stored in the acquired files are the U and V components of wind measured at 10 meters, significant wave heights, mean wave periods and mean wave directions. The files have values for these parameters at each latitude and longitude point for each time step defined in the files.

Weather data is defined four times a day; at 0, 6, 12, and 18 o'clock. The grid created by the latitude and longitude data from the *grib* file is from 90 to minus 90 for the latitude and from 0 to 360 for the longitude. However, the MatLab code transfers the configuration

of the weather data from 0 to 360 degrees longitude to -180 to 180 degrees. The original 90 to -90 degrees configuration of the latitude is changed to -90 to 90 degrees. This is done in order to have the data in compliance with the MatLab structure and the rest of the code.

The direction of the U component of wind is positive for a west to east flow, and for the V component for a south to north flow (ECMWF, 2017a), as seen in Figure 5.2.

The significant wave height is defined in meters and the mean wave period in seconds. The mean wave direction is defined as propagating towards north at 0 degrees, and towards east at 90 degrees (ECMWF, 2017b). Some of these definitions have been changed in the code in order to make the data compatible with the MatLab program.

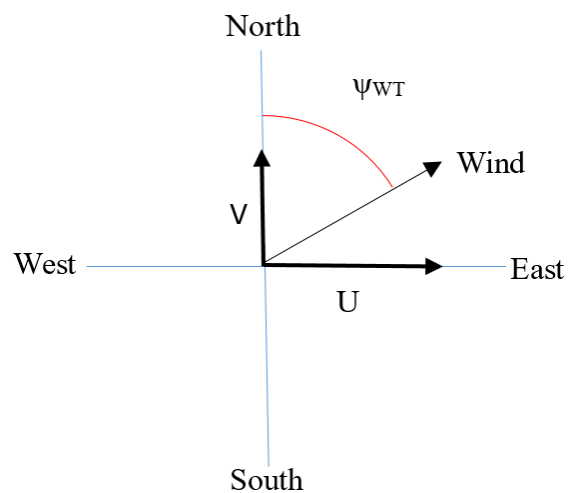


Figure 5.2: Configuration of the V and U wind components given in the *grib* files.

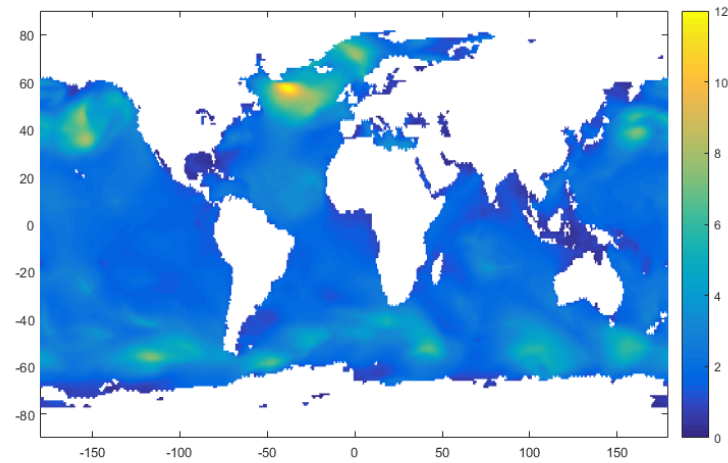


Figure 5.3: Visual representation of the significant wave at an arbitrary time point.

A visualization of the significant wave height at an arbitrary time point is shown in Figure 5.3. The outlines of a world map can clearly be seen in white, as the colored areas represent significant wave height values. In the figure these white areas are equivalent with NaN (not a number) values.

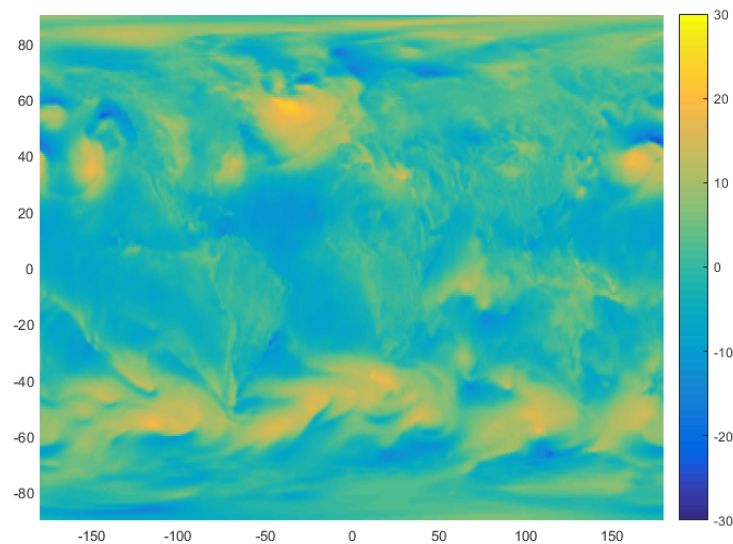


Figure 5.4: Visual representation of the U component of wind at an arbitrary time point.

When the route is defined too close to shore, the weather parameters connected with waves are invalid. The code redefines these values to be 0 in order to avoid calculation errors.

A visualization for the U component of the wind at an arbitrary time point is shown in Figure 5.3. The wind parameters will not have the same problem with NaN values, as the wind is defined both on land and across the oceans.

### 5.2.2 Time Intervals

The larger the *grib* files are, the more computing power is required in order to process them. Thus, the *grib* files are defined for three months at a time for the last five years, resulting in 20 input files for the weather. It was decided that the weather for the last years will give the best indication of future weather.

Another way could have been to choose five arbitrary years from the last 37 years, but as there is no particular reason to do this, it was disregarded. Also, as the world climate is changing it was assumed that the last years will give more accurate results for future operations.

## 5.3 Route Simulation

The route definition created in Google Earth is used in order to create an operational profile in the method. The MatLab code imports the *kml* file and makes variables of the longitude and latitude coordinates respectively. Then the route is divided into a larger number of intervals. The number of intervals between each point is dependent on the distance between the points in order to get the intervals to be as uniform as possible. After the intervals are defined, the coordinates of each interval midpoint is found. It is assumed that variables are constant for each interval and equal to the interval midpoint values. The midpoint values are used when collecting relevant weather data.

The code utilizes the great circle when dividing the intervals, which finds the shortest distance between two points on a sphere. The route will not be linear on a 2D map, but an arc as seen in Figure 5.5. After the latitude and longitude vectors are defined, the same vectors are reversed in order to define the return coordinates for the route. The route simulation in this code will have the ship sail to a destination and returning continuously for the selected period of time.



Figure 5.5: The same route as shown in Figure 5.1 plotted in 2D in MatLab.

The MatLab code which defines the route coordinates is written as a function with the *kml* route data as input.

Using a specified constant speed, the method calculates the time point when the ship will be in an exact position. This is done for all the midpoint values of the intervals for the route crossings, and returns a time matrix. This time matrix thus specifies the time point for which the data must be collected.

The route is continuously running for three months at a time. However, at the end of the third month the code sets some limitations. Firstly, the whole route has to fit inside the three month time interval. This means that if the time points for the last route crossing exceeds the time defined in the three month *grib* file, this route crossing is disregarded. Secondly, the code specifies that the number of route crossings has to be an even number. This is done in order to have an equal number of route crossings traveling to and from the destination.

This will cause some neglected data at the end of each three month interval. However, this is assumed to average over time. The alternative, i.e. allowing odd numbers of route crossings, would result in a 50% larger data collection for the ship traveling one way. This would give unreliable results.

In order to find the weather parameters for the midpoint values of latitude, longitude and

time, a three dimensional interpolation is performed for each interval. This is done separately for the U and V wind components, the significant wave heights, the mean wave periods and the mean wave directions. Thus, the result is five matrices containing the values for each three month interval. These matrices are then combined for all the three month intervals, resulting in a total of five matrices containing the weather data for the last five years.

These matrices are then used as input data in the resistance calculation.

## 5.4 Resistance Increase Due To Environmental Factors

In order to find the added resistance due to environmental and deteriorative effects, the ISO (2015) standard for correcting the results of trial runs is used. This standard can of course not be used completely as is. The standard calculates the increase in resistance due to wind, waves and change in temperature and density in order to correct for these effects. In this thesis this standard is used to find the resistance increase in order to combine it to the calm water resistance. Equation 5.1 shows the main formula for the increase in resistance.

$$\Delta R = R_{AA} + R_{AW} + R_{AS} \quad (5.1)$$

where  $R_{AA}$ ,  $R_{AW}$  and  $R_{AS}$  is the increase in resistance due to wind, waves and temperature and density in Newton, respectively.

However, as will be explained in detail in Section 5.4.3, the proposed method will disregard the effects of temperature and density. The method will however add a contribution to the added resistance due to fouling as shown in Equation 5.2.

$$\Delta R = R_{AA} + R_{AW} + R_{FO} \quad (5.2)$$

where  $R_{AA}$ ,  $R_{AW}$  and  $R_{FO}$  is the increase in resistance due to wind, waves and fouling in Newton, respectively.

When this  $\Delta R$  is found for the intervals in the route crossings, it is combined with the calm water resistance for the constant speed in order to find the total resistance in operational conditions.



The application of the standard comes with limitations for the different parameters. These limitations will be discussed in the sections below.

### 5.4.1 Resistance Increase Due To Wind

A ship with forward speed will experience two kinds of wind. First there is the natural wind, or the shear flow, which is the same wind the ship would experience without the forward speed. The second kind is the uniform wind, which is the wind caused by the movement of the ship.

When performing trial runs, the relative wind velocity and direction is measured directly and used in the formulations. The relative wind is a combination of the true wind and the wind caused by the ship's movement. ISO (2015) uses this relative wind in order to find the true wind. The standard assumes that when measuring the data, a double run is performed. This is normal in trial runs. Then an averaging process is performed in order to find the most accurate result over the double run. As mentioned, this thesis will not use the standard as is, and thus the averaging process for the double runs are disregarded. From the weather data the true wind velocity and direction is easily found directly. These values are used in order to calculate the relative wind velocity and direction. The definition of the angles and velocities used in the calculations is shown in Figure 5.6.

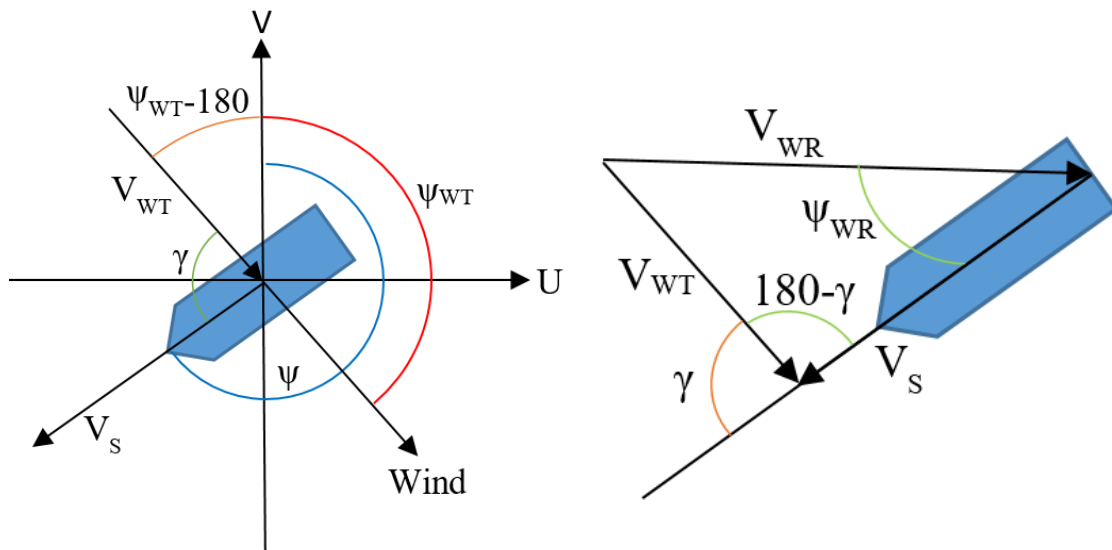


Figure 5.6: Definition of angles and velocities in wind resistance calculations.

Following this is a correction of the true wind due to the vertical position of the anemometer. In trial runs the anemometer is usually at the top of the ship mast. The wind velocity and direc-

tion found at this height must be corrected to the height used in wind tunnel tests to find the resistance coefficient. The correction due to the vertical position of the anemometer is added to the method through the formula shown in Equation 5.3.

$$V_{WTref} = V_{WT} \left( \frac{Z_{ref}}{Z_a} \right)^{1/7} \quad (5.3)$$

where  $V_{WT}$  is the true wind velocity in meters per second,  $Z_{ref}$  is the reference height for the wind resistance coefficient in meters and  $Z_a$  is the vertical position of the anemometer in meters.

Following this, the relative wind velocity and direction is corrected for the new true wind velocity through Equations 5.4, 5.5 and 5.6.

$$V_{WRref} = \sqrt{V_{WTref}^2 + V_S^2 + 2V_{WTref}V_S \cos(\psi_{WT} - \psi)} \quad (5.4)$$

where  $V_{WTref}$  is the corrected true wind velocity in meters per second,  $V_S$  is the ship speed in meters per second,  $\psi_{WT}$  is the true wind direction in degrees and  $\psi$  is the ship heading in degrees.

$$\psi_{WRref} = \tan^{-1} \left( \frac{V_{WTref} \sin(\psi_{WT} - \psi)}{V_S + V_{WTref} \cos(\psi_{WT} - \psi)} \right) \quad (5.5)$$

for  $V_S + V_{WTref} \cos(\psi_{WT} - \psi) \geq 0$

$$\psi_{WRref} = \tan^{-1} \left( \frac{V_{WTref} \sin(\psi_{WT} - \psi)}{V_S + V_{WTref} \cos(\psi_{WT} - \psi)} \right) + 180 \quad (5.6)$$

for  $V_S + V_{WTref} \cos(\psi_{WT} - \psi) < 0$

In this thesis the wind data from ECMWF is measured at 10 meters, which is the same height at which we assume the wind resistance coefficients are calculated for. This assumption is made as there are no information of the reference height of the wind resistance coefficient in the standard. Also, wind coefficients are normally derived in a wind profile defining the wind speed at 10 meters (van den Boom et al., 2013).

Thus, the correction will in this case not have an effect and the values for the relative wind velocity and direction will be the same before and after the correction.

Using the corrected relative wind direction  $\psi_{WRref}$  as the angle of attack, the wind resistance coefficient can be found from the graph shown in Figure 5.7, where  $C_{AA} = -C_X$ . The standard provides graphs for several different types of vessels. The graph provided in the standard is used in a laden condition, as wind tunnel tests were not available for the case ship used in this thesis.

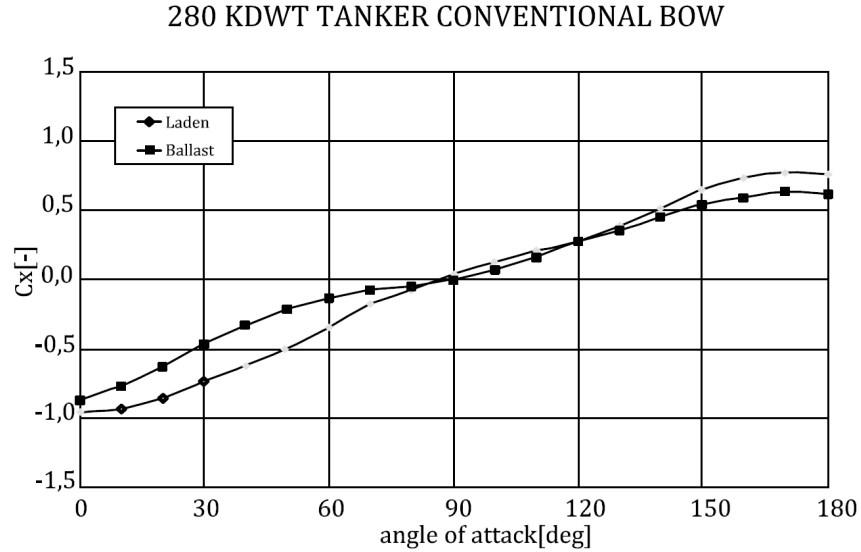


Figure 5.7: Wind resistance coefficients for a 280 KDWT tanker with conventional bow, (ISO, 2015) p. 43

Finally, the added resistance due to wind can be found as shown in Equation 5.7

$$R_{AA} = 0.5\rho_A \cdot C_{AA}(\psi_{WRref}) \cdot A_{XV} \cdot V_{WRref}^2 - 0.5\rho_A \cdot C_{AA}(0) \cdot A_{XV} \cdot V_S^2 \quad (5.7)$$

where the description of the parameters can be found in Section 4.1.1.

In the method a constant ship speed is assumed. Thus, there is no measured speed, and no way of differentiating between ship speed through the water and ship speed above ground. Both parameters are assumed to be the same constant speed,  $V_S$ . In formulas specifying speed above ground  $V_G$ , this has been changed to  $V_S$ .

## 5.4.2 Resistance Increase Due To Waves

As explained in Section 4.1.2, the STAWAVE-1 and STAWAVE-2 methods are used in order to find the added resistance due to waves.

The method evaluates the angle of attack  $\theta$  of each interval in the route crossings, which is defined as shown in Figure 5.8, where MWD is the mean wave direction. The mean wave period, significant wave height and mean wave direction are all found from route simulated weather data.

If the angle of attack is within the  $\pm 45^\circ$  interval, the method goes on to evaluate whether the wave resistance shall be calculated using the STAWAVE-1 or the STAWAVE-2 method. For significant wave heights  $H_{1/3} \leq 2.25\sqrt{L_{PP}/100}$  the STAWAVE-1 method is chosen. For other significant wave heights, the STAWAVE-2 method is used. If the angle of attack is outside the  $\pm 45^\circ$  interval, the effect of the waves is omitted and set equal to 0.

For waves compliant with the STAWAVE-1 method, the calculation is straight forwards, using Equation 5.8.

$$R_{AWL} = \frac{1}{16} \rho_S g H_{1/3}^2 \sqrt{\frac{B}{L_{BWL}}} \quad (5.8)$$

where parameters are defined as in Section 4.1.2.

For waves compliant with the STAWAVE-2 method, the calculation follows the calculation method described in Section 4.1.2, with the governing equation shown in Equation 5.9.

$$R_{AWL} = 2 \int_0^\infty \frac{R_{wave}(\omega, V_S)}{\zeta_A^2} S_\eta(\omega) d\omega \quad (5.9)$$

where all parameters are defined in Section 4.1.2.

The integration limits of the circular frequency  $\omega$  are defined from 0 to infinity. These limits are not valid in the calculations, and different limits are defined in order to compute the results. The relation between the circular frequency  $\omega$  and the wave period  $T$  is given in Equation 5.10 (Faltinsen, 1990).

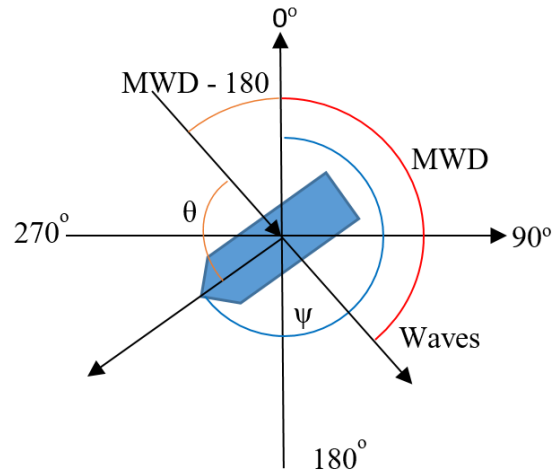


Figure 5.8: Definition of the angle of attack.

$$\omega = \frac{2\pi}{T} \quad (5.10)$$

Using this relation, the limits for  $\omega$  are set for wave periods from 4 seconds to 25 seconds as the upper and lower limit.

The lower limit for the periods was determined due to waves with periods lower than this having very small contributions to the resistance. In the Global Wave Statistics (Hogben et al., 1986), the zero crossing period is measured from a  $< 4$  seconds limit to a  $> 13$  seconds limit. The occurrence of the latter is not frequent. A zero crossing period will always be larger or equal to the wave period by definition.

Thus, it is assumed that the waves which will contribute to the added resistance will be within the defined integration limits.

In the integration the method assumes an  $d\omega$  integration step of 0.1.

In both STAWAVE-1 and STAWAVE-2 the resulting  $R_{AWL} = R_{AW}$ .

### 5.4.3 Evaluation Of $R_{AS}$

It is difficult to gather accurate information of temperature and density for an arbitrary route in the same way which wind and wave components are found. Therefore, the effect of  $R_{AS}$  is evaluated separately for a temperature change of  $\pm 10^\circ C$  in order to determine whether it can be neglected from the new method. This evaluation of  $R_{AS}$  can be found in the *temp.m* file in Appendix E.

The results from this evaluation can be found in Chapter 8.1

## 5.5 Resistance Increase Due To Deteriorative Effects

### 5.5.1 Resistance Increase Due To Roughness

Section 4.2.1 presents the roughness allowance  $\Delta C_F$  as suggested by the 1978 ITTC Standard. This standard is used in most model tests, and the roughness allowance is thus already included in the calm water resistance.

### 5.5.2 Resistance Increase Due To Fouling

As proposed in Section 4.2.2 this thesis assumes a fouling allowance in order to account for the effects of fouling. Thus, a 10% increase in the calm water resistance is added to the total added resistance. This is calculated as shown in Equation 5.11.

$$R_{FO} = 0.10 \cdot R_{Tcalm} \quad (5.11)$$

This allowance assumes the ship to have the hull cleaned every two years.

## 5.6 Powering Prediction

The added resistance due to wind, waves and fouling for each interval in each route crossing is added to the calm water resistance in order to find the total resistance.

The power prediction is automatically performed for each interval in each route crossing.

It is assumed that the wave fraction  $w$ , the thrust deduction factor  $t$  and the relative rotative efficiency  $\eta_R$  are constant for full scale model test data and in operational conditions for a given speed.

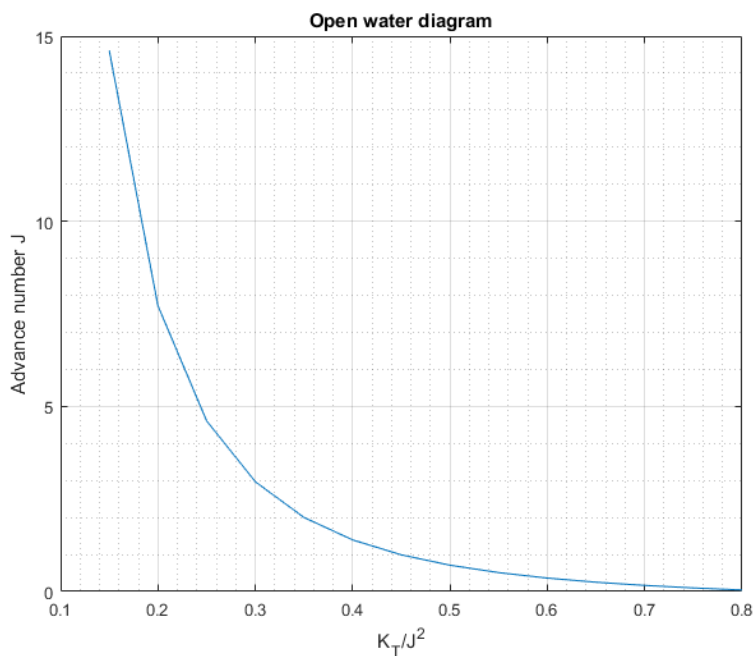


Figure 5.9: Full scale open water diagram for  $KT/J^2$

Using these assumptions and the new total resistance in operational conditions,  $\frac{K_T}{J^2}$  is found as shown in Equation 5.12.

$$\frac{K_T}{J^2} = \frac{R_T}{nprop \cdot \rho_S \cdot (t-1) \cdot D^2 \cdot V_S^2 \cdot (1-w)^2} \quad (5.12)$$

where  $R_T$  is the total resistance in operational conditions in Newtons, i.e. the calm water resistance plus the added resistance calculated from the simulated data.  $nprop$  is the number of propellers,  $\rho_S$  is the sea water density in kilogram per cubic meter,  $t$  is the thrust deduction factor,  $D$  is the full scale propeller diameter in meters,  $V_S$  is the ship speed in meters per second and  $w$  is the wake fraction.

The full scale open water diagram is found from the model test data. The advance coefficient  $J^*$  is found using the calculated  $\frac{K_T}{J^2}$  value in the  $J$  vs  $\frac{K_T}{J^2}$  diagram shown in Figure 5.9.

This value for  $J^*$  is then used in the open water diagram shown in Figure 5.10 in order to find the torque coefficient  $K_Q^*$ .

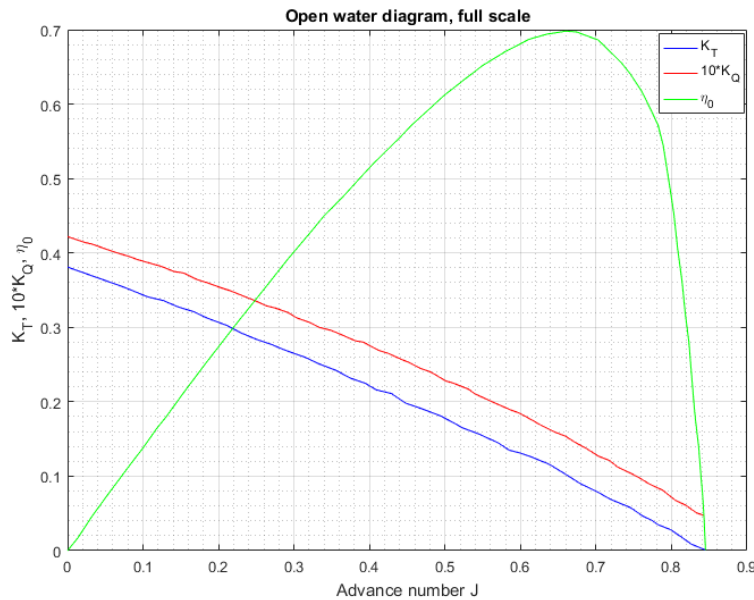


Figure 5.10: Full scale open water diagram

Following these calculations, the rate of revolutions (RPM) is found as shown in Equation 5.13.

$$RPM = \frac{60 \cdot (1 - w)}{D} \cdot \frac{V_S}{J^*} \quad (5.13)$$

where RPM is the rate of revolutions in revolutions per second,  $w$  is the wake fraction,  $V_S$  is the speed of the ship in meters per second,  $D$  is the propeller diameter in meters and  $J^*$  is the advance coefficient found from  $\frac{K_T}{J^2}$ .

Then the delivered power is found as shown in Equation 5.14.

$$P_D(kW) = n_{prop} \cdot \frac{2\pi}{1000} \cdot \rho_S \cdot D^5 \left( \frac{RPM}{60} \right)^3 \cdot \frac{K_Q^*}{\eta_R} \quad (5.14)$$

where  $P_D$  is the delivered power in kilo watts.

Finally, the brake power can be found as shown in Equation 5.15.

$$P_B = \frac{P_D}{\eta_M} \quad (5.15)$$

where  $P_D$  is the delivered power in kilo watts and  $\eta_M$  is the mechanical efficiency. It is assumed that  $\eta_M = 0.97$  as this is common practice.

The same procedure is also performed with the calm water resistance in order to calculate the calm water brake power. This difference between calculated operational brake power and calm water brake power is needed to find the sea margin.

## 5.7 Exclusion Of Extreme Weather Conditions

The sea margin is supposed to be representative of the ship in normal operational conditions. Thus, weather conditions above a certain level should be omitted from the sea margin calculations. In order to limit the weather the Beaufort scale is used. The Beaufort scale is a scale of wind speeds ranging as seen in Table 5.1.

The limit for the operational condition is set at Beaufort 5. This means that if the wind speed is above 10.7 meters per second or the wave height is above 3 meters the data is disregarded. This is done by defining  $\Delta R$  to be 0 if the Beaufort 5 limit is exceeded.

The method keeps these values at 0 throughout the calculations in order to maintain the structure of the matrices used in the MatLab code. After all calculations are done, the resulting



Table 5.1: The Beaufort scale (Pettersen, 2007)

The Beaufort Scale Of Wind			
Beaufort number	Name of wind	Wind speed [m/s]	Wave height [m]
0	Calm	0-0.2	0
1	Light air	0.3-1.5	0-0.2
2	Light breeze	1.6-3.3	0.2-0.5
3	Gentle breeze	3.4-5.4	0.5-1
4	Moderate breeze	5.5-7.9	1-2
5	Fresh breeze	8.0-10.7	2-3
6	Strong breeze	10.8-13.8	3-4
7	Moderate gale (or near gale)	13.9-17.1	4-5.5
8	Fresh gale (or gale)	17.2-20.7	5.5-7.5
9	Stong gale	20.8-24.4	7-10
10	Whole gale (or storm)	24.5-28.4	9-12.5
11	Storm (or violent storm)	28.5-32.6	11.5-16
12-17	Hurricane	32.7 and over	$\geq 14$

brake power  $P_B$  matrix loses its structure when omitting the route intervals which exceed the Beaufort 5 limit. At this point the structure of the matrix is no longer important, as route related information, e.g. plots for a given route, has been found.

## 5.8 The Sea Margin

The sea margin is, as explained in Section 2, a margin which accounts for the environmental and deteriorative effects by making a correction between the calm water power and the average service condition power as shown in Equation 5.16.

$$SM = \left( \frac{P_B}{P_{Bcalm}} - 1 \right) \cdot 100 \quad (5.16)$$

where  $SM$  is the sea margin in percent.

In the method this results in individual sea margin values for each interval in the route crossings. The method then removes the intervals where the weather data is above the Beaufort 5 limit. The sea margin should not include these weather conditions, as it is a margin representative for normal operational conditions.

The total sea margin is found by averaging all the interval sea margins from the route crossings. This results in a sea margin representing the specified route with a constant specified

speed.

## 5.9 Validation Of Wave Resistance In ShipX

ShipX is an analysis tool for ship designs created by SINTEF Ocean. The Veres (Vessel response) tool in ShipX was used in order to check the validity of the calculated added resistance in waves. A ship model for a ship similar to the case ship was available. Using the hull transformation tool in ShipX the parameters of the existing ship model were changed to represent the case ship. A Veres calculation was run with direct pressure integration and post processed in order to find the graph for mean added resistance at 16 knots for wave headings at  $0^\circ$  and  $45^\circ$ .

The resulting graph for mean added resistance in waves for short term statistics is shown in Appendix C. The mean significant wave height found from the simulated data was used as input for the constant significant wave height in ShipX. The wave period range was chosen from the lowest and highest mean wave periods found from the simulated weather data.

The graph from ShipX was manipulated in MatLab in order to show values for the added resistance due to waves. The resulting graph is shown in Figure 5.11.

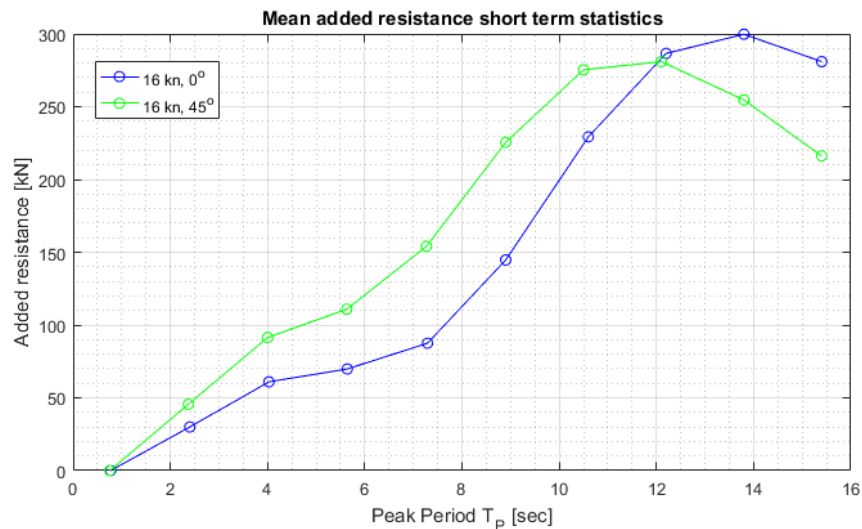


Figure 5.11: Mean added resistance in waves from ShipX, manipulated in MatLab

The values for the calculated added resistance due to waves were found to be in the same order of magnitude as the resistance in Figure 5.11. Thus, the calculated added wave resistance is assumed valid.



# Chapter 6

## MatLab Code

The complete MatLab code can be found in the Digital Appendix, as well as *grib* and *kml* files and saved workspaces. An explanation of the files presented in the Digital Appendix can be found in Appendix A. Below follows a guide on how to execute the method with instructions on which parameters the user has to provide. The complete code can also be found in Appendix D. All the default data presented in the codes are from the case ship and for the Amsterdam to New York route.

The code is divided into two parts of the method. The route simulation, which provides the weather data input from a specified route and speed, and the sea margin calculation. The method is divided like this in order to save calculation time. Once the route simulation has been performed once, the workspace is saved and imported into the sea margin calculation.

### 6.1 Input Parameters

As mentioned in Chapter 5 there are several input parameters needed in order to run the code.

#### 6.1.1 Route Simulation

In order to run the route simulation, one needs to specify the route of the ship and the constant ship speed. The route is specified as the parameter *route\_data* in the *main.m* code. Several example routes are found in the Digital Appendix. However, the user can create a different route

in Google Earth, save this *kml* file in the same folder as the code, and define this route in the *main.m* script.

The constant ship speed is specified in knots as the parameter *V\_knots* in the *grib\_reader.m* code.

The *grib* files needed to run the code for the last five years are included in the code as a default. It is recommended to use these values. However, if a shorter interval is required, the user can remove elements from the *quarter* parameter in the *route.m* script. If a longer interval is needed, *grib* files of three month intervals can be added in the *weatherdata* folder and included in the *quarter* parameter. The parameter *numberofquarters* should also be changed to reflect the number of quarters the code is to run for.

### 6.1.2 Sea Margin Calculation

Some of the parameters defined in the *iso\_input* file will be constant for all ships or found from the weather data. However, the following ship parameters should be changed according to the model test data for the particular ship:

- *V\_S\_knots* - Ship speed in knots.
- *L\_OA* - The ship's length overall in meters.
- *L\_PP* - The ship's length between perpendiculars in meters.
- *L\_BWL* - The distance from the bow to 95% of maximum breadth on the waterline in meters.
- *B* - The ship's breadth in meters.
- *C\_B* - The block coefficient (dimensionless).
- *A\_XV* - Transverse projected area above waterline, included superstructure in square meters.
- *S* - The wetted surface area in square meters.
- *T\_M* - The draft at midships in meters.

Additionally, model test data for the following parameters should be specified in the input file in vector form, varying for the speed range in the model test:

- The speed range in knots:

Example:  $V\_range = [14\ 14.5\ 15\ 15.5\ 16\ 16.50\ 17\ 17.5\ 18\ 18.5\ 19];$

- The calm water resistance in kN:

Example:  $R\_Ts\_range = [589\ 636\ 685\ 738\ 797\ 866\ 955\ 1060\ 1171\ 1321\ 1542]*1000;$

- The wake fraction:

Example:  $w\_range = [0.308\ 0.309\ 0.310\ 0.311\ 0.312\ 0.313\ 0.309\ 0.303\ 0.304\ 0.306\ 0.301];$

- The thrust deduction factor:

Example:  $t\_range = [0.216\ 0.219\ 0.221\ 0.223\ 0.226\ 0.229\ 0.223\ 0.216\ 0.222\ 0.227\ 0.215];$

- The relative rotative efficiency:

Example:  $etaR\_range = [1.016\ 1.018\ 1.020\ 1.023\ 1.025\ 1.026\ 1.026\ 1.027\ 1.027\ 1.026\ 1.025];$

These parameters should be specified in the *iso\_input* script.

The open water diagram values found in the model test data must be specified in the *open-water.m* script.

## 6.2 Route Simulation

The route simulation for the method can be accessed in the *main.m* file. This file calls on other functions and scripts in order to limit the variables presented in the workspace. This code takes several hours to run. In light of this, the workspace for several routes are saved in the *saved\_data* folder for further use. These saved workspaces assumes a constant speed of 16 knots.

The *main.m* code calls on the *route.m* function with the route data as input.

The first thing the *route.m* function does is to call on the *route\_coords.m* function with the same route data as input. The *route\_coords.m* function works as described in Section 5.3, by defining latitude and longitude coordinates for 100 intervals, both to and from the route destination.

Next, the *route.m* function reads the *grib* files containing weather data and calls on the *grib\_reader.m* function to interpolate the weather parameter matrices as described in Section 5.3.

After a route simulation is performed, the user should save the workspace, which will be used later when calculating the sea margin.

## 6.3 Sea Margin Calculation

In order to calculate the sea margin, the user should run the *SM\_calculation.m* script. This script calls on the resistance calculation and the open water diagram data. When all input variables are defined, the resulting sea margin for the whole route simulation is shown in the command window.

### 6.3.1 Added Resistance

The added resistance for the route simulation is calculated in the *resistance.m* script. The first thing the script does is to read the input variables from the *iso\_input.m* file. It then goes on to read the *wind.m*, *criteria.m* and *waves.m* scripts, which are explained below. The *criteria.m* script evaluates whether the ship input is within the criteria for the STAWAVE-2 calculation and writes the results directly into the command window. The method should not be used if the text "Criteria not met" is shown.

After the code runs the calculations for wind and wave resistance as explained below, the total added resistance due to environmental and deteriorative effects is found. The calm water resistance is found by interpolating the calm water resistance input vector using the specified constant speed value.

### 6.3.2 Resistance Due To Wind

The *wind.m* script calculates the resistance due to wind for the route simulation.

The ship velocity is decomposed into U and V components using the ship headings in order to find the relative wind velocity. The angles to be used are manipulated in order to be in com-

pliance with the calculations. The script follows the procedure explained in Section 5.4.1 and gives values for the added resistance due to wind  $R_{AA}$  for each interval of the route crossings simulated.

### 6.3.3 Resistance Due To Waves

The *waves.m* script defines the integration step of the STAWAVE-2 calculation to be 0.1 and manipulates the angles in order to be in compliance with the calculations. Resistance calculated by STAWAVE-2 is found by the use of a for-loop which integrates over  $\omega$ . In the for-loop a function named *R\_wave.m* is run, which contains the calculations described in Appendix B.

The code evaluates if the individual intervals should be calculated using the STAWAVE-1 or STAWAVE-2 method, dependent on the significant wave height. Waves outside of the  $\pm 45^\circ$  section of the bow are omitted and equaled to 0.

This results in wave resistance calculations for each interval along all the simulated routes.

## 6.4 Powering Prediction

As mentioned, the *SM\_calculation.m* script runs both the resistance and the open water scripts. Values for the thrust deduction factor  $t$ , the wake fraction  $w$  and the relative rotative efficiency  $\eta_R$  is found by the code by interpolating the for the specified speed.

The code follows the calculation described in Section 5.6 in order to find the resulting brake power  $P_B$  for each interval in the simulated route crossings and for the calm water resistance. The code removes values for  $P_B$  which is based on weather data above Beaufort 5 and averages the sea margin values.

The resulting sea margin for the simulated route at the specified speed is shown in the command window.





# Chapter 7

## Case Ship

A case ship was selected in order to test out the new method. SFI Smart Maritime provided operational measurements from an open hatch fleet of 24 cargo vessels. The vessels are a part of five different classes, where model test data were available for three of these classes.

### 7.1 Selection And Presentation Of The Case Ship

When choosing the case vessel the most important factor was availability of data. The case ship must have available data from model tests, open water diagram and preferably body plan. The latter was not available when the choice of case ship was made. The ship should have reliable measurements in the sea passage state in order to provide the actual measured sea margin in operation. The ship from the classes with available model test data with the most measured data in the sea passage state was chosen as the case ship.

Presentation of the case ship is shown in Table 7.1.

The model test data for the case class is representative for the case ship, but the parameters are not exactly the same. The data presented in Table 7.1 is from the case class model test data, which is close enough to the case ship to be representative of it.

When using this case ship in the route simulation and sea margin calculation, the design speed without sea margin from the model test was chosen as the constant speed. The data used from the model test data are from the design loading condition in order to best create the conditions of the ship in normal operation.

Table 7.1: Presentation of the case ship

Case ship			Description
$L_{OA}$	208.73	$m$	Length over all
$L_{PP}$	197.40	$m$	Length between perpendiculars
$L_{WL}$	201.90	$m$	Length of waterline
$B$	32.20	$m$	Ship breadth
$T_M$	12.0	$m$	Draft at mid-ship
$C_B$	0.7958	-	Block coefficient
$S$	9512.1	$m^2$	Wetted surface area
$\nabla$	60696.6	$m^3$	Displacement volume
$A_T$	785.40	$m^2$	Transverse area above waterline

## 7.2 Calculating The Sea Margin For The Measured Operational Data

Using the measured operational data provided, the corresponding route which the case ship follows can be visualized as shown in Figure 7.1.

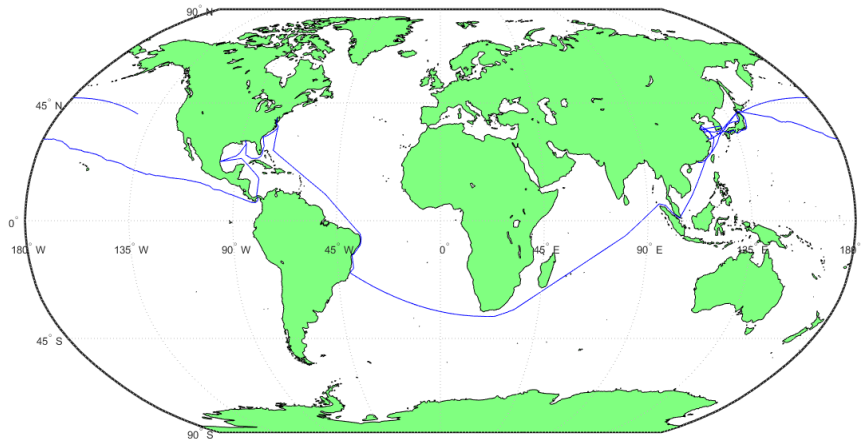


Figure 7.1: The complete travel history of the case ship

The measured operational data contains information about parameters, including draft, speed, Beaufort number and cargo. In order to present the data as similar to the model test as possible, some limitations are introduced to the data set.

Measurements with the following properties are disregarded from the data:

- Speed below 4 knots

- Draft below 9 meters
- Cargo below 35000
- Beaufort number above 5
- Relative wind velocity above 10.8

The Beaufort limitation enforces the same limitation with respect to weather as present in the method developed in this thesis. The relative wind velocity is also enforced in order to disregard too strong weather. The method assumes the ship in a laden condition. Thus, the cargo restriction is made in order to make the method input and the measurement input as similar as possible. The restrictions made for speed and draft are also made for this reason.

The resulting route for which the measurements fulfill these requirements are shown in Figure 7.2 as traveling from Malaysia in Asia to Brazil in South America. This route is simulated later using the method developed in this thesis.

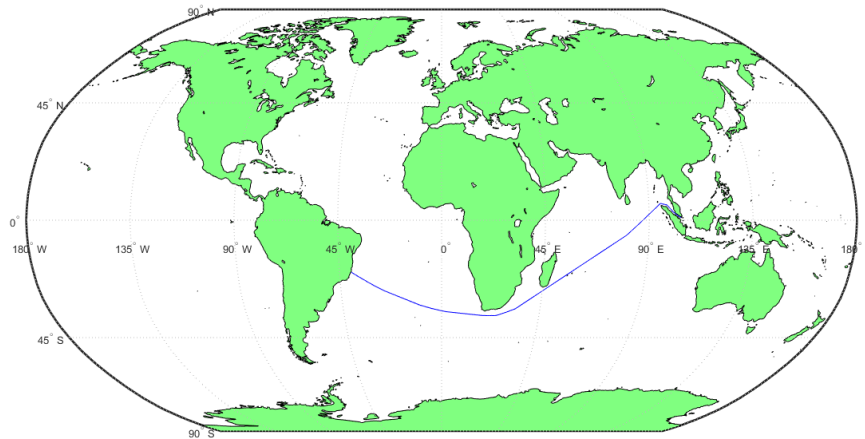


Figure 7.2: The ship route based on filtered data

Using the filtered data, the speed - power relationship is found for the operational condition as shown in Figure 7.3. The graph has been extrapolated for the lower values.

In the figure the measured operational data is shown as blue circles. The mean power and speed from the data was calculated. The figure shows these mean values as red lines. By interpolation, the values for where these mean lines cross the calm water power line is found. The values in these intersections are shown in the figure as black lines.

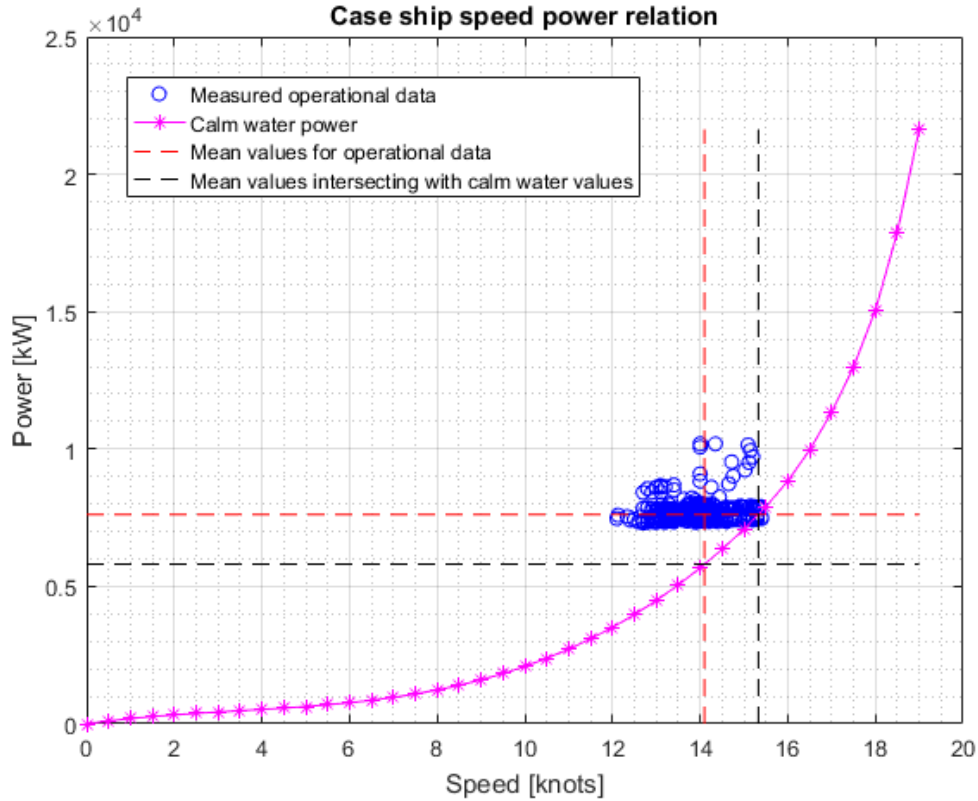


Figure 7.3: Speed power relation of the case ship based on calm water model test data and measured operational data

The difference between the calm water power and the measured power at the mean speed was found and converted to a percentage-wise increase. This increase represents the sea margin in operational conditions at the mean speed.

# Chapter 8

## Results

### 8.1 Evaluation Of $R_{AS}$

An evaluation of the added resistance due to temperature and density has been performed. The calculation method described in Section 4.1.3 was used, with the data from the model test as the reference input at a given speed.

The reference temperature is  $15^{\circ}C$ . The evaluation investigates how much a ten degree Celsius difference will influence the added resistance. Thus, test cases at  $5^{\circ}C$  and  $25^{\circ}C$  were evaluated. Density and kinematic viscosity values for the temperatures investigated were found from the Naval Hydrodynamics Ship Resistance compendium (Steen and Minsaas, 2013).

With a water temperature of  $5^{\circ}C$  and  $25^{\circ}C$  the resulting added resistance due to temperature and density was found as shown in Table 8.1.

Table 8.1: Results for  $R_{AS}$  evaluation.

<b>Added resistance due to temperature and density:</b>		
Temperature:	$R_{AS}$	
$5^{\circ}C$	18.4618	kN
$25^{\circ}C$	-15.5454	kN

## 8.2 Case Ship In Simulated Routes

The developed method has been tested for three routes. In the following sections the added resistance  $\Delta R$ , the total resistance in operational conditions, the brake power  $P_B$  and the sea margin is presented for the different routes. The input data is from the case ship exclusively. The graphs presented shows the results for one route crossing, unless otherwise specified. The resulting sea margin for each route takes all the simulated crossings for that route into account.

### Amsterdam - New York Route

Figure 8.1 shows the route for which the route simulation has been run for, and thus where the weather data has been collected.

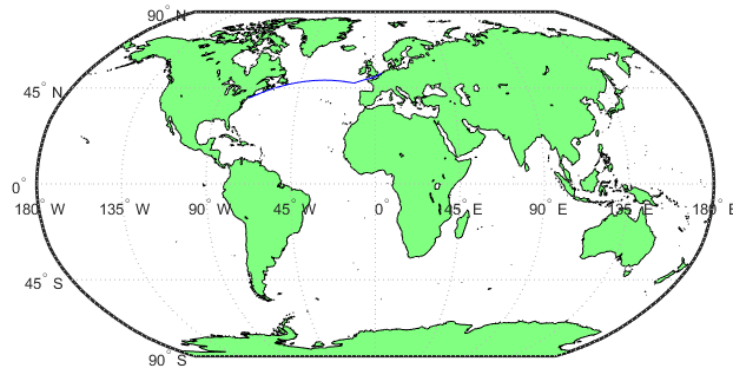


Figure 8.1: Route from Amsterdam to New York

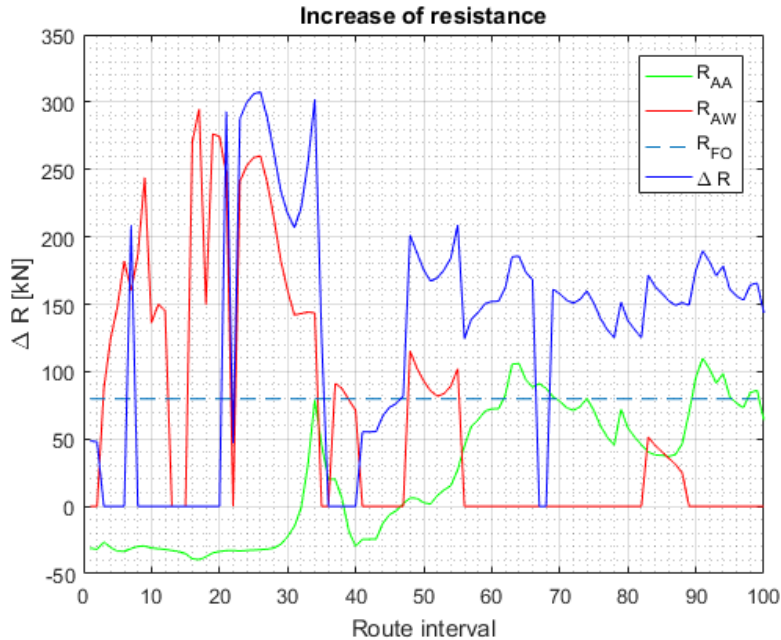


Figure 8.2: Components of the added resistance for route crossing number 14

Figure 8.2 shows the components of the added resistance.  $R_{AA}$ ,  $R_{AW}$  and  $R_{FO}$  is the resistance increase due to wind, waves and fouling, respectively.  $\Delta R$  is the sum of all the contributions at this particular route. It can be seen that the wind gives both an increase and a decrease of the total resistance, dependent of where in the route the ship is. The waves does not have a contribution for all the route intervals. This is because the method used to calculate the wave resistance only takes waves within a  $\pm 45^\circ$  limit off the bow into account. The resistance due to fouling is seen as constant across the whole route crossing, which is consistent with the definition of the fouling allowance in the defined method. Finally, the total increase of resistance  $\Delta R$  is seen to add all the components into a resulting resistance increase. It can be seen that in some intervals  $\Delta R$  is zero, even though there are contributions from the other resistance components. This is due to weather above Beaufort 5 being omitted. In areas where this is the case, as for interval number 10, the weather conditions are too large to be accounted for in this method.



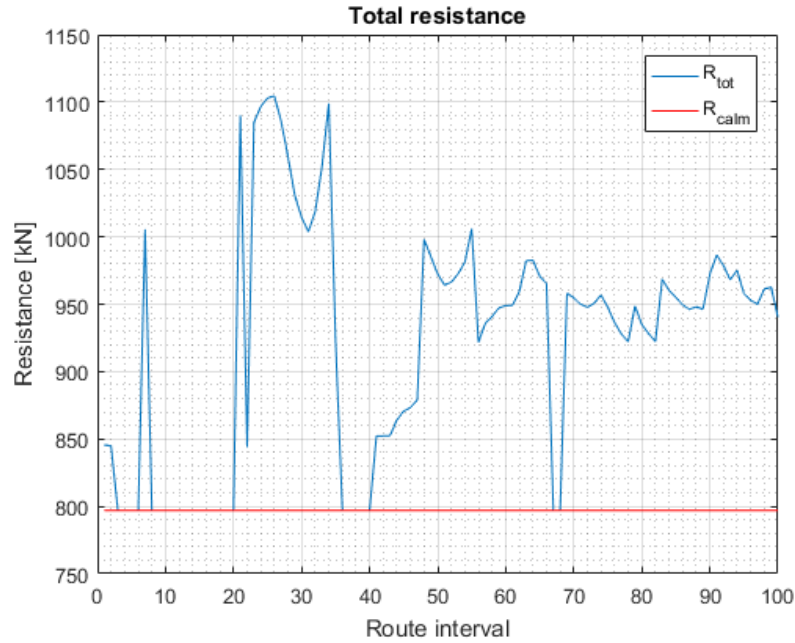


Figure 8.3: The operational resistance for route crossing number 14

Figure 8.3 shows the total resistance in operational conditions, which is found as  $R_{calm} + \Delta R$ . It also shows the calm water resistance for the specified speed, as a reference. This graph is a good visualization of the stochastic nature of the resistance of a ship in wind and waves.

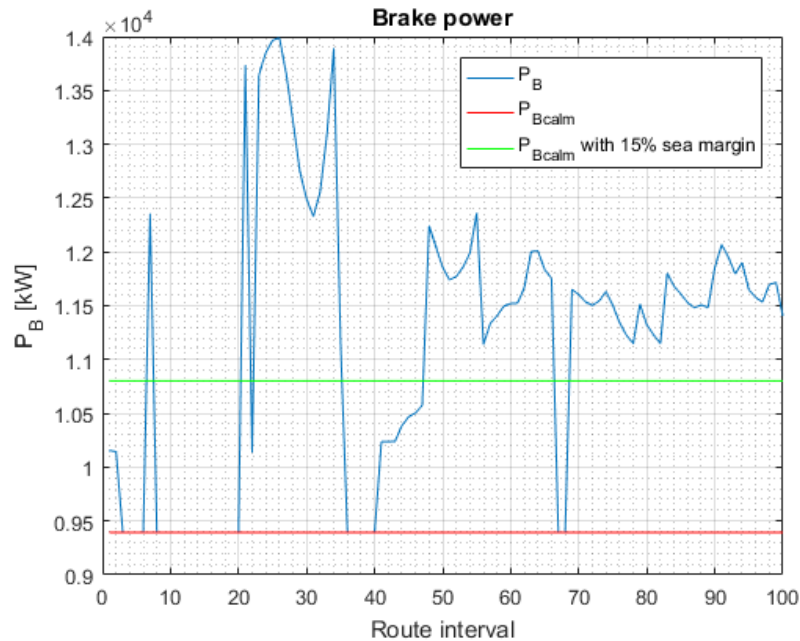


Figure 8.4: The operational brake power for route crossing number 14

Figure 8.4 visualizes the resulting brake power for the same route.  $P_B$  is the actual brake power for this route crossing, which is calculated using data from the route simulation. The calm water brake power  $P_{B_{calm}}$  is shown as a reference, as well as the calm water brake power with a 15% sea margin. The latter is shown to illustrate how large the operational brake power is in comparison with the typical assumed 15% sea margin.

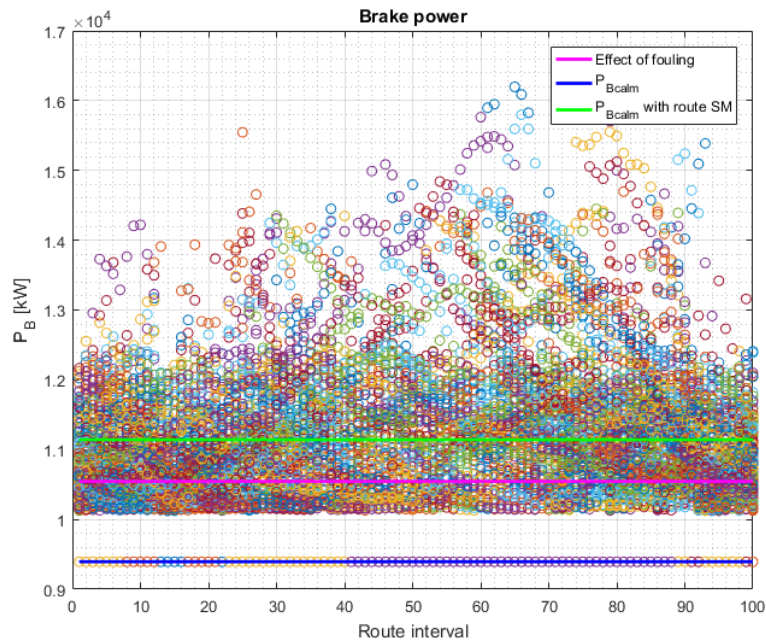


Figure 8.5: Total  $P_B$  distribution for all route crossings combined, for the Amsterdam - New York route

Figure 8.5 illustrates the distribution of all the calculated brake power values over the route simulated. The calm water brake power is included as a reference. The total calculated sea margin limit is also shown. As a reference, the brake power due to fouling is shown, to illustrate that the brake power values also can be below this value. This is due to the wind having a negative contribution to the resistance, as was seen in Figure 8.2.

For the intervals where the weather exceeds Beaufort 5, the added resistance is set to zero, and thus the resulting brake power will be equal to the calm water brake power. This explains the values for the interval brake powers equal to the calm water brake power. These values are not taken into account when calculating the sea margin.

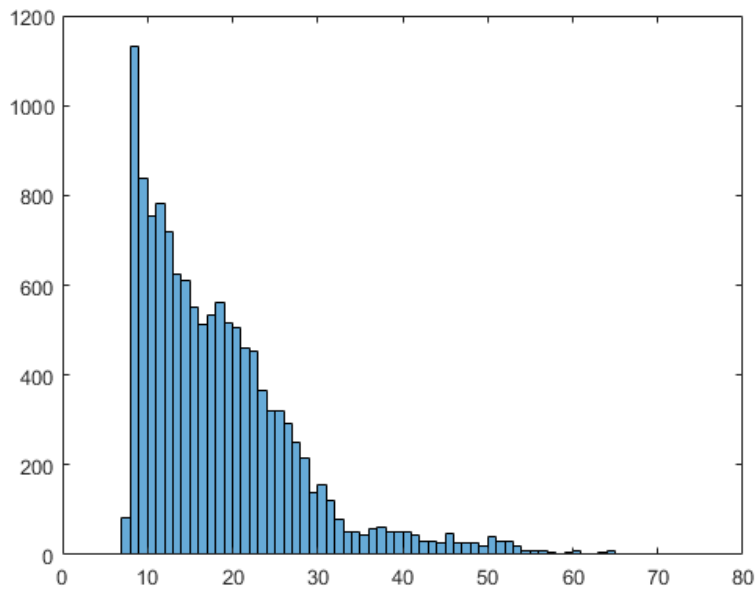


Figure 8.6: Sea margin histogram for all route crossings, for the Amsterdam - New York route

Figure 8.6 shows a histogram of the distribution of all the sea margin values which does not exceed the Beaufort 5 limit. These are the values which are averaged in order to find the total sea margin for the route. It can be seen from the figure that there are large concentrations of for sea margins between 10 and 20%. Then the concentrations for the higher values trail off quickly.

In this case, where the route is from Amsterdam to New York, the overall sea margin is found to be 18.6043%.

### Route Specified For Case Ship

Figure 8.7 shows the route for which the route simulation has been run for, and thus where the weather data has been collected. This route is between Malaysia and Brazil.

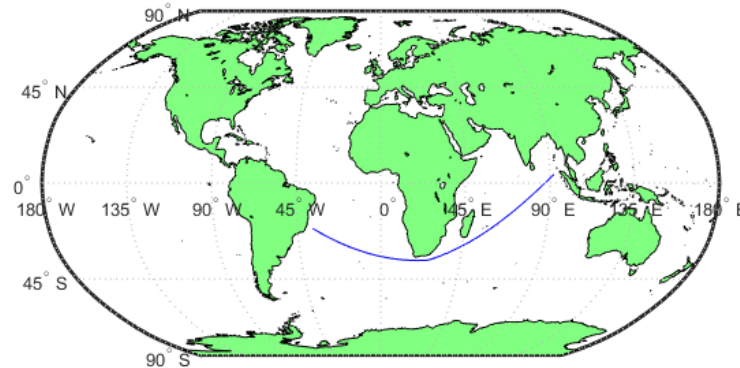


Figure 8.7: Route specified for case ship

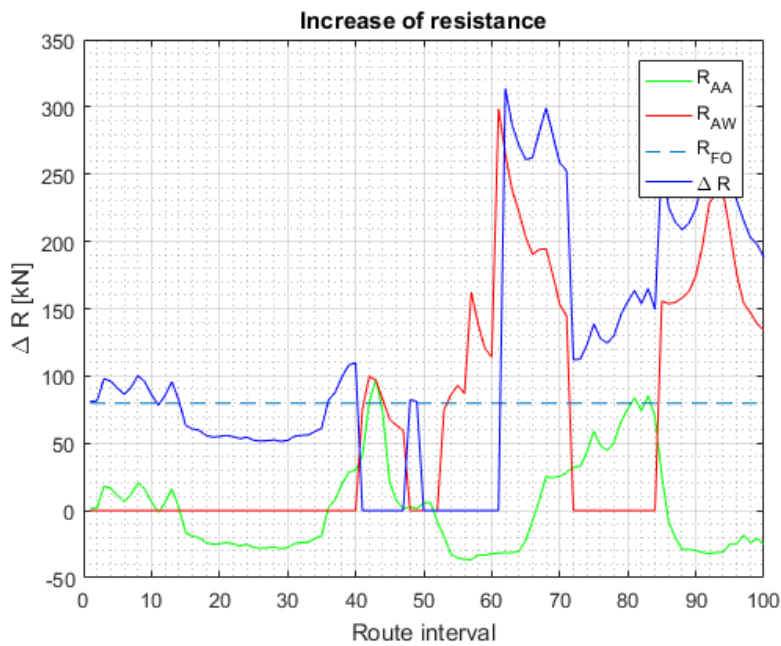


Figure 8.8: Components of the added resistance for route crossing number 14

Figure 8.8 shows the components of the added resistance, with components defined as for Figure 8.2. Here it can be seen that the resistance due to the wind for this route crossing gives a negative contribution to the resistance for some parts of the route, and a positive contribution at other parts. This illustrates well that the ship operates in winds varying between tailwind and

headwind for this route crossing.

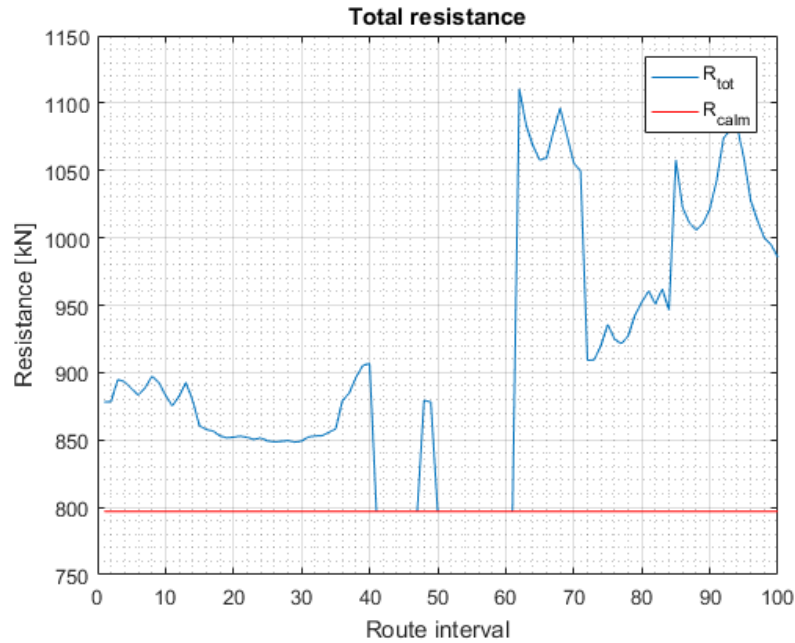


Figure 8.9: The operational resistance for route crossing number 14

Figure 8.9 shows the total resistance in operational conditions, as well as the calm water resistance for the specified speed as a reference line. It can clearly be seen where the weather data is omitted for wind speeds and wave heights above Beaufort 5, where the operational resistance is equal to the calm water resistance.

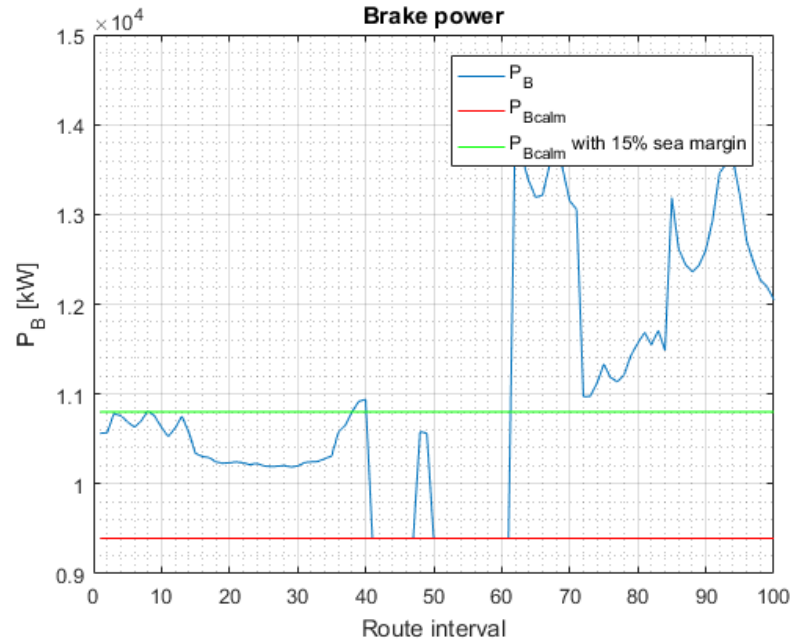


Figure 8.10: The operational brake power for route crossing number 14

Figure 8.10 visualizes the resulting brake power for the same route. The calm water brake power  $P_{Bcalm}$  and the calm water brake power with a 15% sea margin are shown as references to the obtained values. This is route crossing 14, an even number, which means that the ship is traveling to Brazil from Malaysia. For this route crossing it is evident that the ship experiences more weather in the second part of the route, as the corresponding power is higher for these values.

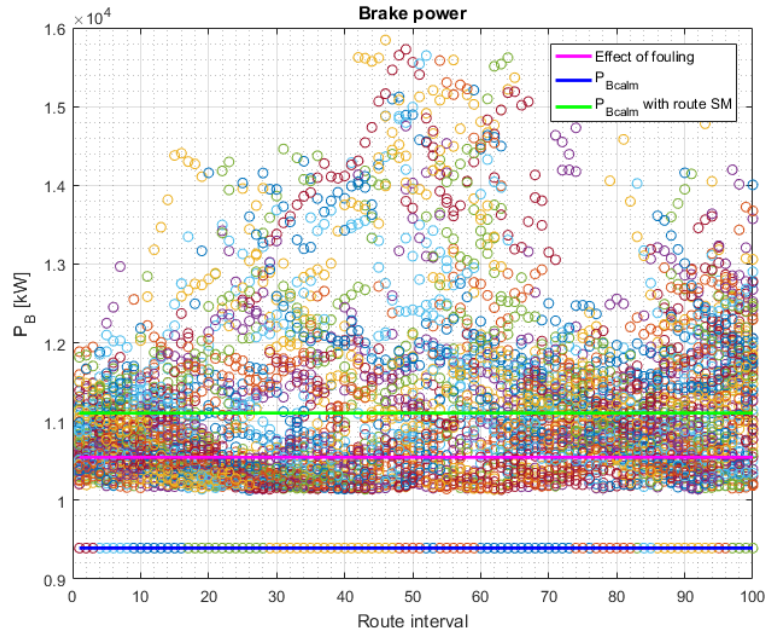


Figure 8.11: Total  $P_B$  distribution for all route crossings combined, for the case ship specified route

Figure 8.11 illustrates the distribution of all the calculated brake power values over the route simulated. The components are as described for Figure 8.5. It can be seen from the figure that the ship typically experiences milder weather in the start of the route. Here the power is concentrated at lower values than later in the route crossing.

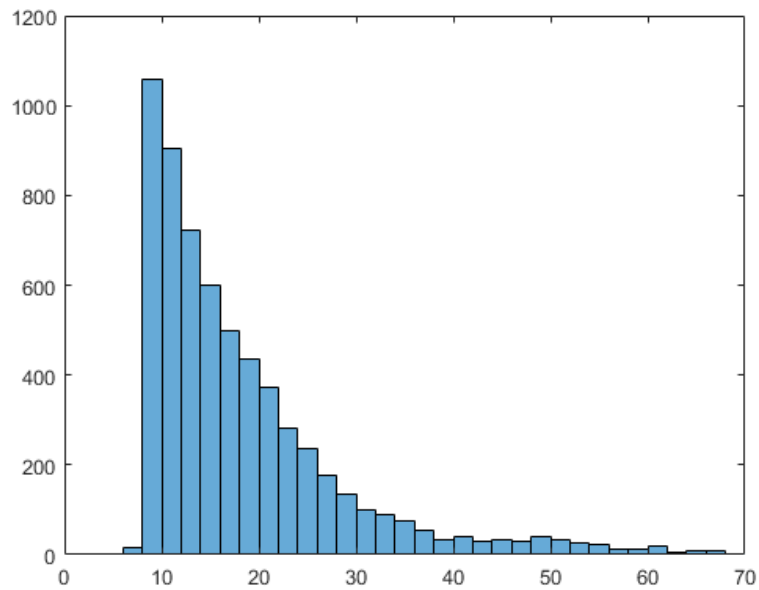


Figure 8.12: Sea margin histogram for all route crossings, for the case route

Figure 8.12 shows a histogram of the sea margin values which does not exceed the Beaufort 5 limit. The histogram shows a clear peak at around 10% and is steadily declining for higher values. The distribution of sea margins for this route is much more uniform than for the route from Amsterdam to New York.

In this case, where the route is from Malaysia to Brazil, the overall sea margin is found to be 18.2475%.

### **Georgetown - Cape Town Route**

Figure 8.13 shows the route for which the route simulation has been run for, and thus where the weather data has been collected.



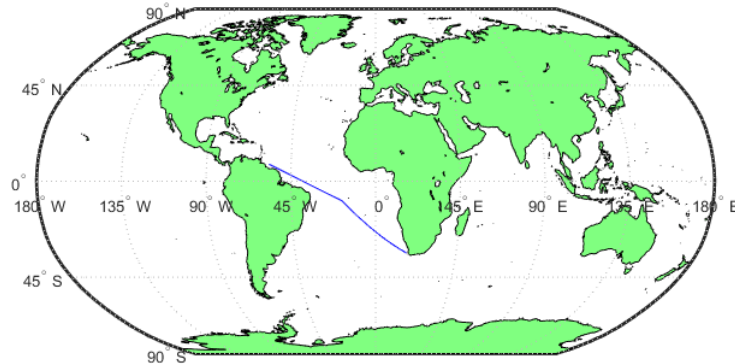


Figure 8.13: Route from Georgetown to Cape Town

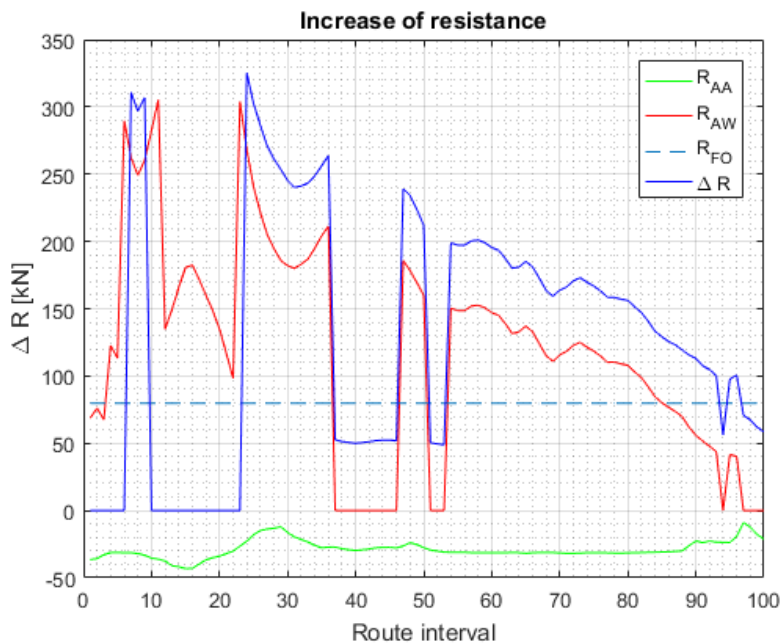


Figure 8.14: Components of the added resistance for route crossing number 14

Figure 8.14 shows the components of the added resistance, with components described as for Figure 8.2. In in this particular route crossing the added resistance due to waves gives a contribution for almost the whole route crossing. This is equivalent with the ship experiencing waves interacting with the ship within a  $\pm 45^\circ$  limit off the bow. The wind gives negative values

for the added resistance throughout the route crossing, which means that the ship is operating in tailwind throughout the route.

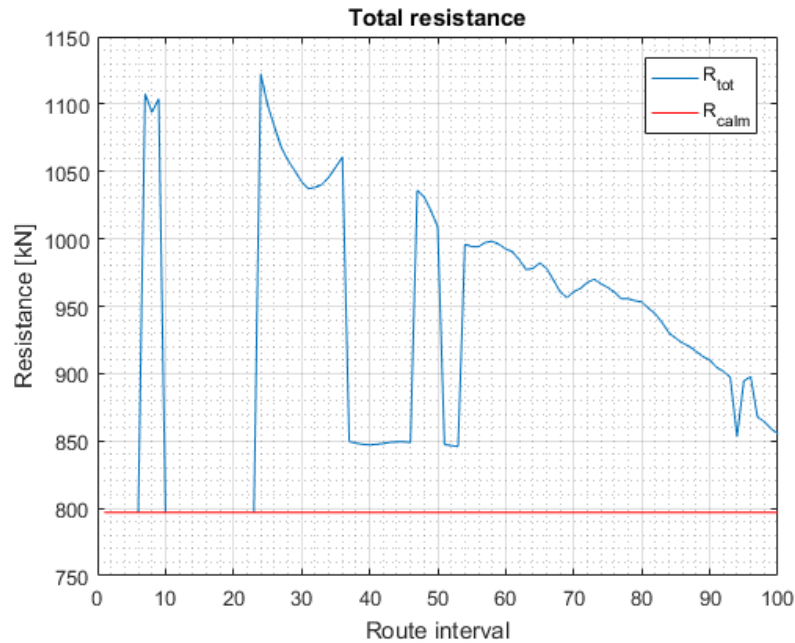


Figure 8.15: The operational resistance for route crossing number 14

Figure 8.15 shows the total resistance in operational conditions, as well as the calm water resistance for the specified speed as a reference line. In this particular route crossing the number of omitted results due to weather being above Beaufort 5 is low. This can be seen as the majority of the operational total resistance values are not equal to the calm water resistance line. The graph is declining for increasing route interval number, which means that for this route crossing the ship experiences milder weather as the route crossing progresses.

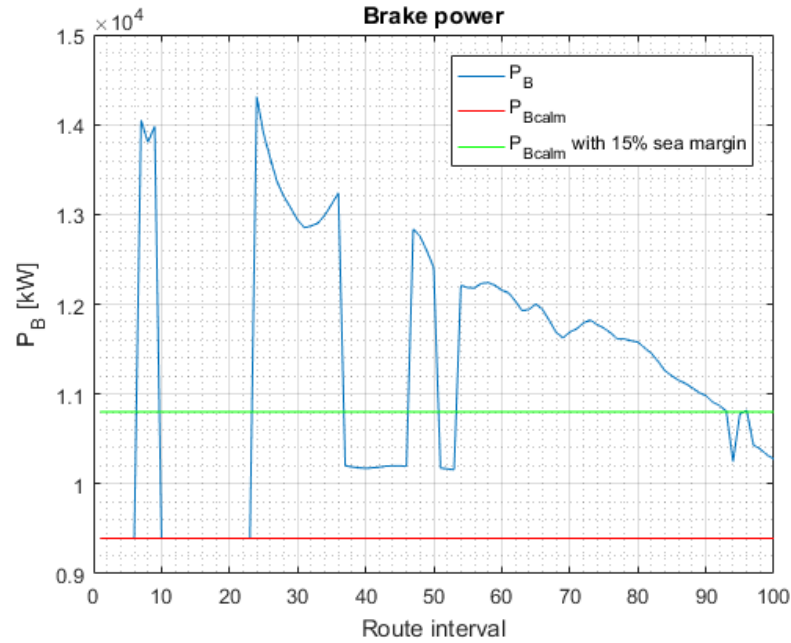


Figure 8.16: The operational brake power for route crossing number 14

Figure 8.16 visualizes the resulting brake power for the same route. The components of this figure are as described for Figure 8.5. For this route crossing it is seen that the majority of the operational brake power values are above the typical 15% sea margin limit. In other words, if the sea margin was to be calculated for this route crossing alone, it could have been seen from this figure that the sea margin would be above 15%.

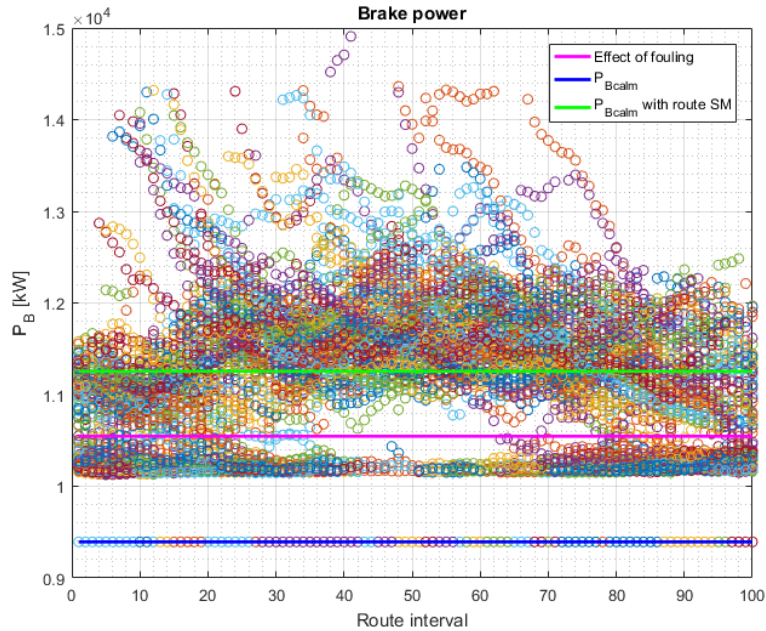


Figure 8.17: Total  $P_B$  distribution for all route crossings combined, for the Georgetown - Cape Town route

Figure 8.17 illustrates the distribution of all the calculated brake power values over the route simulated, with components as described for Figure 8.5. It can be seen from the figure that the ship typically experiences rougher weather in the middle of the route crossings. The middle of the route crossings is located in the middle of the Atlantic Ocean, as can be seen in Figure 8.13. Here the power is typically concentrated at higher values than in the beginning and in the end of the route crossings.

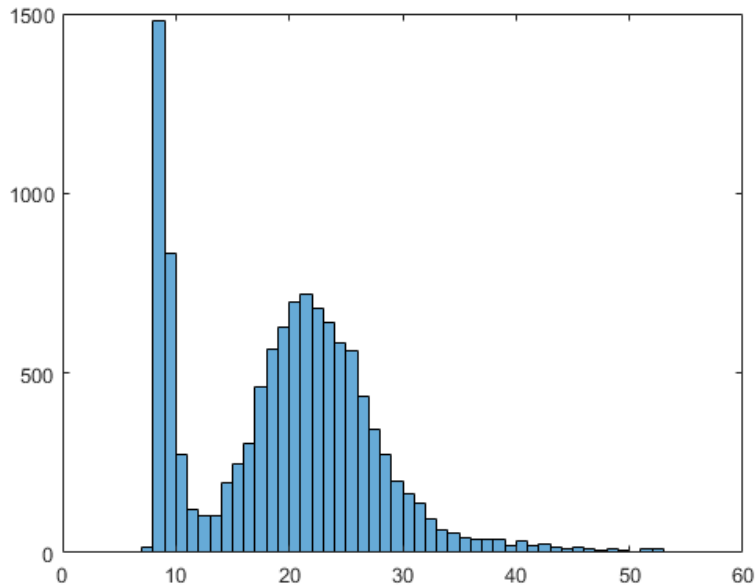


Figure 8.18: Sea margin histogram for all route crossings, for the Georgetown - Cape Town route

Figure 8.18 shows the sea margin histogram for the simulated routes. A large concentration of values can be seen for sea margin of approximately 9% and then a second peak at about 24%. The shape of the sea margin for this simulated route is found to differ quite a lot from the histograms found for the earlier routes. This gap in values around 14% can also be seen from Figure 8.17. There the concentration of power values is less dense.

In this case, where the route is from Georgetown to Cape Town, the overall sea margin is found to be 19.8052%.

### 8.3 Sea Margin From Operational Data

Following the calculation method described in Section 7.2 the mean speed of the measured operational data was found to be 14.1 knots. The mean power of the data was found to be 7619.6 kW. Interpolating to the calm water power line, the corresponding value for the power was found to be 5807.3 kW.

This gives a  $\Delta P$  of 1812.3 kW, which is equal to a 31.21% sea margin for the specified speed.

## 8.4 Application Of Method In Varying Speed

The Amsterdam - New York route simulation was run for varying speeds. Four simulations were performed, at 14, 16, 18 and 19 knots. This was done in order to evaluate how the added resistance and the sea margin changes with speed. In this evaluation the total resistance was filtered for extreme weather in the same way as the sea margin was filtered in the method. Then the resistance was averaged in order to have one representative value for the route simulation. The resistance margin is defined as the change in resistance between averaged, simulated operational resistance and calm water resistance.

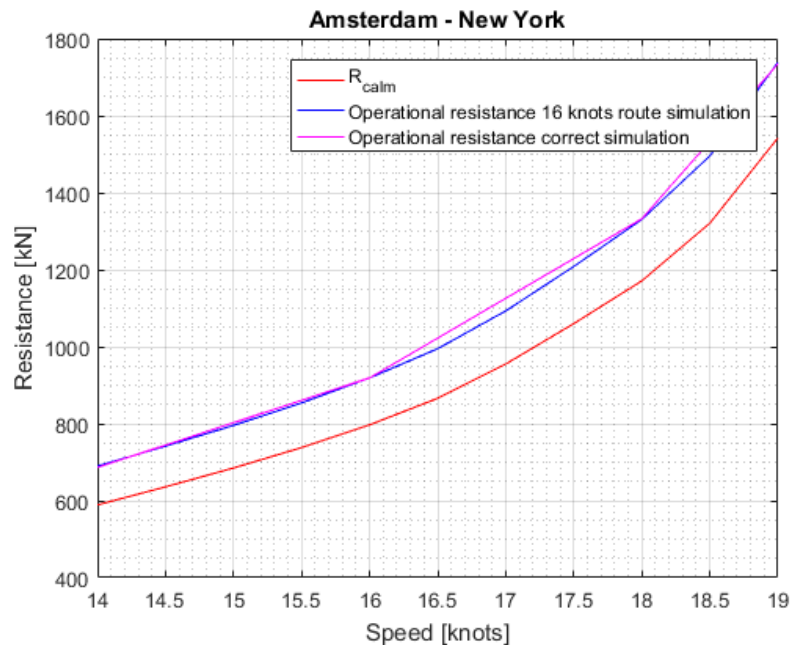


Figure 8.19: Resistance for the Amsterdam - New York route for varying speed

Figure 8.19 shows how the averaged simulated total resistance behaves in varying speed compared to the calm water resistance. The figure shows two lines for the total resistance. The blue line is calculated using the route simulated weather data constant for 16 knots, but the speed in the resistance calculation varying for speed. The pink line is calculated based on route simulations and resistance calculations for the actual speed values. The comparison of these lines are made in order to evaluate whether the simulated weather data for one speed can be used as input in sea margin calculations with different speeds. The route data simulation only uses the speed in order to evaluate where the ship will be at which time.

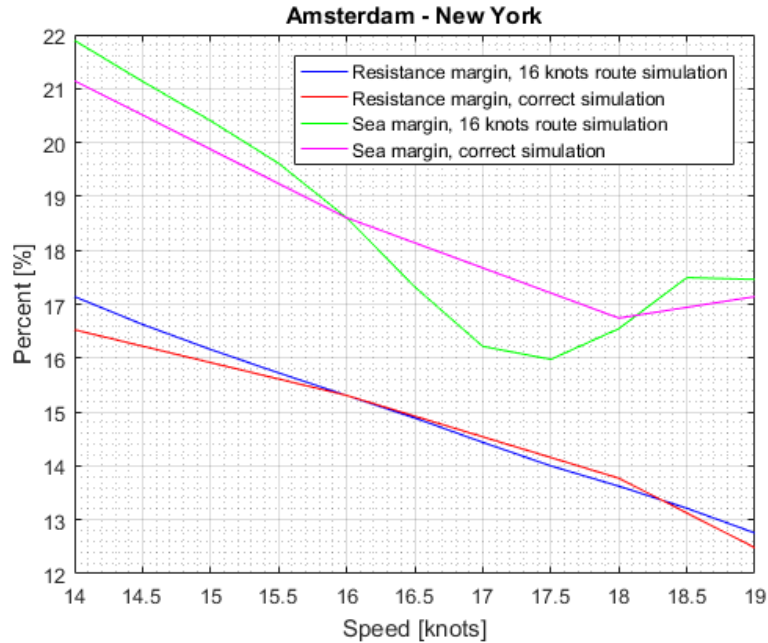


Figure 8.20: Resistance margin and sea margin for the Amsterdam - New York route for varying speed

Figure 8.20 shows how the resistance margin and the sea margin decreases with increasing speed. Identically to the figure above, this figure includes both data for correctly simulated weather data with respect to the speed used in the calculations and weather data simulated at a constant 16 knots speed.

The difference in percentage points, i.e. in margin values, of the resistance margin and sea margin using a speed varying route simulation and a constant route simulation at 16 knots is shown in Table 8.2. The percentage change in total simulated resistance for the two calculation methods is also shown.

Table 8.2: The difference between weather data simulation at a constant speed of 16 knots and for simulations at varying speed

Speed [knots]	Resistance margin [percentage points]	Sea margin [percentage points]	Total resistance [%]
14	0,6145	0,7509	-0,5246
16	0	0	0,0000
18	-0,1483	-0,196	0,1305
19	0,2735	0,3186	-0,2426

# Chapter 9

## Discussion

### 9.1 Evaluation Of $R_{AS}$

The effects of a  $\pm 10^{\circ}C$  change in the temperature caused a change in the added resistance of 18.5 kN and minus 14.5 kN. This is equivalent to a 2.32% and minus 1.95% change in the calm water resistance. In comparison, this is a change in the resulting sea margin of 2.88 and minus 2.38.

It is seen that for increased temperatures, the added resistance has a negative value and will thus decrease the total resistance. This is due to a decrease in the kinematic viscosity. This leads to smaller friction between the ship hull and the water, and thus a decrease in resistance. In other words, it will be beneficial with respect to the resistance to have a ship operating in higher temperatures.

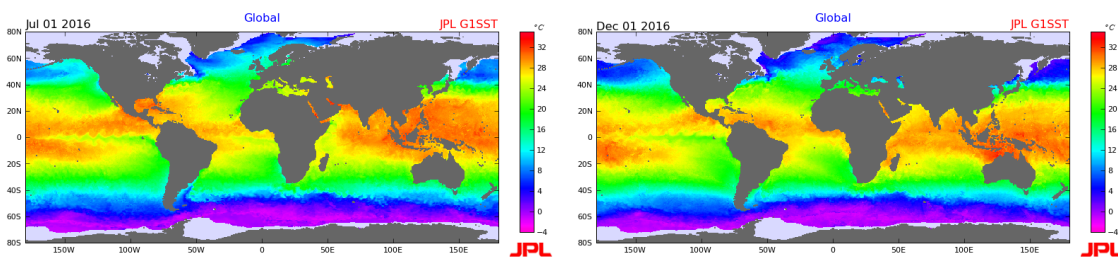


Figure 9.1: Ocean temperatures in July and December 2016, (JPL OurOcean Portal via NASA, 2017)

As seen in Figure 9.1, the ocean temperatures will seldom be outside the  $\pm 10^{\circ}C$  interval of the reference temperature. Also, a ship operating in the routes defined in this thesis is more



likely to encounter higher temperatures than temperatures lower than the reference.

Due to the small overall difference in resistance and that the ship most likely will experience a decrease in resistance due to temperatures, the effects of temperature and density are omitted from the method.

## 9.2 Sea Margin From Route Simulations

All of the routes simulated at the given speed resulted in similar sea margins. The Amsterdam to New York route had a sea margin of 18.60%, the case ship route had a sea margin of 18.25% and the Georgetown to Cape Town route had a sea margin of 19.81%. These sea margin values are slightly higher than the traditional 15% sea margin. Thus, the power of a ship with the traditional sea margin implemented would be underestimated for operations in these routes.

The number of routes the method is implemented for in this thesis is not large enough for to determine a general sea margin for the ship at the given speed. If this is the goal, a strategic choice of representative routes should be made and the resulting sea margins averaged for the routes.

## 9.3 Sea Margin From Measured Operational Data

From Figure 7.3 it can be seen that the ship operates with a varying speed and a constant power. This makes a direct comparison between the measured operational data and the simulated operational data hard to perform. The sea margin at the mean speed of the provided data was found to be 31.21%. The mean speed of the provided data was found to be 14.1 knots.

The sea margin from the route simulated at 14.1 knots was found to be 20.7041%. Thus, the simulated sea margin was underestimated. This can be explained by the fact that the case ship is operated with constant power, which can cause unreliable results of the actual sea margin. Also, the effect of fouling on the actual ship is not known. The fouling effect of the measured data is dependent on when the last hull cleaning was performed.

## 9.4 Speed Dependence Of Added Resistance And Sea Margin

As found in Section 8.4 the added resistance decreases compared with the calm water resistance for increasing speed. The sea margin shows a general reduction as well with varying speed.

The results following a route simulated at a constant speed and with varying speed shows generally small differences in percentage points. Thus, in order to get an idea of the magnitude of the sea margin a route simulation at a constant speed can be used in order to save time. However, it is recommended to perform the route simulations with varying speed in order to get the most reliable results.

## 9.5 Proposed Method In Comparison With Existing Methods

The developed method for calculating the sea margin in this thesis uses many parts of the earlier sea margin calculation methods. The concept of the service margin method is used by adding a percentage on the calm water power. However, the method of finding this percentage is widely more complex in this method than just choosing one based on experience.

The method proposed also uses elements found in Levine and Hawkins' method (Levine and Hawkins, 1970). The proposed method includes the effects of environmental and deteriorative effects, and it is decision based, with a constant speed and specified route.

Swifts method takes the stochastic nature of the ship speed in operation into consideration (Swift, 1975). It assumes a ship, a route, the time in each area of the route, the ship heading and sea state frequency of occurrence. The proposed method differs here by assuming a constant speed. However, the assumptions mentioned have been made for the proposed method as well. This results in a representation of how the resistance is stochastic in nature, dependent on the environmental conditions the ship meets.

Parts from Stasiak's method has not been utilized in the proposed method. Similarly to the ITTC method (ITTC, 2008*b*) the added power is found using the powering prediction method for the proposed method. However, this is where the similarities end between the two methods. Both Stasiak's method and the ITTC method assumes a probabilistic model in order to account for the environmental effects, while the proposed method uses a route simulation for the weather data.

Cho, Kim and Kim's prediction method for the sea margin is the most similar method to the one proposed in this thesis. Both utilizes given routes, the STAWAVE-1 and STAWAVE-2 resistance calculations and the same calculation method for wind resistance.

The proposed method in this thesis has been inspired by many of the earlier works on the subject. However, the resulting method is innovative through the route simulation and provides a new proposition on how to find a rational sea margin.

## 9.6 Limitations Of The Method

The route simulation is not a good estimation of wave data close to shore. Due to the interpolation in latitude and longitude coordinates, some wave parameters are closest to the onshore values, which are non-existent. In this method these non-existing values are set equal to zero in order to disregard them. Data for the route close to shore should be found other ways, or the route should not be defined close to shore. This is not a problem for the wind data, as these are defined onshore as well.

The route simulation does not utilize all the data provided in each three month interval file. This is in order to have an even number of route crossings, and thus an equal number of routes to and from the destination. Some of the time in the end of each file is neglected. This will not have a large influence on the overall calculations.

The method assumes a the limit for extreme weather at Beaufort 5. This is done in order to have a resulting sea margin which represents normal operational conditions, as well as limiting the sea states the method processes. The ISO 15016 standard which is used assumes small sea states, and by limiting the weather above Beaufort 5 the method is more in compliance with the standard.

The method does not include the effect of waves outside of the  $\pm 45^\circ$  limit off the bow. This is specified for the ISO (2015) standard and is due to head waves having the largest effect on the resistance. However, the waves meeting the ship at other angles will also have an effect on the ship resistance. It stands to reason that the sea margin could be affected overall by these as well.

# Chapter 10

## Conclusion And Further Work

### 10.1 Summary And Conclusion

The sea margin describes how much added power is required in operational conditions compared to the calm water conditions in order to maintain a speed in environmental and deteriorative effects. Traditionally a 15% sea margin has been used, based on data from similar ships or experience. In this thesis a more rational method for calculating the sea margin a ship has been proposed and tested.

A literary study has been performed in order to get a greater understanding of what has been done on the subject before. Important parameters which should be implemented in the developed method were found by evaluating the literature.

The added resistance in wind and waves has been calculated using calculation methods from ISO 15016. The effects of water temperature and density on the resistance were evaluated. It was found that these changes represents a small difference in the overall results. In addition, no reliable data for temperature for the individual routes was found. Thus, the effects of temperature and density was neglected.

A route simulation has been developed and implemented in the method. The simulation requires a route and a constant speed as input and delivers weather data for the last five years. Using this weather data, ship parameters and model test data, the sea margin is calculated using the powering prediction method.

The method has been tested for a case ship. The speed was chosen to be the design speed

and three routes were tested: Amsterdam to New York, Malaysia to Brazil and Georgetown to Cape Town. The corresponding sea margins for the routes were found to be 18.60%, 18.25% and 19.81%, respectively. All of the sea margins were found to be higher than the traditional 15% sea margin. Thus, a ship operating at design speed in these routes will be underestimated if the traditional sea margin is implemented. This gives a good indication that the traditional sea margin should not be implemented for operations for the specified speed and routes. The number of routes the method is implemented for in this thesis is not large enough for to determine a general sea margin for the ship at the given speed, but route based sea margins are found.

Measured operational data was available for the case ship. Using this, the sea margin at the average speed of operation was found to be 31.21% at a mean speed of 14.1 knots. The corresponding sea margin for the same speed from the developed method was found to be 20.70%. Thus, the proposed sea margin from the developed method is an underestimation of the actual conditions. However, these results are slightly unreliable, as the case ship is operated at a constant power. Also, the effect of fouling on the actual ship is not known, which can contribute to a large increase in resistance and power. The fouling effect of the measured data is dependent on when the last hull cleaning was performed.

As the sea margin is known to be speed dependent, the proposed method is also used for varying speeds. The change in the added resistance margin and in the sea margin due to speed was found by running the method separately for a range of speeds. This showed that the added resistance margin and the sea margin both decreases with increasing speed.

The proposed method in this thesis has been inspired by the earlier literature on the subject. However, the resulting method is innovative through the route simulation and provides a new proposition on how to find a rational sea margin.

## **10.2 Recommendations For Further Work**

In order to make the proposed method more accurate, several things can be improved on or developed further. The model should be expanded in order to make use of all wave data from the route simulation, not just the waves in the bow section.

The effects of temperature and density on the resistance should be included. Reliable data for the temperature for given routes should be found in order to implement this contribution to the method.

The fouling allowance should be based on more extensive research and use a more exact way of including the effects of marine growth.



# References

Arribas, P. F. (2007), 'Some methods to obtain the added resistance of a ship advancing in waves', *Ocean Engineering* 34(7): 946-955 .

Carlton, J. S. (2012), *Marine Propellers and Propulsion*, Elsevier. 3rd edition.

Cho, Y. R., Kim, Y. T. and Kim, J. G. (2016), 'Prediction of sea margin on the specific route for a vlcc in design stage', *Energy Efficient Ships* .

ECMWF (2017a), 'Direction convention of wave components', <http://www.ecmwf.int/en/faq/what-direction-convention-u-and-v-components-winds>. Online; accessed May 16 2017.

ECMWF (2017b), 'Direction convention of wave fields', <https://www.ecmwf.int/en/faq/what-direction-convention-wave-fields>. Online; accessed June 6 2017.

Faltinsen, O. M. (1990), *Sea Loads On Ships and Offshore Structures*, Cambridge University Press.

Faltinsen, O. M., Minsaas, K. J., Liapis, N. and Skjørdal, S. O. (1980), 'Prediction of resistance and propulsion of a ship in a seaway', *Proc. Thirteenth Symp. on Naval Hydrodynamics* . p. 505-530.

Gerritsma, J. and Beukelman, W. (1972), 'Analysis of the resistance increase in waves of a fast cargo ship', *International Shipbuilding Progress* **19 (217)**.

Grin, R. (2015), 'On the prediction of wave-added resistance with empirical methods', *Journal of Ship Production and Design* 31(3): 181-191. .



- Hellio, C. and Yebra, D. M. (2009), *Advances in Marine Antifouling Coatings and Technologies*, Elsevier Science, Burlington. Woodhead Publishing Series in Metals and Surface Engineering.
- Hogben, N., Dacunha, N. M. C. and Olliver, G. F. (1986), *Marin Teknikk 3 - Hydrodynamikk*, British Maritime Technology by Unwin Brothers Limited.
- ISO (2015), *Ships and Marine technology - Guidelines for the Assessment of Speed and Power Performance by Analysis of Speed Trial Data*, second edn, International Standard. ISO 15016.
- ITTC (2008a), *Recommended Procedures and Guidelines: Performance, Propulsion 1978 ITTC Performance Prediction Method*, revision 01 edn, International Towing Tank Conference. 7.5 - 02 03 - 01.4.
- ITTC (2008b), *Recommended Procedures and Guidelines: Testing and Extrapolation Methods, Propulsion, Performance, Predicting Powering Margins*, revision 01 edn, International Towing Tank Conference. 7.5 - 02 03 - 01.5.
- JPL OurOcean Portal via NASA (2017), 'Global 1-km sea surface temperature (gl1sst)', <https://ourocean.jpl.nasa.gov/SST/>. Online; accessed June 4 2017.
- Levine, G. H. and Hawkins, S. (1970), 'Comments on service margins for ships (with discussion)', *Society of Naval Architects and Marine Engineers* **SNAME Order 511**.
- Molland, A. F., Turnock, S. R. and Hudson, D. A. (2011), *Ship Resistance and Propulsion: Practical Estimation of Ship Propulsive Power*, Cambridge University Press.
- Pettersen, B. (2007), *Marin Teknikk 3 - Hydrodynamikk*, Akademika Forlag. Compendium.
- Stasiak, J. (2004), 'Service margin - solution of the problem or a problem waiting for a solution', *Polish Maritime Research, special issue*.
- Steen, S. and Minsaas, K. (2013), *Naval Hydrodynamics - Ship Resistance*, Akademika Forlag. Compendium.
- Swain, G. W., Kovach, B., Touzot, A., Casse, F. and Kavanagh, C. (2007), 'Measuring the performance of today's antifouling coatings', *Journal of Ship Production* **Vol. 23, No. 3**. p. 164–170.

Swift, P. M. (1975), 'An approach to the rational selection of the power service margin', *The University of Michigan, College of Engineering* **No. 174**.

The Motor Ship (2016), 'Image copyright © Mercator Media', [http://www.motorship.com/\\_data/assets/image/0024/428253/Hull-fouling.jpg](http://www.motorship.com/_data/assets/image/0024/428253/Hull-fouling.jpg). Online; accessed December 1 2016.

Townsin, R. L. (1985), 'The ittc line - its genesis and correlation allowance', *The Naval Architect*, .

Townsin, R. L. (2003), 'The ship hull fouling penalty', *Biofouling*, 19:S1, 9-15.

University of Stavanger (2013), 'Working under extreme conditions', <http://www.uis.no/news/working-under-extreme-conditions-article69473-8865.html>. Online; accessed December 1 2016.

van den Boom, H., Huisman, H. and Mennen, F. (2013), 'New guidelines for speed/power trials'. Found at <http://www.marin.nl/web/JIPs-Networks/JIPs-public/STA.html>.



# Appendix A

## Digital Appendix

Attached to this thesis there is a file containing several MatLab scripts, weather data in *grib* files, routes in *kml* files and saved workspaces. Following is a brief presentation of what the files contains.

### MatLab Files

The following list of MatLab files are attached in the digital appendix:

- main.m  
*Main script for route simulation.*
- route.m  
*Function. Calls on other functions and creates resulting weather matrices.*
- route\_coords.m  
*Function. Manipulates the route coordinates.*
- grib\_reader.m  
*Function. Uses weather data input files and route information in order to find the relevant data.*
- iso\_input.m  
*Input file for ship parameters and model test data.*

- wind.m  
*Calculates the added resistance due to wind.*
- waves.m  
*Calculates the added resistance due to waves. Calls on R\_waves.m.*
- R\_waves.m  
*Function. Calculates the STAWAVE-2 method.*
- criteria.m  
*Evaluates whether the STAWAVE-2 method can be applied.*
- resistance.m  
*Calculates the total added resistance and the corresponding total resistance for the simulated route.*
- openwater.m  
*Input data file for the open water test.*
- SM\_calculation.m  
*Calculates the sea margin through powering prediction.*
- temp.m  
*Evaluates the effect of a  $\pm 10^{\circ}$  change in the water temperature.*

Additionally, three *kml* files are included, which is the input data for the three routes described in the thesis.

The folder *weatherdata* contains *grib* files which are used automatically as input in the route simulation. The files are divided into three month intervals. Due to a limitation in the allowed size of the digital appendix, only weather data for the last three years are included. When using the code, the *route.m* script must be changed in order reflect this as specified in Section 6.1.1.

The folder *saved\_data* contains results from three route simulations. This data can be used directly in the sea margin calculations. The *nctoolbox-1.1.3* folder contains code which is implemented automatically in the route simulations. The *kml2struct.m* code is implemented automatically in order to read the route input data from the *kml* files.

# Appendix B

## STAWAVE-2 Calculations

All formulations in this appendix can be found in ISO (2015). The mean resistance increase in long crested irregular waves in Newtons:

$$R_{AWL} = 2 \int_0^{\infty} \frac{R_{wave}(\omega, V_S)}{\zeta_A^2} S_{\eta}(\omega) d\omega$$

The empirical transfer function,  $R_{wave}$ :

$$R_{wave} = R_{AWML} + R_{AWRL}$$

Mean resistance increase due to wave reflection:

$$R_{AWML} = 4\rho s g \zeta_A^2 \frac{B^2}{L_{PP}} r_{aw}^-(\omega)$$

with

$$r_{aw}^-(\omega) = \bar{\omega}^{b_1} \exp\left(\frac{b_1}{d_1}(1 - \bar{\omega}^{d_1})\right) a_1 Fr^{1.50} \exp(-3.50Fr)$$

$$\bar{\omega} = \frac{\sqrt{\frac{L_{PP}}{g}} \sqrt[3]{k_{yy}}}{1.17Fr^{-0.143}} \omega$$

$$a_1 = 60.3C_B^{1.34}$$

$$b_1 = \begin{cases} 11.0 & \text{for } \bar{\omega} < 1 \\ -8.50 & \text{elsewhere} \end{cases}$$

$$d_1 = \begin{cases} 14.0 & \text{for } \bar{\omega} < 1 \\ -566 \left( \frac{L_{PP}}{B} \right)^{-2.66} & \text{elsewhere} \end{cases}$$

The motion induced resistance:

$$R_{AWRL} = \frac{1}{2} \rho_S g \zeta_A^2 B \alpha_1(\omega)$$

$$\alpha_1(\omega) = \frac{\pi^2 I_1^2(1.5kT_M)}{\pi^2 I_1^2(1.5kT_M) + K_1^2(1.5kT_M)} f_1$$

$$f_1 = 0.692 \left( \frac{V_S}{\sqrt{T_M g}} \right)^{0.769} + 1.81 C_B^{6.95}$$

Where

$\rho_S$  is the water density in full scale [ $kg/m^3$ ].

$g$  is the gravitational acceleration [ $m/s^2$ ].

$\zeta_A$  is the the wave amplitude [m].

$L_{PP}$  is the ship's length between perpendiculars [m].

$B$  is the breadth of the ship [m].

$T_M$  is the midships draught [m].

$C_B$  is the block coefficient.

$Fr$  is the Froude number.

$V_S$  is the speed of the ship through the water [m/s].

$k_{yy}$  is the non-dimensional radius of gyration in the lateral direction.

$I_1$  is the modified Bessel function of the first kind of order 1.

$K_1$  is the modified Bessel function of the second kind of order 1.

$k$  is the wave number [rad/m].

The Pierson-Moskowitz frequency spectrum:

$$S_{\eta} = \frac{A_{fw}}{\omega^5} \exp\left(-\frac{B_{fw}}{\omega^4}\right)$$

where

$$A_{fw} = 173 \frac{H_{1/3}^2}{T_{01}^4}$$

and

$$B_{fw} = \frac{691}{T_{01}^4}$$

Where

$\omega$  is the circular frequency of regular waves [rad/s].

$H_{1/3}$  is the significant wave height [m].

$T_{01}$  is the mean wave period [s].





# Appendix C

## ShipX Graph

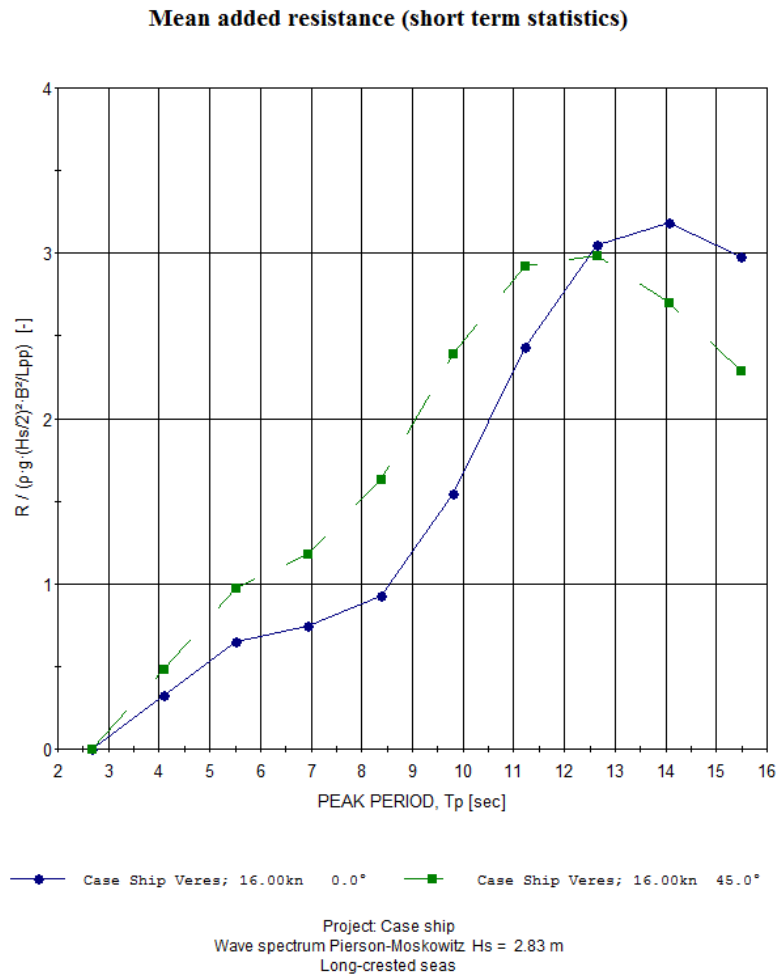


Figure C.1: Coefficients for mean added resistance in waves from ShipX



# Appendix D

## MatLab Code - Route Simulation

### main.m

```
1 % ----- Route simulation -----
2 route_data = 'amsterdam_newyork.kml';
3 tic
4 [U_wind_matrix, V_wind_matrix, H_13_matrix, MWP_matrix, MWD_matrix, ...
5     arclength_m, azimuth, arclength_m_return, azimuth_return, latitude, ...
6     longitude, latitude_return, longitude_return, time_points] = ...
7     route (route_data);
8
9 wtime = toc;
10 fprintf ( 1, ' MY_PROGRAM took %f seconds to run.\n', wtime );
11
12
13 % Plot the route from Google Earth in a world map in MatLab
14 % Performed in order to visually check that the route is correct
15 figure
16 worldmap world
17 geoshow('landareas.shp', 'FaceColor', [0.5 1.0 0.5])
```

```
18 geoshow(latitude ,longitude)
```

## route.m

```
1 function [U_wind_matrix, V_wind_matrix, H_13_matrix, MWP_matrix, ...
2         MWD_matrix,arclength_m, azimuth, arclength_m_return, ...
3         azimuth_return, latitude ,longitude, latitude_return, ...
4         longitude_return ,time_points] = route (route_data)
5 %-----
6 [latitude , longitude , latitude_return , longitude_return , ...
7         latitude_points , longitude_points , longitude_return_points , ...
8         latitude_return_points] = route_coords (route_data);
9
10 % ----- Defining grib files for five years -----
11 quarter = { '2012_Q1.grib' ; '2012_Q2.grib' ; '2012_Q3.grib' ; '2012_Q4.grib' ; ...
12             '2013_Q1.grib' ; '2013_Q2.grib' ; '2013_Q3.grib' ; '2013_Q4.grib' ; ...
13             '2014_Q1.grib' ; '2014_Q2.grib' ; '2014_Q3.grib' ; '2014_Q4.grib' ; ...
14             '2015_Q1.grib' ; '2015_Q2.grib' ; '2015_Q3.grib' ; '2015_Q4.grib' ; ...
15             '2016_Q1.grib' ; '2016_Q2.grib' ; '2016_Q3.grib' ; '2016_Q4.grib' };
16
17 numberofmonths = 20;
18 file = fullfile('weatherdata',quarter);
19 file = char(file);
20
21 % ----- Run simulation for five years -----
22 for j=1:numberofmonths
23     grib = ncgeodataset(file(j,:));
24     [U_wind_mat, V_wind_mat, H_13_mat, MWD_wave_mat, MWP_wave_mat, ...
25         arclength_m, azimuth, arclength_m_return, azimuth_return ,...
26         time_points] = grib_reader(grib , latitude_points , ...
```

```

27     longitude_return_points, latitude_return_points, longitude_points, ...
28     longitude, latitude, latitude_return, longitude_return);
29
30 % ----- Saving matrices created in each run -----
31 filename_Uwind = ['U_wind_' num2str(j)];
32 save(filename_Uwind, 'U_wind_mat');
33
34 filename_Vwind = ['V_wind_' num2str(j)];
35 save(filename_Vwind, 'V_wind_mat');
36
37 filename_H13 = ['H_13_' num2str(j)];
38 save(filename_H13, 'H_13_mat');
39
40 filename_MWP = ['MWP_' num2str(j)];
41 save(filename_MWP, 'MWP_wave_mat');
42
43 filename_MWD = ['MWD_' num2str(j)];
44 save(filename_MWD, 'MWD_wave_mat');
45 end
46
47 % ----- Loading the matrices from the simulation -----
48 for j = 1:numberofmonths
49     filename_Uwind = ['U_wind_' num2str(j)];
50     U_wind_load(j) = load(filename_Uwind, 'U_wind_mat');
51
52     filename_Vwind = ['V_wind_' num2str(j)];
53     V_wind_load(j) = load(filename_Vwind, 'V_wind_mat');
54
55     filename_H13 = ['H_13_' num2str(j)];
56     H_13_load(j) = load(filename_H13, 'H_13_mat');

```

```
57
58 filename_MWD      = [ 'MWD_' num2str(j) ];
59 MWD_load(j)       = load(filename_MWD, 'MWD_wave_mat');
60
61 filename_MWP      = [ 'MWP_' num2str(j) ];
62 MWP_load(j)       = load(filename_MWP, 'MWP_wave_mat');
63 end
64
65 % ----- Combining values from all the runs, making one resulting matrix -----
66 U_wind_table = struct2cell(U_wind_load);
67 V_wind_table = struct2cell(V_wind_load);
68 H_13_table = struct2cell(H_13_load);
69 MWD_table = struct2cell(MWD_load);
70 MWP_table = struct2cell(MWP_load);
71
72 U_wind_test  = cell2mat(U_wind_table);
73 V_wind_test  = cell2mat(V_wind_table);
74 H_13_test   = cell2mat(H_13_table);
75 MWD_test    = cell2mat(MWD_table);
76 MWP_test    = cell2mat(MWP_table);
77
78
79 U_wind_cell = num2cell(U_wind_test,[1,2]);
80 U_wind_matrix = cat(1,U_wind_cell{:});
81
82 V_wind_cell = num2cell(V_wind_test,[1,2]);
83 V_wind_matrix = cat(1,V_wind_cell{:});
84
85 H_13_cell = num2cell(H_13_test,[1,2]);
86 H_13_matrix = cat(1,H_13_cell{:});
```

```

87
88 MWP_cell = num2cell(MWP_test,[1,2]);
89 MWP_matrix = cat(1,MWP_cell{:});
90
91 MWD_cell = num2cell(MWD_test,[1,2]);
92 MWD_matrix = cat(1,MWD_cell{:});
93
94 % ----- Changing all NaN values to 0 -----
95 U_wind_matrix(isnan(U_wind_matrix)) = 0;
96 V_wind_matrix(isnan(V_wind_matrix)) = 0;
97 H_13_matrix(isnan(H_13_matrix)) = 0;
98 MWD_matrix(isnan(MWD_matrix)) = 0;
99 MWP_matrix(isnan(MWP_matrix)) = 0;
100 end

```

## route\_coords.m

```

1 function [latitude , longitude , latitude_return , longitude_return , ...
2         latitude_points , longitude_points , longitude_return_points , ...
3         latitude_return_points] = route_coords (route_data)
4 %
5 clearvars latitude1
6 clearvars longitude1
7 addpath('nctoolbox-1.1.3');
8 setup_nctoolbox;
9
10 % ----- Import kml file from Google Earth -----
11 s = kml2struct(route_data);
12
13 % ----- Define latitude and longitude vectors -----

```



```

14 Lat = s.Lat;
15 Lon = s.Lon;
16
17 % ----- Arclengths and azimuths between coordinates in vector form -----
18 for i = 1:length(Lat)-1
19     [arclen1(i),az(i)] = distance(Lat(i),Lon(i),Lat(i+1),Lon(i+1),...
20         'degrees');
21 end
22
23 % ----- Summation of arclengths -----
24 arclen = sum(arclen1);
25
26 % ----- Make the route have 100 intervals -----
27 intervalnumber = 100;
28 for i = 1:length(Lat)-1
29     if (intervalnumber /arclen)*arclen1(i) < 1
30         splitperint(i) = 1;
31     else
32         splitperint(i) = (intervalnumber /arclen)*arclen1(i);
33     end
34 end
35 splitperint = round(splitperint);
36
37 % ----- Dividing the vector into more intervals -----
38 for i = 1:length(Lat)-1
39     [latitude1{i},longitude1{i}] = gcwaypts(Lat(i),Lon(i),Lat(i+1), ...
40         Lon(i+1),splitperint(i));
41 end
42
43 latitude1 = cell2mat(latitude1');

```

```

44 latitude1 = round(latitude1 , 10);
45 latitude_points = latitude1 ([1, diff(latitude1 ')]~=0);
46 latitude_return_points = flipud(latitude_points);
47
48 longitude1 = cell2mat(longitude1 ');
49 longitude1 = round(longitude1,10);
50 longitude_points = longitude1 ([1, diff(longitude1 ')]~=0);
51 longitude_return_points = flipud(longitude_points);
52
53 % -- Making mid-values in the coordinates to represent the interval -----
54 latitude           = zeros ();
55 longitude          = zeros ();
56 latitude_return    = zeros ();
57 longitude_return    = zeros ();
58
59 for i = 1:1:length(latitude_points)-1
60     latitude(i) = ((latitude_points(i)+latitude_points(i+1))/2);
61     longitude(i) = ((longitude_points(i)+longitude_points(i+1))/2);
62     latitude_return(i) = ((latitude_return_points(i) + ...
63         latitude_return_points(i+1))/2);
64     longitude_return(i) = ((longitude_return_points(i) + ...
65         longitude_return_points(i+1))/2);
66 end
67 latitude = latitude ';
68 longitude = longitude ';
69 latitude_return = latitude_return ';
70 longitude_return = longitude_return ';
71
72 end

```

**`grib_reader.m`**

```

1 function [U_wind_mat, V_wind_mat, H_13_mat, MWD_wave_mat, MWP_wave_mat, ...
2     arclength_m, azimuth, arclength_m_return, azimuth_return, ...
3     time_points] = grib_reader(grib, latitude_points, ...
4     longitude_return_points, latitude_return_points, longitude_points, ...
5     longitude, latitude, latitude_return, longitude_return)
6 % ----- Speed -----
7 % Assign value to the constant speed in knots:
8 V_knots    = 16;
9 V_des      = V_knots * 1852/3600; % [m/s]
10
11 % ----- Read weather file -----
12 % Take a look at the variables available within the dataset:
13 grib.variables;
14
15 % Determine the shape of the selected variable (Each the same size):
16 grib.size('10_metre_U_wind_component_surface');
17 grib.size('10_metre_V_wind_component_surface');
18 grib.size('Significant_wave_height_msl');
19 grib.size('Significant_wave_height_msl');
20 grib.size('Mean_wave_period_msl');
21
22 % Creating geovvariable object to access data in MATLAB style indexing:
23 U_wind1    = grib.geovvariable('10_metre_U_wind_component_surface');
24 V_wind1    = grib.geovvariable('10_metre_V_wind_component_surface');
25 H_13       = grib.geovvariable('Significant_wave_height_msl');
26 MWD        = grib.geovvariable('Mean_wave_direction_msl');
27 MWP        = grib.geovvariable('Mean_wave_period_msl');
28

```

```

29 % The range of time instances available in the grib file:
30 time_max = length(U_wind1.data(:,1,1));
31
32 % The dimensions are 'time', 'lat' and 'lon' for all components:
33 grib.dimensions('10_metre_U_wind_component_surface');
34 grib.dimensions('10_metre_V_wind_component_surface');
35 grib.dimensions('Significant_wave_height_msl');
36 grib.dimensions('Mean_wave_direction_msl');
37 grib.dimensions('Mean_wave_period_msl');
38
39 % ----- Checking the size and class of the components -----
40 % U component of the wind:
41 size(U_wind1);
42 class(U_wind1);
43 % V component of the wind:
44 size(V_wind1);
45 class(V_wind1);
46 % Significant wave height:
47 size(H_13);
48 class(H_13);
49 % Wave direction:
50 size(MMD);
51 class(MMD);
52 % Wave period:
53 size(MMP);
54 class(MMP);
55
56 % ----- The arrangement of the dimensions -----
57 % The arrangement is as follows: time = row, lat = column, and lon = page.
58 % A subset of (1, :, :) means that the code grabs the first time step

```

```

59 % and the entire spatial domain of the dataset.
60 U_wind      = U_wind1.data (:, :, :);
61 V_wind      = V_wind1.data (:, :, :);
62 H_13        = H_13.data (:, :, :);
63 MMD         = MMD.data (:, :, :);
64 MWP         = MWP.data (:, :, :);
65
66 % Change arrangement: lat = row, lon = column, time = page:
67 U_wind      = permute(U_wind,[2 3 1]);
68 V_wind      = permute(V_wind,[2 3 1]);
69 H_13        = permute(H_13,[2 3 1]);
70 MMD         = permute(MMD,[2 3 1]);
71 MWP         = permute(MWP,[2 3 1]);
72
73 % It may be necessary to remove singleton dimensions for Matlab
74 % commands like plotting using the function squeeze.
75 U_wind      = squeeze(double(U_wind));
76 V_wind      = squeeze(double(V_wind));
77 H_13_wave   = squeeze(double(H_13));
78 MWD_wave    = squeeze(double(MMD));
79 MWP_wave    = squeeze(double(MWP));
80
81 % ----- Create vectors for coordinates, to save operational time -----
82 % Latitude is now from -90 to 90, not 90 to -90, due to Matlab coding
83 coords_latitude = -90:0.75:90;
84 coords_longitude = -180:0.75:179.25;
85 coords_lat      = coords_latitude';
86 coords_lon      = coords_longitude';
87
88 % Flip values as latitude coordinates are now from -90 to 90.

```

```

89 U_wind           = flipud (U_wind) ;
90 V_wind           = flipud (V_wind) ;
91 H_13_wave        = flipud (H_13_wave) ;
92 MWD_wave         = flipud (MWD_wave) ;
93 MWP_wave         = flipud (MWP_wave) ;
94
95 % Move values in compliance with lon coords from -180 to 180
96 skip             = length (U_wind) / 2;
97 U_wind           = circshift (U_wind, [0 , skip] ) ;
98 V_wind           = circshift (V_wind, [0 , skip] ) ;
99 H_13_wave        = circshift (H_13_wave, [0 , skip] ) ;
100 MWP_wave         = circshift (MWP_wave, [0 , skip] ) ;
101 MWD_wave         = circshift (MWD_wave, [0 , skip] ) ;
102
103 % --- Calculate the time spent in each interval with a constant speed ---
104 % Arclengths and azimuths with the route divided into intervals
105 arclength        = zeros () ;
106 azimuth          = zeros () ;
107 arclength_return = zeros () ;
108 azimuth_return   = zeros () ;
109
110 % Arclength in degrees:
111 for i = 1:length (latitude_points)-1
112     [arclength (i) , azimuth (i)] = distance (latitude_points (i) , ...
113         longitude_points (i) , latitude_points (i+1) , longitude_points (i+1) , ...
114         'degrees' ) ;
115     [arclength_return (i) , azimuth_return (i)] = ...
116         distance (latitude_return_points (i) , longitude_return_points (i) , ...
117         latitude_return_points (i+1) , longitude_return_points (i+1) , ...
118         'degrees' ) ;

```

```

119 end
120
121 % Arclength in meters:
122 arclength_m          = distdim(arclength, 'deg', 'm');
123 arclength_m_return   = distdim(arclength_return, 'deg', 'm');
124
125 % Summation of arclengths in degrees:
126 arclength_sum        = sum(arclength);
127 arclength_sum_return = sum(arclength_return);
128
129 % Summation of arclengths in meters:
130 arclength_sum_m      = sum(arclength_m);
131 arclength_sum_m_return = sum(arclength_m_return);
132
133 % Time in each interval: time = distance/speed
134 time_interval        = arclength_m./V_des;
135 time_interval_return = arclength_m_return./V_des;
136
137 % ----- Calculating crossing time of route -----
138 time_tot              = arclength_sum_m/V_des; %[s]
139 time_tot_minute       = time_tot / 60; % [min]
140 time_tot_hour         = time_tot_minute / 60; % [hour]
141 time_tot_six          = time_tot_hour / 6; % Grib data time steps
142 time_tot_day          = time_tot_hour / 24; % [days]
143
144 % ----- Create startpoints for continous route crossings -----
145 time_min = 0;
146 start_points = time_min:time_tot_six:time_max-time_tot_six;
147
148 % ----- Creating a time matrix, with an even number of routes -----

```

```

149 time_interval = time_interval./(60*60*6);
150 time_interval_return = time_interval_return./(60*60*6);
151
152 clearvars time_mat;
153 for i = 1:length(start_points)
154     if mod(i,2) == 0 % even numbers
155         time_loop = [start_points(i) time_interval_return];
156         time_mat(i,:) = time_loop;
157     else % odd numbers
158         time_loop = [start_points(i) time_interval];
159         time_mat(i,:) = time_loop;
160     end
161 end
162
163 time_points_int = cumsum(time_mat,2);
164
165 if mod(size(time_points_int,1),2) ~= 0
166     time_points_int(end,:) = [];
167 end
168
169 for j = 1:size(time_points_int, 1)
170     for i = 1:(size(time_points_int, 2)-1)
171         time_points(j,i) = ((time_points_int(j,i)+time_points_int(j,i+1))/2);
172     end
173 end
174 % ----- Create route time vector for interpolation -----
175 coords_time = 0:1:time_max-1;
176
177 % ----- Integrate U_wind in time and space -----
178 % Add that even numbers are return and odd numbers are to destination.

```



```

179 U_wind_route = zeros();
180 U_wind_mat= zeros();
181 for j = 1:1:size(time_points, 1)
182     for i = 1:1:length(longitude)
183         if mod(j,2) == 0 % even numbers
184             U_wind_route(i) = interp3(coords_lon, coords_lat, ...
185                 coords_time, U_wind, longitude_return(i), ...
186                 latitude_return(i), time_points(j, i));
187             U_wind_mat(j, i) = U_wind_route(i);
188         else
189             U_wind_route(i) = interp3(coords_lon, coords_lat, ...
190                 coords_time, U_wind, longitude(i), latitude(i), ...
191                 time_points(j, i));
192             U_wind_mat(j, i) = U_wind_route(i);
193         end
194     end
195 end
196 % ----- Integrate V_wind in time and space -----
197 V_wind_route = zeros();
198 V_wind_mat = zeros();
199 for j = 1:1:size(time_points, 1)
200     for i = 1:1:length(longitude)
201         if mod(j,2) == 0 % even numbers
202             V_wind_route(i) = interp3(coords_lon, coords_lat, ...
203                 coords_time, V_wind, longitude_return(i), ...
204                 latitude_return(i), time_points(j, i));
205             V_wind_mat(j, i) = V_wind_route(i);
206         else
207             V_wind_route(i) = interp3(coords_lon, coords_lat, ...
208                 coords_time, V_wind, longitude(i), latitude(i), ...

```

```

209         time_points(j , i));
210         V_wind_mat(j , i) = V_wind_route(i);
211     end
212 end
213 end
214 % ----- Integrate H_13 in time and space -----
215 H_13_route = zeros();
216 H_13_mat = zeros();
217 for j = 1:1:size(time_points , 1)
218     for i = 1:1:length(longitude)
219         if mod(j,2) == 0 % even numbers
220             H_13_route(i) = interp3(coords_lon , coords_lat , ...
221                 coords_time , H_13_wave , longitude_return(i) , ...
222                 latitude_return(i) , time_points(j , i));
223             H_13_mat(j , i) = H_13_route(i);
224         else
225             H_13_route(i) = interp3(coords_lon , coords_lat , coords_time , ...
226                 H_13_wave , longitude(i) , latitude(i) , time_points(j , i));
227             H_13_mat(j , i) = H_13_route(i);
228         end
229     end
230 end
231 % ----- Integrate MWD in time and space -----
232 MWD_wave_route = zeros();
233 MWD_wave_mat = zeros();
234 for j = 1:1:size(time_points , 1)
235     for i = 1:1:length(longitude)
236         if mod(j,2) == 0 % even numbers
237             MWD_wave_route(i) = interp3(coords_lon , coords_lat , ...
238                 coords_time , MWD_wave , longitude_return(i) , ...

```

```

239         latitude_return(i),time_points(j,i));
240     MWD_wave_mat(j,i) = MWD_wave_route(i);
241     else
242         MWD_wave_route(i) = interp3(coords_lon,coords_lat,...
243             coords_time,MWD_wave,longitude(i),latitude(i),...
244             time_points(j,i));
245         MWD_wave_mat(j,i) = MWD_wave_route(i);
246     end
247 end
248 end
249 % ----- Integrate MWP in time and space -----
250 MWP_wave_route = zeros();
251 MWP_wave_mat = zeros();
252 for j = 1:1:size(time_points, 1)
253     for i = 1:1:length(longitude)
254         if mod(j,2) == 0 % even numbers
255             MWP_wave_route(i) = interp3(coords_lon,coords_lat,...
256                 coords_time,MWP_wave,longitude_return(i),...
257                 latitude_return(i),time_points(j,i));
258             MWP_wave_mat(j,i) = MWP_wave_route(i);
259         else
260             MWP_wave_route(i) = interp3(coords_lon,coords_lat,...
261                 coords_time,MWP_wave,longitude(i),latitude(i),...
262                 time_points(j,i));
263             MWP_wave_mat(j,i) = MWP_wave_route(i);
264         end
265     end
266 end
267 end

```

# MatLab Code - Calculate Sea Margin

## iso\_input.m

```
1 % ----- Load weather data from route simulation -----
2 load('saved_data/amsterdam_newyork_5yrs_16kn');
3
4 % ----- Constants -----
5 % The mass density of air in kg/m^3:
6 rho_A = 1.225;
7 % The gravitational acceleration in m/s^2:
8 g = 9.81;
9 % The water densisty in kg/m^3
10 rho_S = 1025.89;
11 % Kinematic viscosity for 15 degrees celsius
12 nu = 1.18830 * 10^-6;
13
14 % ----- Ship speed -----
15 % The ship speed in knots:
16 V_S_knots = 16;
17 V_S = V_S_knots *(1852/3600); %[m/s]
18
19 % ----- Input from model test data -----
20 % Insert values to interpolate between from model test data:
```

```

21 % Speed [knots]:
22 V_range = [14 14.5 15 15.5 16 16.50 17 17.5 18 18.5 19];
23 % Calm water resistance [kN]:
24 R_Ts_range = [589 636 685 738 797 866 955 1060 1171 1321 1542]*1000;
25 % Calm water effective power [kN]:
26 PE_range = [4245 4740 5283 5886 6557 7348 8352 9539 10846 12572
15070]*1000;
27 % Wake fraction:
28 w_range = [0.308 0.309 0.310 0.311 0.312 0.313 0.309 0.303 0.304 0.306
0.301];
29 % Thrust deduction factor:
30 t_range = [0.216 0.219 0.221 0.223 0.226 0.229 0.223 0.216 0.222 0.227
0.215];
31 % Relative rotative efficiency:
32 etaR_range = [1.016 1.018 1.020 1.023 1.025 1.026 1.026 1.027 1.027 1.026
1.025];
33
34 % ----- Azimuth angle to and from destination -----
35 azimuth_angle = zeros();
36 for j = 1:size(MWD_matrix, 1)
37     for i = 1:length(longitude)
38         if mod(j,2) == 0 % even numbers
39             azimuth_angle(j, i) = azimuth_return(:, i);
40         else % odd numbers
41             azimuth_angle(j, i) = azimuth(:, i);
42         end
43     end
44 end
45
46 azimuth_rad = deg2rad(azimuth_angle); % rad

```

```

47
48 % ----- Ship heading degrees -----
49 psi = wrapTo180(azimuth_angle);
50
51 % ----- Wind calculation constants -----
52 % The reference height for the wind resistance coefficient in metres:
53 Z_ref = 10 ;
54 % The vertical position of the anemometer in metres:
55 Z_a = 10;
56 % The wind resistance coefficient in head wind:
57 C_AA_0 = 0.960;
58
59 % ----- Ship and propeller parameters -----
60 % The ship's length overall in metres:
61 L_OA = 208.73;
62 % The ship's breadth in metres:
63 B = 32.20;
64 % The distance of the bow to 95% of maximum breadth on the waterline in
65 % meters:
66 L_BWL = 13.4995;
67 % The ship's length between perpendiculars in meters:
68 L_PP = 197.4;
69 % The block coefficient:
70 C_B = 0.7958;
71 % Length of waterline
72 L_WL = 201.90;
73 % The draft at midships in metres:
74 T_M = 12;
75 % The Froude number: should be LWL.
76 Fr = V_S/(sqrt(g*L_WL));

```

```

77 % Transverse projected area above waterline , incl superstructure in m^2:
78 A_XV = 785.40;
79 % The wetted surface area in m^2:
80 S = 9512.1;
81 % The number of propellers:
82 nprop = 1;
83 % The propeller diameter [m]:
84 D = 6.8;
85 % The mechanical efficiency (typical value is 0.97):
86 eta_M = 0.97;

```

## wind.m

```

1 % ----- Wind resistance calculation R_AA -----
2 % Decompose the ship speed into V and U components:
3 for j = 1:size(azimuth_angle,1)
4     for i = 1:size(azimuth_angle,2)
5         if azimuth_angle(j,i) >= 0 && azimuth_angle(j,i) <= 90
6             V_ship(j,i) = cosd(azimuth_angle(j,i))*V_S;
7             U_ship(j,i) = sind(azimuth_angle(j,i))*V_S;
8         elseif azimuth_angle(j,i) > 90 && azimuth_angle(j,i) <= 180
9             V_ship(j,i) = -(sind(azimuth_angle(j,i)- 90)*V_S);
10            U_ship(j,i) = cosd(azimuth_angle(j,i)- 90)*V_S;
11        elseif azimuth_angle(j,i) > 180 && azimuth_angle(j,i) <= 270
12            V_ship(j,i) = -(cosd(azimuth_angle(j,i)- 180)*V_S);
13            U_ship(j,i) = -(sind(azimuth_angle(j,i)- 180)*V_S);
14        elseif azimuth_angle(j,i) > 270 && azimuth_angle(j,i) <= 360
15            V_ship(j,i) = sind(azimuth_angle(j,i)- 270)*V_S;
16            U_ship(j,i) = -(cosd(azimuth_angle(j,i)- 270)*V_S);
17        end

```

```

18     end
19 end
20
21 % Finding the relative velocity components in V and U directions:
22 relative_V = V_wind_matrix - V_ship;
23 relative_U = U_wind_matrix - U_ship;
24
25 % Mean value of measured rel wind velocity at vertical pos m/s:
26 V_WR = sqrt(relative_V.^2 + relative_U.^2);
27
28 % True wind direction in degrees [0, 360]:
29 % (Acting on point, not from point, thus -180 degrees)
30 psi_WT = atan2d(U_wind_matrix, V_wind_matrix) -180 + ...
31     360*(U_wind_matrix<0);
32 wind_dir_rad = deg2rad(psi_WT); %rad
33
34 % Difference between the ship heading and true wind velocity:
35 azimuth_rad = deg2rad(azimuth_angle); % rad
36 wind_dir_rel = angdiff(azimuth_rad, wind_dir_rad); % rad
37 gamma = rad2deg(wind_dir_rel); % degrees
38
39 % True wind velocity in m/s:
40 V_WT = sqrt(U_wind_matrix.^2 + V_wind_matrix.^2);
41
42 % The relative wind velocity:
43 for j = 1:size(V_WR,1)
44     for i = 1:size(V_WR,2)
45         if gamma(j, i) < 0
46             psi_WR(j, i) = -acosd((V_S^2+V_WR(j, i)^2-V_WT(j, i)^2) / ...
47                 (2*V_WR(j, i)*V_S));

```



```

48     elseif gamma(j , i) >= 0
49         psi_WR(j , i) = acosd((V_S^2 + V_WR(j , i)^2 - V_WT(j , i)^2) / ...
50             (2 * V_WR(j , i) * V_S));
51     end
52 end
53 end
54
55 % Correction for the vertical position of the anemometer:
56 for j = 1:size(V_WR,1)
57     for i = 1:size(V_WR,2)
58         V_WTref(j , i) = V_WT(j , i) * ((Z_ref) / (Z_a))^(1/7);
59     end
60 end
61
62 % Relative wind velocity at reference height:
63 V_WRref = zeros(1, 10);
64 for j = 1:size(V_WR,1)
65     for i = 1:size(V_WR,2)
66         V_WRref(j , i) = sqrt (V_WTref(j , i)^2 + V_S^2 + ...
67             2 * V_WTref(j , i) * V_S * cosd(psi_WT(j , i) - psi(j , i)));
68     end
69 end
70
71 % Relative wind direction at reference height:
72 psi_WRref = zeros(1, 10);
73 %
74 for j = 1:size(V_WR,1)
75     for i = 1:size(V_WR,2)
76         if V_S + V_WTref(j , i) * cosd(psi_WT(j , i) - psi(j , i)) >= 0
77             psi_WRref(j , i) = atand((V_WTref(j , i) * sind(psi_WT(j , i) ...

```

```

78         -psi(j,i)))/(V_S + V_WTref(j,i)*cosd(psi_WT(j,i) ...
79         -psi(j,i))));
80     elseif V_S + V_WTref(j,i)*cosd(psi_WT(j,i)-psi(j,i)) < 0
81         psi_WRref(j,i) = atand((V_WTref(j,i)*sind(psi_WT(j,i) ...
82         -psi(j,i)))/(V_S +V_WTref(j,i)*cosd(psi_WT(j,i) ...
83         -psi(j,i))))+180;
84     end
85 end
86 end
87 psi_WRref = wrapTo180(psi_WRref);
88
89 % Graph in ISO for C_X
90 C_X_degrees = [0 9.92 20.1 29.8 39.9 49.4 59.8 69.8 79.7 90 99.6 110 ...
91     120 130 140 150 160 170 180];
92
93 C_X_graph = [-0.960 -0.943 -0.863 -0.740 -0.620 -0.510 -0.347 -0.179 ...
94     -0.0816 0.0332 0.121 0.210 0.267 0.395 0.497 0.642 0.726 0.766 0.752];
95
96 % Interpolating for the relative wind directions for the route:
97 C_X = zeros(size(V_WR,1), size(V_WR,2));
98 for j = 1:size(V_WR,1)
99     for i = 1:size(V_WR,2)
100         C_X(j,i) = interp1(C_X_degrees, C_X_graph, abs(psi_WRref(j,i)));
101     end
102 end
103
104 C_AA = -C_X;
105
106 % Calculating the added resisance due to wind:
107 R_AA = zeros(size(U_wind_matrix,1), size(U_wind_matrix,2));

```

```

108
109 for j = 1:size(V_WR,1)
110     for i = 1:size(V_WR,2)
111         R_AA(j,i) = 0.5 * rho_A * C_AA(j,i) * A_XV * (V_WRref(j,i))^2 ...
112             - 0.5 * rho_A * C_AA_0 * A_XV * V_S^2;
113     end
114 end

```

## waves.m

```

1  % ----- Resistance due to waves -----
2  % Omega step to use in integration:
3  domega = 0.1;
4
5  % ----- Wave parameters -----
6  % Angle between ships heading and component in waves (0 = head)
7  MWD_towards_ship = MWD_matrix - 180;
8  MWD_360 = wrapTo360(MWD_towards_ship);
9  MWD_rad = deg2rad(MWD_360);
10
11 theta_m_rad = angdiff(MWD_rad, azimuth_rad);
12 theta_m = rad2deg(theta_m_rad);
13
14 % The significant wave height in metres:
15 H_13 = H_13_matrix;
16 % Mean wave period:
17 T_01 = MWP_matrix;
18
19 % ----- Integration limits for omega -----
20 % Omega is the circular frequency of regular waves in rad/s:

```

```

21 om_start = 2*pi/25;
22 om_stop = 2*pi/4;
23
24 % STAWAVE-2 calculations:
25 R_AWL = zeros(size(MWP_matrix,1), size(MWP_matrix,2));
26 for omega = om_start:domega:om_stop
27     [R_wave, S_eta] = R_waves(T_01, omega, U_wind_matrix, ...
28         V_wind_matrix, H_13, H_13_matrix, MWD_matrix, MWP_matrix, ...
29         longitude, latitude, azimuth, azimuth_return);
30     equation= R_wave.*S_eta;
31     R_AWL = R_AWL + (equation.*domega);
32 end
33 R_AWL_ST2 = 2*R_AWL;
34
35 % Calculating the added reistance due to waves:
36 limit = (2.25 * sqrt(L_PP/100));
37 for j = 1:size(MWP_matrix,1)
38     for i = 1:size(MWP_matrix,2)
39         % STAWAVE-1
40         if H_13_matrix(j,i) <= limit && abs(theta_m(j,i)) <= 45
41             R_AWL(j,i)= 1/16*rho_S*g*H_13_matrix(j,i)^2*B*sqrt(B/L_BWL);
42
43         elseif H_13_matrix(j,i) <= limit && abs(theta_m(j,i)) > 45
44             R_AWL(j,i) = 0;
45
46         % STAWAVE-2
47         elseif H_13_matrix(j,i) > limit && abs(theta_m(j,i)) <= 45
48             R_AWL(j,i) = R_AWL_ST2(j,i);
49
50         elseif H_13_matrix(i) > limit && abs(theta_m(j,i)) > 45

```

```

51         R_AWL(j, i) = 0;
52     end
53 end
54 end
55
56 R_AW = R_AWL;

```

## R\_wave.m

```

1 function [R_wave, S_eta] = R_waves (T_01, omega, U_wind_matrix, ...
2     V_wind_matrix, H_13, H_13_matrix, MWD_matrix, MWP_matrix, ...
3     longitude, latitude, azimuth, azimuth_return)
4 iso_input;
5 % The wave number in rad/m:
6 k = omega^2/g;
7 bess = 1.5*k*T_M;
8
9 % The modified bessel function of the first kind of order 1:
10 I_1 = besseli(1,bess);
11 % The modified bessel function of the second kind of order 1:
12 K_1 = besserk(1,bess);
13 % The non-dimensional radius of gyration in the lateral direction:
14 k_yy = 0.25*L_PP;
15
16 % ----- Pierson Moskowitz spectrum -----
17 A_fw = 173.*((H_13_matrix.^2)./(T_01.^4));
18 B_fw = ((691)./(T_01.^4));
19 S_eta =((A_fw)./(omega^5)).*exp(-(B_fw)/(omega^4));
20
21 % -----

```

```

22
23 a_1 = 60.3*C_B^1.34;
24
25 omega_line = ((sqrt(L_PP/g)*(k_yy)^(1/3))/(1.17*Fr^(-0.143)))*omega;
26 if omega_line < 1
27     b_1 = 11.0;
28     d_1 = 14.0;
29 else
30     b_1 = -8.50;
31     d_1 = -566*(L_PP/B)^(-2.66);
32 end
33
34 r_aw_line = omega_line^(b_1)*exp((b_1/d_1)*(1-omega_line^(d_1)))*a_1* ...
35     Fr^(1.50)*exp(-3.50*Fr);
36 R_AWML = 4*rho_S*g*(B^2/L_PP)*r_aw_line;
37 f_1 = 0.692*((V_S)/(sqrt(T_M*g))).^(0.769) + 1.81*C_B^(6.95);
38 alpha_1= ((pi^2*I_1^2)/(pi^2*I_1^2+K_1^2))*f_1;
39 R_AWRL = 0.5*rho_S*g*B*alpha_1;
40 R_wave = R_AWML + R_AWRL;
41
42 end

```

## criteria.m

```

1 % ----- Criteria for STAWAVE-2 -----
2 % STAWAVE-2 can only be applied under the following conditions:
3 % 75 < L_PP
4 % 4.0 < L_PP/B < 9.0
5 % 2.2 < B/T_M < 9.0
6 % 0.10 < Fr < 0.30

```

```
7 % 0.50 < C_B < 0.90
8
9 if L_PP > 75
10     disp('L_PP > 75m.           Criteria met.')
```

11 else

```
12     disp('L_PP <= 75m.         Criteria not met.')
```

13 end

14

```
15 if L_PP/B > 4 && L_PP/B < 9
16     disp('4 < L_PP/B > 9.       Criteria met.')
```

17 else

```
18     disp('L_PP/B outside interval. Criteria not met.')
```

19 end

20

```
21 if all((B./T_M >= 2.2) & (B./T_M < 9.0))
22     disp('2.2 < B/T_M < 9.0.     Criteria met.')
```

23 else

```
24     disp('B/T_M outside interval. Criteria not met.')
```

25 end

26

```
27 if all((Fr > 0.1) & (Fr < 0.3))
28     disp('0.10 < Fr < 0.30.     Criteria met.')
```

29 else

```
30     disp('Fr outside interval.   Criteria not met.')
```

31 end

32

```
33 if C_B > 0.5 && C_B < 0.9
34     disp('0.50 < C_B < 0.90.     Criteria met.')
```

35 else

```
36     disp('C_B outside interval.   Criteria not met.')
```

37 **end**

## resistance.m

```

1  % ----- Resistance increase -----
2  % ----- Run scripts -----
3  iso_input;
4  wind;
5  criteria;
6  waves;
7
8  % ----- Calm water resistance -----
9  R_TS = interp1(V_range, R_Ts_range, V_S_knots);
10 R_Ts_mat = R_TS*ones(size(U_wind_matrix,1), size(U_wind_matrix,2));
11
12 % ----- Fouling allowance -----
13 R_FO = 0.10*R_Ts_mat;
14
15 % ----- Total added resistance -----
16 DeltaR = R_AA + R_AW + R_FO;
17
18 % ----- Limit for extreme weather - Beaufort 5 -----
19 beaufort5wind = 10.8;
20 beaufort5waves = 3;
21
22 % ----- Neglect values above Beaufort 5 -----
23 for j = 1:size(U_wind_matrix,1)
24     for i = 1:size(U_wind_matrix,2)
25         if H_13_matrix(j,i) >= beaufort5waves || V_WT(j,i) >= beaufort5wind
26             DeltaR(j,i) = NaN;

```



```

27 end
28     end
29 end
30 DeltaR(isnan(DeltaR))= 0;
31
32 % ----- Resistance increase in kN -----
33 Delta_R = DeltaR/1000;
34
35 % ----- Total resistance in each interval -----
36 R_tot = R_TS + DeltaR;

```

## openwater.m

```

1 % ----- Open water diagram data -----
2 % Data from digitalization of open water diagram (Only used for plot)
3 % ----- K_T -----
4 K_T_tab = [0.381 0.368 0.354 0.341 0.336 0.328 0.321 0.312 0.303 0.292...
5           0.284 0.277 0.269 0.260 0.251 0.242 0.232 0.225 0.216 0.211 0.198 ...
6           0.190 0.181 0.173 0.165 0.157 0.145 0.135 0.131 0.126 0.116 0.103 ...
7           0.0895 0.0793 0.0690 0.0576 0.0463 0.0406 0.0349 0.0280 0.0190 ...
8           0.00881 0.000794];
9
10 J_Kt = [0 0.0359 0.0747 0.106 0.127 0.145 0.167 0.186 0.210 0.231 0.250...
11         0.270 0.289 0.314 0.333 0.356 0.374 0.394 0.409 0.429 0.448 0.471 ...
12         0.494 0.509 0.523 0.544 0.570 0.585 0.600 0.614 0.638 0.659 0.680 ...
13         0.701 0.719 0.746 0.762 0.774 0.782 0.799 0.812 0.826 0.845];
14
15 % ----- K_Q -----
16 K_Q_tab = 0.1*[ 0.422 0.414 0.412 0.405 0.401 0.395 0.391 0.386 0.382 ...
17               0.375 0.373 0.364 0.360 0.354 0.349 0.342 0.336 0.329 0.326 0.320 ...

```

```

18     0.313  0.306  0.300  0.296  0.290  0.282  0.280  0.269  0.265  0.257  0.253  ...
19     0.245  0.240  0.228  0.225  0.217  0.211  0.202  0.197  0.189  0.185  0.175  ...
20     0.169  0.159  0.154  0.145  0.138  0.127  0.121  0.112  0.103  0.0961  0.0893...
21     0.0813  0.0677  0.0609  0.0507  0.0473];
22
23 J_Kq = [ 0 0.0231 0.0320 0.0514 0.0628 0.0822 0.0928 0.110 0.124 0.141...
24         0.154 0.172 0.185 0.201 0.216 0.233 0.248 0.263 0.275 0.292 0.303  ...
25         0.322 0.333 0.349 0.363 0.381 0.392 0.412 0.425 0.442 0.452 0.467  ...
26         0.481 0.501 0.511 0.531 0.539 0.558 0.569 0.587 0.598 0.616 0.626  ...
27         0.646 0.659 0.673 0.686 0.703 0.718 0.729 0.748 0.760 0.771 0.788  ...
28         0.805 0.819 0.833 0.843  ];
29
30 % ----- eta_0 -----
31 eta_0 = [ 0 0.0174 0.0464 0.0779 0.117 0.138 0.164 0.179 0.214 0.249  ...
32         0.308 0.351 0.392 0.428 0.449 0.479 0.497 0.520 0.555 0.572 0.596  ...
33         0.611 0.631 0.652 0.670 0.687 0.694 0.698 0.697 0.686 0.675 0.655  ...
34         0.641 0.618 0.606 0.585 0.572 0.544 0.525 0.480 0.453 0.406 0.361  ...
35         0.320 0.280 0.242 0.193 0.173 0.139 0.0987 0.0770 0.0443 0.000828];
36
37 J_eta0 = [0 0.0138 0.0326 0.0552 0.0840 0.100 0.118 0.130 0.155 0.181  ...
38         0.226 0.260 0.292 0.322 0.339 0.368 0.384 0.405 0.440 0.456 0.482  ...
39         0.498 0.523 0.550 0.579 0.611 0.635 0.660 0.674 0.703 0.714 0.734  ...
40         0.745 0.760 0.766 0.776 0.782 0.789 0.792 0.799 0.803 0.808 0.814  ...
41         0.818 0.823 0.826 0.830 0.832 0.836 0.839 0.841 0.843 0.845];
42
43
44 % ----- Plots -----
45 figure
46 subplot(1,2,1)
47 plot(J_Kt, K_T_tab, '-b', J_Kq, 10*K_Q_tab, '-r', J_eta0, eta_0, '-g')

```

```
48 legend('K_T', '10*K_Q', '\eta_0')
49 grid on
50 grid minor
51 title('Open water diagram, full scale')
52 xlabel('Advance number J')
53 ylabel('K_T, 10*K_Q, \eta_0')
54
55 % ----- Data from model test data -----
56 % KT/J^2 values:
57 K_T_O = 0.1*[3.288 3.088 2.881 2.668 2.451 2.230 2.005 1.776 ...
58     1.543 1.305 1.060 0.807 0.544 0.268];
59
60 K_Q_O = 0.01*[3.741 3.559 3.368 3.169 2.963 2.751 2.532 2.306 2.072 ...
61     1.828 1.574 1.307 1.025 0.725];
62
63 J = [0.150 0.200 0.250 0.300 0.350 0.400 0.45 0.500 ...
64     0.550 0.600 0.650 0.700 0.750 0.800];
65
66 K_T_J2_tab = K_T_O./J.^2;
67
68 subplot(1,2,2)
69 plot(J, K_T_J2_tab, '-')
70 grid on
71 grid minor
72 title('Open water diagram')
73 ylabel('K_T/J^2')
74 xlabel('Advance number J')
```

## SM\_calculation.m

```

1 % ----- Calculating the brake power from self propulsion test -----
2 clear all
3 clc
4 % ----- Run scripts -----
5 resistance;
6 openwater;
7
8 % ----- Calm water thrust deduction factor, wake fraction -----
9 % ----- and relative rotative efficiency -----
10 w = interp1(V_range, w_range, V_S_knots);
11 t = interp1(V_range, t_range, V_S_knots);
12 eta_R = interp1(V_range, etaR_range, V_S_knots);
13
14 % ----- Brake power calculation -----
15 K_T_J2 = R_tot / (nprop*rho_S*(1-t)*D^2*V_S^2*(1-w)^2);
16 J_star = interp1(K_T_J2_tab, J, K_T_J2);
17
18 % Finding K_Q_star from J_star in open water diagram:
19 K_Q_star = interp1(J, K_Q_O, J_star);
20
21 RPM = (60*(1-w)*V_S) ./ (D.*J_star);
22 % Calculating delivered and brake power:
23 P_D = nprop*(2*pi/1000)*rho_S * D^5.*(RPM/60).^3.*(K_Q_star./eta_R);% kW
24 P_B = P_D /eta_M; %kW
25
26 % ----- Calm water brake power -----
27 K_T_J2_calm = R_Ts_mat / (nprop*rho_S*(1-t)*D^2*V_S^2*(1-w)^2);
28 J_star_calm = interp1(K_T_J2_tab, J, K_T_J2_calm);
29 K_Q_star_calm = interp1(J, K_Q_O, J_star_calm);
30 RPM_calm = (60*(1-w)*V_S) ./ (D.*J_star_calm);

```

```

31 P_D_calm = nprop * (2*pi/1000) * rho_S * D^5.*(RPM_calm/60).^3.* ...
32     (K_Q_star_calm./eta_R); %kW
33 P_B_calm = P_D_calm /eta_M; %kW
34
35 P_B_mat_15 = P_B_calm * 1.15;
36
37 % ----- Calculating and averaging the sea margin -----
38 SM_mat = (P_B./P_B_calm-1)*100;
39 for j = 1:size(U_wind_matrix,1)
40     for i = 1:size(U_wind_matrix,2)
41         if DeltaR(j,i) == 0
42             SM_mat(j,i) = NaN;
43         end
44     end
45 end
46 SM_mat(isnan(SM_mat)) = [];
47 SM_tot = mean(SM_mat);
48
49 disp('Total sea margin for the whole route simulation');
50 disp(SM_tot);
51
52 figure
53 histogram(SM_mat)
54
55 % Brake power for calm water plus fouling resistance:
56 K_T_J2_fouling = (R_TS+R_FO)/(nprop*rho_S*(1-t)*D^2*V_S^2*(1-w)^2);
57 J_star_fouling = interp1(K_T_J2_tab, J, K_T_J2_fouling);
58 K_Q_star_fouling = interp1(J, K_Q_O, J_star_fouling);
59 RPM_fouling = (60*(1-w)*V_S)./(D.*J_star_fouling);
60 P_D_fouling = nprop * (2*pi/1000) * rho_S * D^5.*(RPM_fouling/60).^3.* ...

```

```

61     (K_Q_star_fouling./eta_R); %kW
62 P_B_fouling = P_D_fouling /eta_M; %kW
63
64 % ----- Plots -----
65 % Each plot visualizes the data for ONE route crossing.
66
67 % Choose which route crossing to be plotted (range: 1 to number of columns
68 % in matrices.
69 run_number = 14;
70 % i is the number of intervals in a route crossing
71 i = [1:1:size(U_wind_matrix,2) ];
72
73 % Plotting the increase of resistance:
74 figure
75 plot(i, R_AA(run_number,:)/1000, '-g', i, R_AW(run_number,:)/1000, ...
76      '-r', i, R_FO(run_number,:)/1000, '--', i, DeltaR(run_number,:)/1000, '-b')
77 legend('R_{AA}', 'R_{AW}', 'R_{FO}', '\Delta R')
78 grid on
79 grid minor
80 title('Increase of resistance')
81 xlabel('Route interval')
82 ylabel('\Delta R [kN]')
83
84 % Plotting the calm water and the operational resistance:
85 figure
86 plot(i, R_tot(run_number,:)/1000, '-', i, R_Ts_mat(1,:)/1000, '-r')
87 legend('R_{tot}', 'R_{calm}')
88 grid on
89 grid minor
90 title('Total resistance')

```

```

91 ylabel('Resistance [kN]')
92 xlabel('Route interval')
93
94 figure
95 plot(i, P_B(run_number,:), '-r', i, P_B_calm(run_number,:), '-r', i, ...
96     P_B_mat_15(run_number,:), '-g')
97 legend('P_B', 'P_{Bcalm}', 'P_{Bcalm} with 15% sea margin')
98 grid on
99 grid minor
100 title('Brake power')
101 xlabel('Route interval')
102 ylabel('P_B [kW]')
103
104 % -----
105 % Plotting the calm water and the operational brake power:
106 for j = 1:size(P_B,1)
107     i_mat(j,:) = i;
108 end
109
110 P_B_SM = (1+SM_tot/100) * P_B_calm;
111
112 figure
113 plot(i, P_B_fouling(1,:), '-m', i, P_B_calm(1,:), '-b', i, P_B_SM, '-g', ...
114     'LineWidth', 2)
115 legend('Effect of fouling', 'P_{Bcalm}', 'P_{Bcalm} with route SM')
116 hold on
117 for j = 1:size(P_B,1)
118     scatter(i_mat(j,:), P_B(j,:))
119     hold on
120 end

```

```
121 plot(i, P_B_calm(1,:), '-b', i, P_B_SM, '-g', i, P_B_fouling(1,:), '-m', ...
122       'LineWidth', 2)
123 hold on
124
125 grid on
126 grid minor
127 title('Brake power')
128 xlabel('Route interval')
129 ylabel('P_B [kW]')
```





# Appendix E

## Evaluation Of Temperature Change

### temp.m

```
1 % ----- Effect of water temperature and water density -----
2 % ----- Speed -----
3 V_S_knots = 16; % [knots]
4 V_S = V_S_knots *(1852/3600); % [m/s]
5
6 % ----- Water density for test cases: 5, 15 and 25 degrees celsius -----
7 % Water density for actual water temperature and salt content:
8 rho_S_5 = 1027.7225; % [kg/m^3]
9 rho_S_25 = 1023.3873; % [kg/m^3]
10 % Water densisty for reference water temperature and salt content:
11 rho_S0 = 1025.89; % [kg/m^3]
12
13 % --- Kinematic viscosity for test cases: 5, 15 and 25 degrees celsius ---
14 nu_15 = 1.18830* 10^-6; % [m^2/s]
15 nu_5 = 1.5762 * 10^-6; % [m^2/s]
16 nu_25 = 9.3713* 10^-7; % [m^2/s]
17
```

```

18 % ----- Ship parameters -----
19 %The ship's length overall:
20 L_OA = 208.73; % [m]
21 % The wetted surface area:
22 S = 9512.1; % [m^2]
23
24 % ----- Reynolds number for all cases -----
25 R_N_15 = V_S * L_OA / nu_15;
26 R_N_5 = V_S * L_OA / nu_5;
27 R_N_25 = V_S * L_OA / nu_25;
28
29 % ----- The frictional resistance coefficient -----
30 % For the actual water temperature and water density:
31 C_F_5 = 0.075 / (log10(R_N_5) - 2)^2;
32 C_F_25 = 0.075 / (log10(R_N_25) - 2)^2;
33 % For the reference water temperature and water density:
34 C_F0 = 0.075 / (log10(R_N_15) - 2)^2;
35
36 % --- Total resistance coefficient for the reference water temperature ---
37 % (C_T0 value from model test)
38 C_T0 = 2.410 * 10^-3;
39
40 % ----- Frictional resistance for the test cases -----
41 R_F_5 = 0.5 * rho_S_5 * S * V_S.^2 .* C_F_5; % [N]
42 R_F_25 = 0.5 * rho_S_25 * S * V_S.^2 .* C_F_25; % [N]
43
44 % The resulting added resistance due to water density and temperature:
45 R_T0 = 0.5 * rho_S0 * S * V_S.^2 * C_T0;
46 R_AS_5 = R_T0 * ((rho_S_5) / (rho_S0) - 1) - R_F_5 * ((C_F0) / (C_F_5) - 1);
47 R_AS_25 = R_T0 * ((rho_S_25) / (rho_S0) - 1) - R_F_25 * ((C_F0) / (C_F_25) - 1);

```

48

```
49 disp('Added resistance due to temperature and density [kN], +/- 10 degrees  
    celsius');
```

```
50 disp(R_AS_5/1000);
```

```
51 disp(R_AS_25/1000);
```